A MINERALOGICAL AND TEXTURAL STUDY OF THE CENTRAL NORTH ISLAND TEPHRA, OKAREKA ASH AND ITS OVERLYING TEPHRIC LOESS DEPOSITS

A Thesis Presented as Partial Fulfillment for the Degree of Master of Science in Soil Science

by

Lynette Anne Benny

Massey University,
New Zealand

1982

ACKNOWLEDGEMENTS

I wish to thank my supervisors Dr. J.H. Kirkman, and Mr. R.B. Stewart for their guidance, encouragement and advice during my thesis work.

I wish also to extend my thanks to Dr. W.A. Pullar and Mr N.M. Kennedy, Soil Bureau, Rotorua, for their invaluable assistance in collecting soil samples for this study, and worthwhile discussion in the field.

I am grateful to Mr. D. Hopcroft and Mr. R.J. Bennett of the Electron Microscope Lab. D.S.I.R., for their technical assistance in the electron optical work, and printing of the electron micrographs.

To Miss. J.S. Rowarth and Mr. R.C. Wallace, my thanks for your critical reading of, and helpful comments about the manuscript.

I would also like to thank my mother, Mrs. A.F. Benny, who typed this thesis, and finally, both my parents for their continuing support.

ABSTRACT

In Central North Island, New Zealand, Post-Okareka tephric loess rests upon Okareka Ash (c.17,000 years B.P.). Tephric loess accumulation occurred under semi-arid conditions which coincided with glacial advances in southern areas of New Zealand.

Morphological and grain-size evidence indicates the tephric loess has been derived from a localised source, most probably that of Okareka Ash material, reworked and redeposited by aeolian processes. Optical and electron optical evidence reveals that Okareka Ash particles are angular and relatively unweathered, whereas tephric loess grains are subangular and more weathered.

The sand and clay mineralogy of the tephra and tephric loess are similar. Sand fractions contain mainly rhyolitic volcanic glass, quartz, plagioclase feldspar, biotite, hypersthene, hornblende, titanomagnetite and traces of cristobalite, tridymite and augite, whereas clay fractions contain halloysite, allophane, imogolite and gibbsite in varying amounts.

Grain-size analysis reveals Okareka Ash deposits show decreasing mean grain-size with increasing distance from source, are poorly-sorted, fine-skewed, and lepto/platykurtic. In contrast to tephra, tephric loess samples exhibit a narrow mean grain-size range, and are better sorted, but show similar skewness and kurtosis values to ash. Grain-size results also indicate that due to minimal weathering of Okareka Ash and Post-Okareka loess, the distinction between the two deposits is less well-defined than data from similar deposits reported by Fisher (1966). Furthermore, where ash deposits are thin, in distal areas from source, and under certain environmental conditions, textural and morphological characteristics of the tephra are similar to those of the tephric loess. Nevertheless, grain-size parameters may be used to differentiate airfall tephra and tephric loess deposits, although this

differentiation is enhanced by post-depositional weathering.

The contrasting clay mineralogies of tephra and tephric loess samples from sections of similar topography, altitude, drainage and rainfall, illustrates the problems of field sampling in weathering studies.

TABLE OF CONTENTS

LIST OF TABLES

LIST OF FIGURES

NOMENCLATURE

Sections: (except for Trunk Rd, sections sampled are given a letter symbol, listed below, with increasing distance from Okareka Ash source)

G Gavin Rd
A Okareka Quarry
I Lynmore
H Te Ngae
B Pukehangi Rd
J Ngongotaha
C Tarukenga
D Dalbeth Rd
E Highland Hill
K Kuhatahi

At Trunk Rd section, due to the thickness of Okareka Ash, samples were labelled according to -

firstly, the predominance of

R rhyolitic (pale grey)

or B basaltic (dark grey-black) material

and secondly, the grain-size by a letter subscript -

A ash
L lapilli
c coarse
f fine

Ash and Loess: loess samples were labelled -

L loess
A Ash

and given a number subscript, from top to base, depending upon the number of samples taken -

e.g. Okareka Quarry - section A

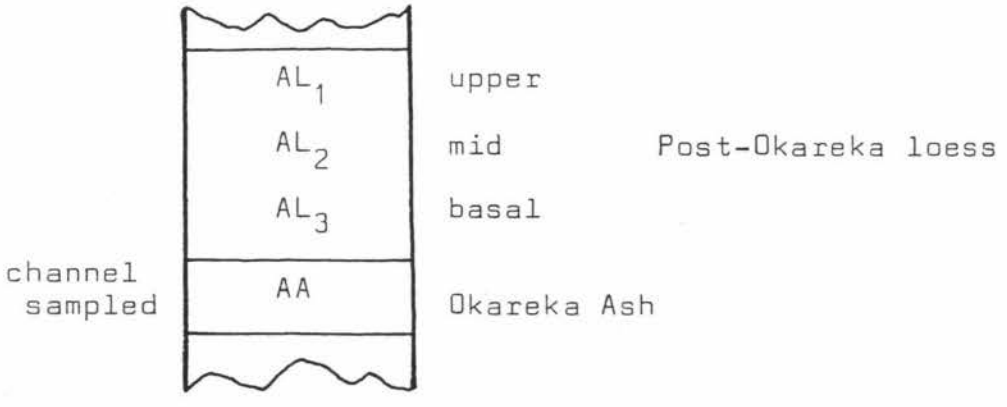

ABBREVIATIONS

Al	Aluminium
Å	angstrom (10^{-7} m)
An	anorthite
Cpx	augite
Bt	biotite mica
cm	centimetre (10^{-2}m)
^{o}C	degrees celsius
DTA	differential thermal analysis
Fds	feldspar (includes alkali and plagioclase)
g	gram
>	greater than
Hb	hornblende
H	hydrogen
Opx	hypersthene
IR	infra-red spectroscopy
kHz	kilohertz
km	kilometre
Kw	kilowatt
K_G	kurtosis
<	less than
Mz	mean grain-size
m	metre
µm	micrometre (10^{-6}m)
mg	milligram (10^{-3}g)
mm	millimetre (10^{-3}m)
O	oxygen
%	percent
Qz	quartz
Ø	phi scale
(v)ps	(very) poorly-sorted
RI	refractive index
SEM	scanning electron microscope
Si	silica
SK_I	skewness
(s)fs	(strongly) fine-skewed
sym	symmetrical
σ_I	sorting
θ	theta

FeO	titanomagnetite
TEM	transmission electron microscope
VG	volcanic glass (rhyolitic)
XRD	X-ray diffraction

N.B. for consistency all grain-size calculations were carried out at μm sizes to equal Ø (phi-scale) divisions (e.g. 63μm = 4.5Ø)

Chapter 1: INTRODUCTION

Loess deposits consisting of rhyolitic volcanic glass, feldspar, quartz, and an igneous mafic mineral assemblage overlie late Pleistocene tephras in areas of Central North Island, New Zealand (Pullar and Birrell, 1973a). These 'tephric loess' deposits (Pullar and Pollok, 1973), possess characteristics which indicate derivation from underlying tephra beds (Vucetich and Pullar, 1969).

During late Quaternary times, when climatic conditions were cooler and drier than at present, extensive loess deposition occurred in central areas of North Island (Cowie and Milne, 1973). Glaciation occurred in South Island regions during these periods, whereas areas of North Island experienced periglacial conditions, facilitating erosion of a tephra-covered landscape and subsequent accumulation of loess comprising predominantly tephric constituents (McGraw, 1975). Recent investigations suggest that tephric loess deposits are mineralogically similar to the underlying tephra units, and therefore, are largely derived from them (Vucetich and Pullar, 1969; Pullar and Birrell, 1973a, 1973b; Cowie and Milne, 1973).

Much controversy exists over use of the term 'tephric loess', as loess deposits can comprise either primary or secondary material. Primary loess consists of quartzo-felspathic material ultimately derived from braided rivers, to which airfall tephric material may have been added. Aeolian material which has been reworked and redeposited is defined as secondary loess. Loess deposits found in Central North Island are of this type (McGraw, 1975).

Difficulty is encountered in distinguishing between tephra nad tephric loess, both in the field and laboratory (Pullar and Birrell, 1973a; Birrell, 1974). Kennedy (1980) has outlined possible pedological criteria to aid field discrimination of airfall tephra and tephric loess in Central North Island. However, differentiation of tephric loess and tephra by analytical techniques

would aid characterisation of each deposit, and, therefore, have a greater application to Quaternary studies.

This study attempts to elucidate the relationship between tephra, tephric loess and loess on the basis of grain-size, mineralogy and morphology. The Okareka Ash, erupted c.17,000 years B.P. (Pullar, 1980), and overlying loess deposits which accumulated prior to deposition of Rerewhakaaitu Ash (NZ716 14,700 $\pm$ 200 years B.P.), were selected for detailed investigation. The mineralogical and morphological properties of the ash and loess, together with the grain-size distribution of airfall tephra and tephric loess were studied. Results from the present study were compared to those of similar studies by other workers, the aim being to identify parameters that may assist differentiation of tephra, tephric loess and loess deposits. For convenience the thesis is presented in two parts. Section A reports on mineralogical and morphological characteristics of airfall tephra and tephric loess, and Section B deals with grain-size distribution of these two deposits.

SECTION A:

MINERALOGY AND MORPHOLOGY

Chapter 2: LITERATURE REVIEW

2.1 Distribution of airfall deposits in New Zealand

Loess, dune sand and volcanic ash deposits comprise material which has been transported and laid down by wind and localised air turbulence. Such aeolian deposits form extensive subsurface and surface cover beds in both islands of New Zealand (McGraw, 1975).

Loess of the Northern Hemisphere is a product of periglacial processes in regions of continental glaciation. It consists essentially of unbedded, well-sorted aeolian silt with a variable calcium carbonate content, and has a homogenous structure with high porosity (Selby, 1976). In New Zealand, however, loess deposits are generally noncalcareous (Cowie and Milne, 1973). McGraw (1975) defined loess in New Zealand as "any fine textured deposit of aeolian origin where transport has been chiefly by suspension irrespective of organic matter content, mineralogical composition, calcium carbonate content or degree of compaction, other than sand dunes or tephra".

In South Island, loess which is widely distributed over hills, downlands, inland basins and older terraces on the east coast (Selby, 1976), is largely a product of wind and fluvioglaciation (McGraw, 1975). During Pleistocene glacials, rivers deposited large quantities of glacial detritus in extensive outwash fans. Concomitantly, particles of fine sand and silt were uplifted from wide, braided river beds by prevailing north westerly winds and deposited on adjacent areas (McGraw, 1975). Older deposits generally occur as a thin veneer on upper terraces and older plains, while thicker, younger deposits are widespread on downlands, fans and younger terraces (Raeside, 1964). Recent studies have shown South Island loess deposits may be subdivided according to source area, dependent upon prevailing climatic conditions (Ives, 1973). During late Pleistocene times, thicker deposits of loess, laid down rapidly during an immediate post-stadial period

of warming, were derived from a fluvioglacial source. However, interstadial loess, which accumulated at a slower rate, often on surfaces adjacent to major rivers, was derived from a more localised source area during periods of river aggradation (interstadials). A substantial amount of this interstadial loess became eroded during later cooler (stadial) periods of river degradation (Ives, 1973). Likewise, much loess associated with hilly and steep areas was eroded, and became redeposited as secondary or 'reworked' loess (McGraw, 1975).

In Manawatu, Wairarapa and Hawke's Bay regions of North Island, loess units derived from river alluvium occur as surface deposits (McGraw, 1975) (Figure 1). The major sources of alluvium were rapidly aggrading river beds built up due to accelerated erosion accompanying periods of cooler climate that coincided with glacial advances in South Island (Cowie and Milne, 1973). In contrast to eastern and southern areas, Central North Island loess deposits typically contain loess interstratified with tephra units (Cowie and Milne, 1973). Despite the small number of sizeable rivers, loess is widespread in Central North Island (Pullar and Birrell, 1973a), and its distribution suggests that it is derived from tephra rather than river fans (Cowie and Milne, 1973). During the Pleistocene, glaciation in North Island was restricted to isolated parts of Tararua Ranges and Mt. Ruapehu (McGraw, 1975). Northern areas, therefore, were typified by periglacial processes occurring in more cold, desert-like rather than glacial conditions (Pullar and Kennedy, 1978). These conditions were similar to those that resulted in the deposition of 'interstadial' loess in South Island (Ives, 1973). Aeolian deposits were derived from reworking of tephra and from fine fractions of alluvium derived from pyroclastic material (McGraw, 1975).

In New Zealand, loess deposits show wide variation in composition which reflect changes in provenance within

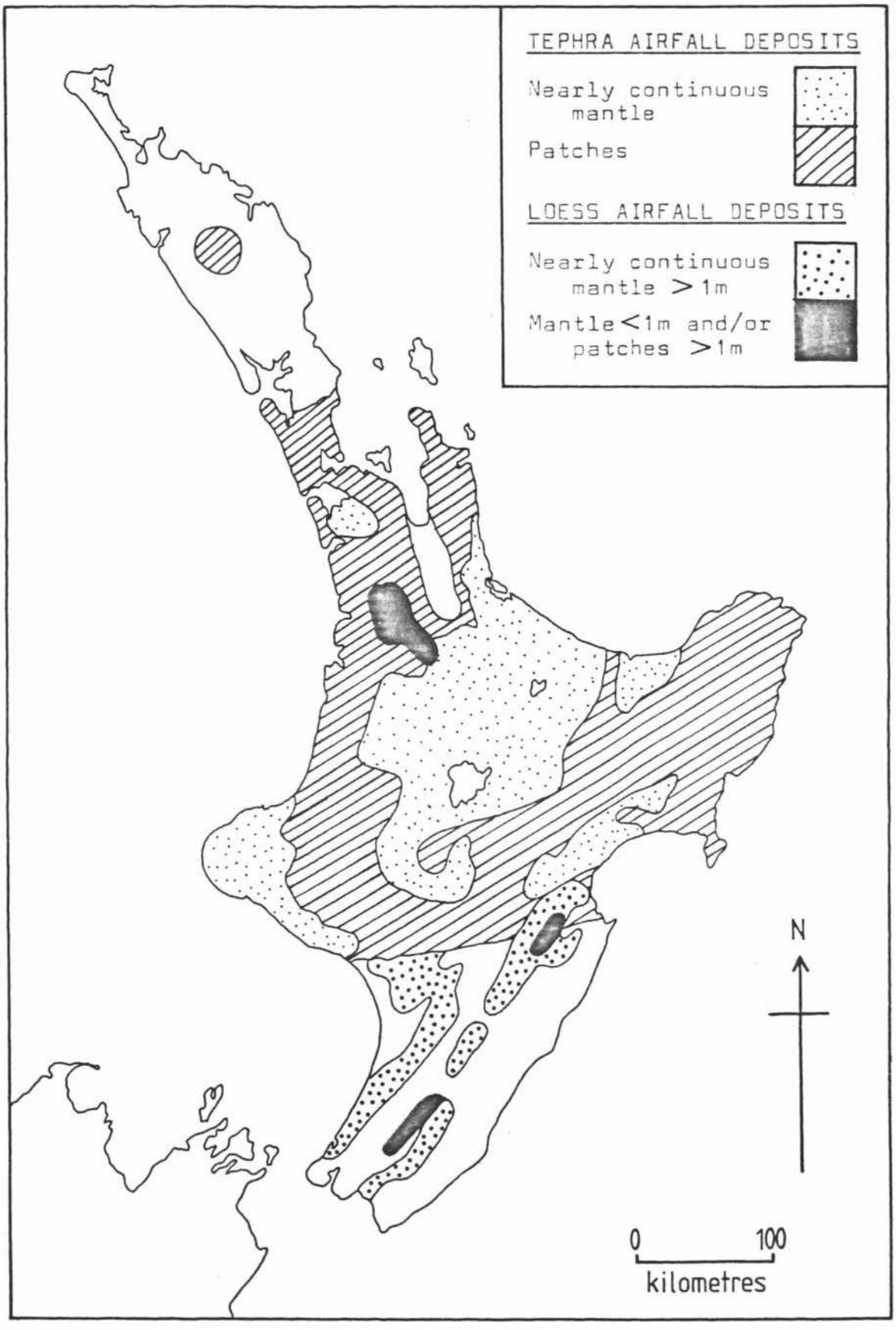

FIGURE 1: Generalised Map of airfall deposits in North Island, New Zealand, (from McGraw, 1975).

and between regions. Loess deposits of South Island are dominated by quartz and feldspar of greywacke or schist origin with occasional micaceous minerals and volcanic glass. Volcanic glass content steadily increases northwards until it becomes a dominant constituent in loess of Central North Island (Cowie and Milne, 1973; McGraw, 1975).

2.2 Tephra and loess deposits of Central North Island

The Otiran glaciation occurred between c.80,000 - 14,000 years B.P. (Cowie and Milne, 1973). In Central North Island, during later stages of this event, considerable loess accumulated, with greatest deposition in colder periods (stadials) when vegetation was minimal (Kennedy, 1980). Intermittent additions of volcanic material are revealed by stratigraphic sequences of alternating tephric and loessial deposits (Vucetich and Pullar, 1969). The dates of eruption of several of these tephras are known and have proved to be of considerable assistance to dating of loess deposits. Furthermore, sedimentary sequences recording stadial periods within Otiran Glacial at Kumara, West Coast (Suggate and Moar, 1970) have been correlated to events occurring in Central North Island (Vucetich and Pullar, 1969) (Table 1)

Greatest loess accumulation in Central North Island is associated with late Pleistocene tephras, including Okareka Ash c.17,000 years B.P., Te Rere Ash c.19,000 years B.P., Kawakawa Tephra 19,850 $\pm$ 310 years B.P., and Rotoehu Ash (NZ1126 41,700 $\pm$ 3500 years B.P.) (Kennedy and Pullar, 1977). Loessial deposits are also associated with Poihipi Tephra c.20,500 years B.P., Okaia Tephra c.25,000 years B.P. and Tahuna Tephra c.36,000 years B.P., and are thought to occur within Hamilton Ash Formation c.120,000 years B.P. and between much older formations associated with Pahoia Tuffs c.200,000 years B.P. (Kennedy, 1980). Poihipi Tephra, Kawakawa Tephra and Te Rere Ash, together with associated loess and sand dune

EPOCH	STAGE	YEARS (10^3) B.P.	TEPHRA STRATIGRAPHY	NORTH WESTLAND GLACIALS
HOLOCENE	ARANUIAN			
PLEISTOCENE (14,000 - 2×10^6 years B.P.)	OTIRAN (14,000 - 70,000 years B.P.)	14.7	Rerewhakaaitu	KUMARA-3
		17.0	Okareka	
		19.0	Te Rere	KUMARA-2_2
		19.8	Kawakawa	
		20.5	Poihipi	
		25.0	Okaia	
		35.0	Tahuna	
		42.0	Rotoehu	

TABLE 1: Correlation of late Pleistocene tephra deposits in Central North Island, with North Westland glacial advances (adapted from Fleming, 1975; McGraw, 1975).

deposits were deposited during a stadial corresponding to Kumara-2_2 glacial advance c.24,000 - 18,000 years B.P. (Vucetich and Pullar, 1969). During this period, paleosols associated with tephras are found to be rare or absent, and root channels indicate that more robust vegetation (sedges and grasses) was present. Furthermore, sand dunes are found overlying Te Rere Ash which suggests that this period, especially c.19,000 - 17,000 years B.P., was colder and more arid than in preceding periods (Kennedy, 1980). However, cool, semi-arid conditions appear to have continued in Central North Island beyond the time of the glacial advance recorded at Kumara, as loess deposits are found overlying Okareka Ash c.17,000 years B.P. (Kennedy, 1980). The absence of loess associated with tephras younger than Okareka Ash tends to imply progressive warming from c.15,000 years B.P. (Kennedy, 1980). However, on the West Coast, a further advance, Kumara-3 is suggested between c.16,000 - 14,000 years B.P. (Suggate and Moar, 1970), coinciding with deposition of Rerewhakaaitu Ash 14,700 $\pm$ 200 years B.P. (Vucetich and Pullar, 1969).

In Central North Island, deposits of aeolian origin were first recognised by Pullar (1967), and later found to be closely associated with underlying tephra beds (Vucetich, 1968; Vucetich and Pullar, 1969). The material was described by Vucetich and Pullar (1969) as "almost homogeneous unbedded deposits of medium and fine sand composed of subangular pumice and glass particles". Distribution was found to be localised, with deposits easily mistaken for shower-bedded ash (Vucetich and Pullar, 1969). Field studies revealed that loess deposits of Central North Island are composed largely of reworked tephra, probably derived from underlying airfall tephra by processes of erosion and deposition, and were termed 'tephric loess' by Pullar and Pollok (1973). It has been suggested that in cooler periods when the ignimbrite sheets of Central North Island resembled cold mini-deserts, aeolian material was blown along narrow valleys and gulches

by prevailing northwesterly winds (Pullar and Kennedy, 1977). Loess was distributed on steep valley sides, interfluves, and broad upland surfaces in Rotorua and Taupo areas (Pullar and Birrell, 1973b; Cowie and Milne, 1973).

In Taranaki, studies of andesitic tephras by Neall (1975) established an aeolian origin for deposits composed largely of redeposited tephric material. These deposits were distinguished from interbedded proximal airfall and airflow tephra on the basis of weak stratification in deposits. Stewart et al. (1977) identified a 'tephric loess' bed in Taranaki with 70% andesitic component and 30% interregional quartz component. During the last glacial period, sea level was lower than at present,and as a result a land bridge became exposed between Nelson and Taranaki (Lewis and Eade, 1974). Material of metamorphic-plutonic origin removed from the exposed land bridge is suggested as source of the loess component (Stewart et al. 1977).

Mineralogically and morphologically, deposits of tephric loess in Central NorthIsland closely resemble the tephra from which they are derived but lack the distinctive paleosols and basal layers typical of tephras (Pullar and Birrell, 1973 a & b). Work by Pullar and Birrell (1973a), Birrell (1974), and Kennedy (1980) revealed that subtle differences in colour, texture and consistency occur between tephra and tephric loess. However, at some sites these differences were found to be inconclusive (Birrell, 1974). Furthermore, laboratory data (clay %, organic C, Tamms extractable Al + Fe, dry bulk density and total porosity) showed only slight differences (Pullar and Birrell, 1973a; Birrell, 1974). It is possible to distinguish between loess and underlying tephra deposits when the two deposits are derived from a chemically and mineralogically different provenance (i.e. Neall, 1975; Stewart et al. 1977). However, in Central North Island, differentiation of the two types of deposit becomes difficult where tephras become indistinct or thinly

bedded with distance from source, and where post-depositional pedogenic processes are increasingly involved (Lowe, 1981). Nevertheless, discrimination between tephra and overlying tephric loess should provide insight into climatic and geological relationships that occurred in late Quaternary times (Kennedy, 1980).

2.3 Okareka Ash and overlying loess deposits

The most extensive loess deposits occur overlying Okareka Ash and Kawakawa Tephra (Pullar and Birrell, 1973b), and both tephras are widespread throughout Rotorua and Taupo districts. However, the younger age of Okareka Ash, and hence its greater accessibility in road sections, make this tephra more suitable for study.

Okareka Ash was first recognised by Vucetich and Pullar (1969) as a tephra formation unconformably underlying Rerewhakaaitu Ash c.14,700 $\pm$ 200 years B.P. and overlying the "buried soil of Te Rere Ash" c.19,000 years B.P. Previous work had tentatively named the more weakly weathered Okareka and Te Rere Ash beds overlying Hinuera Formation as 'Tirau Ash' (Thompson, 1958). However, studies by Vucetich and Pullar (1963, 1964 and 1969), clearly identified several late Pleistocene tephras within this one deposit. Each of the beds described by Vucetich and Pullar (1969), particularly Okareka Ash and Te Rere Ash, were found to have associated loess deposits which were easily confused with their underlying tephra bed.

Okareka Ash is a biotite-bearing rhyolitic tephra which has its source near Mt. Tarawera (Vucetich and Pullar, 1969). Its distribution is strongly influenced by the prevailing westerly wind (Figure 2). Changes in direction of the wind and the eruption are indicated by a multi-lobate isopach distribution pattern (Pullar and Birrell, 1973b). Okareka Ash distribution extends from Waikato to western areas of East Cape, northwards to Bay of Plenty coast and south as far as Taupo. The

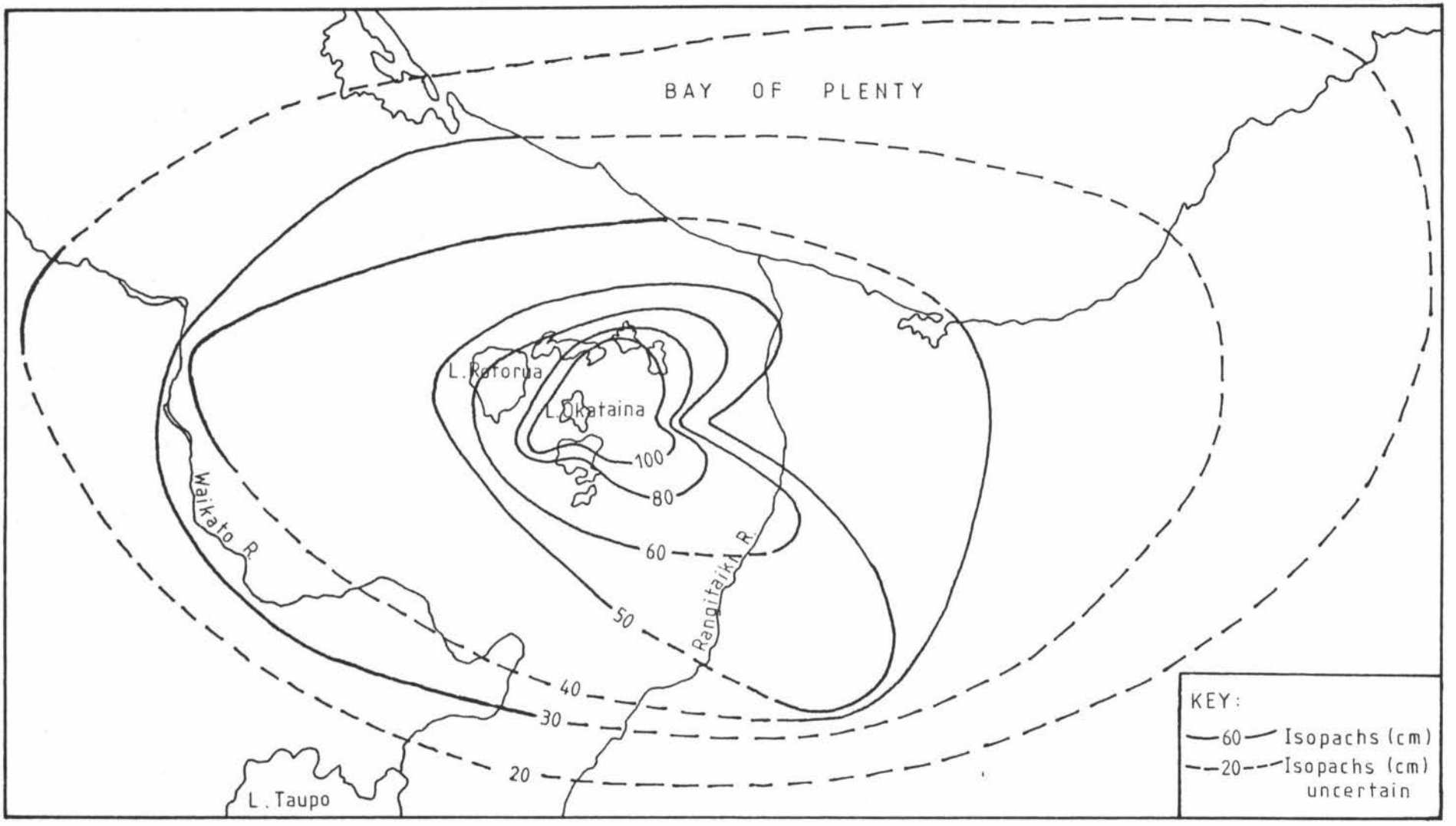

FIGURE 2: Isopachs showing distribution of Okareka Ash (from Pullar and Birrell, 1973b).

thickest deposits are localised in Rotorua district, especially downwind from source (Cowie and Milne, 1973). Loess derived from Okareka Ash appears to be widespread in eastern Waikato, and scattered locations of Rotorua and Bay of Plenty regions (Cowie and Milne, 1973). A radiometric age of 20,700 $\pm$ 450 years B.P. for Okareka Ash was recorded by Vucetich and Pullar (1969), but later studies revised this date to an estimate c.17,000 years B.P. (Kennedy and Pullar, 1977).

Thick deposits of Okareka Ash usually exhibit finely laminated shower material grading upwards from a mixture of coarse and fine ash to fine ash. The coarse fraction consists of vesicular pumice, and fine fraction of subangular fragments of shards and plates (Vucetich and Pullar, 1969). There is considerable range in colour of Okareka Ash. In the east it varies from pale yellow to olive while in peripheral areas where the ash is thinner, colour varies from pale yellow-brown to olive-brown (Vucetich and Pullar, 1969).

2.4 Weathering studies of tephra and tephra-derived soils

In Central North Island accumulation of loessial material often extended over many thousands of years. This is in contrast to airfall tephra deposits which were laid down in a much shorter length of time. The longer depositional interval of the loess has thus allowed post-depositional processes and pedogenesis to occur to a greater extent within tephric loess (Cowie and Milne, 1973).

Weathering pathways in tephra and tephra-derived soils are determined by soil forming factors such as parent material composition, drainage, vegetation, topography, climate, as well as time. To a great extent, variation in these factors also govern the nature of weathering products found in such deposits (Parfitt *et al.* in press). As mineralogical composition of tephra and tephric loess deposits is essentially similar, occurrence of the dominant

weathering product allophane, and smaller amounts of halloysite, imogolite and gibbsite (Pullar and Birrell, 1973a) indicate weathering processes may be broadly similar. It is pertinent, therefore, to review the work which has contributed to our present understanding of the weathering processes which take place in tephra and associated materials.

The occurrence of allophane was first observed in New Zealand soils by Taylor (1933) in a study of weathering processes in volcanic ash-derived soils. During the ensuing twenty-five years field and laboratory evidence gathered by several workers led to description of the properties of allophane, and a realisation of its importance as a principal constituent of clay fractions of tephra and tephra-derived soils.

During the 1950's, Fieldes and co-workers correlated chemical and morphological evidence of short-range order materials in volcanic ash soils, which resulted in the first attempted characterisation of allophane in New Zealand soils. They proposed a weathering sequence for clays derived from glass and feldspar constituents in rhyolitic and andesitic ashes:

(Fieldes, 1955)

Fieldes (1955) demonstrated the presence of discrete amorphous silica, which he termed allophane B, at an early stage of tephra weathering. Allophane B was identified by a 800cm^{-1} absorption band on IR spectra, with no high temperature exothermic peak on differential thermal curves. Whereas allophane B was common in young ash-derived soils, allophane A, which exhibited an endothermic peak at about 150^{o}C, an exotherm at about 900^{o}C on differential thermal curves, and no absorption

at 800cm^{-1} on IR spectra, was common in older soils.

In Japan, despite early recognition of short-range order constituents in volcanic ash soils by Seki (1913), mineralogical examination to establish the presence of allophane was not made until the early 1950's. Studies by Sudo (1953, 1954), Aomine and Yoshinaga (1955), and many other workers demonstrated that allophane is a dominant constituent of volcanic ash soils, sometimes associated with minor amounts of kaolinite, halloysite, gibbsite and 14Å clay minerals (Nagasawa, 1978). Identification by X-ray diffraction and differential thermal methods classified the allophane as Fieldes' allophane A (1955). However, studies of fine fractions (< 0.2μm) of certain young Japanese ash-derived soils by Miyauchi and Aomine (1964) revealed no 900°C exothermic peak on thermal curves, yet a strong 800cm^{-1} absorption band on IR spectra was observed, which they attributed to cristobalite. This work, together with later studies, led Japanese workers to the conclusion that allophane B does not exist in Japanese soils.

Improvements in instrumental techniques during the 1960's greatly facilitated study of allophane and its formation in soils. Of major importance were developments in electron microscopy which advanced morphological studies of clay particles, in particular allophane and associated clay minerals. Early studies (e.g. Birrell and Fieldes, 1952; Aomine and Yoshinaga, 1955) suggested allophane consisted of aggregates of very fine particles, showed no external regularity, and were almost beyond the resolution of the electron microscope. However, improved instrumentation allowed Kitigawa (1971), and Henmi and Wada (1976) to postulate that the structural unit of allophane is a hollow spherical particle of about 55Å external diameter.

Recent advances in characterisation of short-range order and poorly-crystalline minerals included investigation of imogolite. This mineral was first described by Yoshinaga and Aomine (1962b) as a hydrous

alumino-silicate possessing long-range order with physical and chemical properties similar to allophane. Electron microscopy has shown it to possess a thread-like morphology in contrast to globular particles of allophane (Wada, 1978). Imogolite was identified in New Zealand volcanic ash soils by Yoshinaga et al. (1973). It was found to be closely associated with allophane, and sometimes with gibbsite. Initially, it was seen as a possible intermediate weathering product between allophane and halloysite (Masui et al. 1966), but work by Farmer and coworkers (1977, 1978, 1979) demonstrated that it forms from solution and can be synthesised in the laboratory.

The occurrence of halloysite as a weathering product of volcanic glass or feldspar was suggested in the sequence proposed by Fieldes (1955). Whereas allophane was found to occur in young ash soils, clays of older ash soils were dominated by metahalloysite. Subsequent extensive study of Japanese volcanic ash soils under temperate humid conditions enabled workers to propose a weathering sequence which tended to confirm the earlier suggestions by Fieldes (1955).

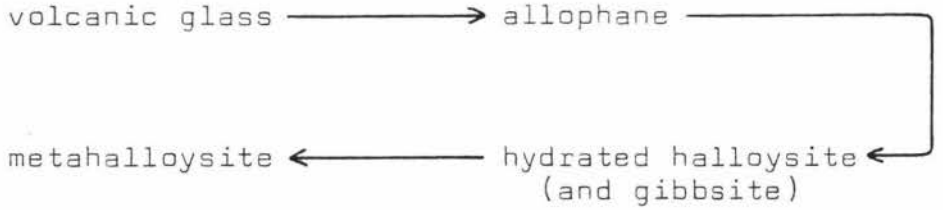

(Aomine and Wada, 1962)

In both New Zealand and Japan, however, these studies had assumed that chemical weathering of volcanic materials increases with depth, thus constituting a measure of weathering time since deposition (Aomine and Wada, 1962). Differential weathering studies of halloysite and allophane by Aomine and Wada (1962) showed such an assumption might be correct only at a megascopic level and that other factors overshadow its effect. Their work suggested transition from allophane to hydrated halloysite in volcanic ash soils proceeds via

intermediates and is a continuous process largely determined by local variations in leaching activity associated with some biotic effects.

Since the study by Aomine and Wada (1962), much work on halloysite morphology and formation in soils has been carried out in New Zealand and Japan. Electron optical work reveals halloysite assumes several morphological forms dependent upon the mode of formation. Whereas squat cylinders or ellipsoids derived by a possible spiral mechanism (Kirkman, 1977) are typical of halloysite weathered from allophane, halloysite formed from feldspar assumes a curled flake or tubular morphology (Kirkman, 1975; Sudo and Yotsumoto, 1977; Saigusa et al. 1978).

Much evidence against differentiation of allophane into separate and distinct A, AB or B forms, its transformation to metahalloysite, and eventual weathering to kaolinite, as suggested by Fieldes (1955) was adduced during the late 1960's and early 1970's. Furthermore, reinvestigation by Fieldes and Furkert (1966) of soils studied in 1955 tended to confirm the view held by Japanese workers that allophane B did not exist. Several studies, including Campbell et al. (1968) established that the high temperature exothermic peak is dependent upon pH, carbon content and particle size, and therefore, can not be used to identify allophane B. Furthermore, Kirkman (1975) showed that the 800cm^{-1} absorption band attributed to allophane B can be ascribed to volcanic glass, as well as to cristobalite (Miyauchi and Aomine, 1964). In a study of Central North Island rhyolitic tephras, Kirkman (1975), revealed hydrated halloysite is the normal halloysite component of tephras and tephra-derived soils, and forms metahalloysite only when dried at temperatures as low as 50^{o}C in the laboratory under conditions of low humidity. During extensive study, Kirkman (1978) found no evidence of halloysite altering to kaolinite in New Zealand soils and tephras. This conclusion is not stated, but was implicit in the later work of

Fieldes and his coworkers (i.e. Fieldes and Furkert, 1966). By the early 1970's it was generally concluded by most workers in Japan, New Zealand and the USA that allophanes show wide variation in composition morphology, structure and reactivities, and it is these features, together with pedogenic conditions, which determine its course in the weathering environment.

Recent studies have resulted in the definition: "Allophane exists as a series of naturally occurring hydrous aluminosilicate clays" (Wada, 1977), "which includes materials of Al/Si ratios extending from 1.0 to 2.5" (Parfitt et al. 1980). Investigations in New Zealand show that much allophane has an Al/Si = 2, and a structure similar to that of imogolite. The term proto-imogolite allophane was suggested by Parfitt and Henmi (1980) to describe this material. Evidence suggests that Al-rich allophane, with proto-imogolite structure and Al/Si = 2 occurs in andesitic tephra and tephra-derived soils, and that it does not usually alter to halloysite. In contrast to andesitic allophane, allophane formed from rhyolitic material is silica-rich, with Al/Si = 1, and possesses a highly condensed structure (Parfitt et al. in press). The structure, chemical composition, and bonding characteristics of rhyolitic glass persists in the allophane to which it weathers, and is appropriate for eventual formation of halloysite (Kirkman and McHardy, 1980).

At present, weathering sequences postulated for rhyolitic and andesitic tephras are as follows:

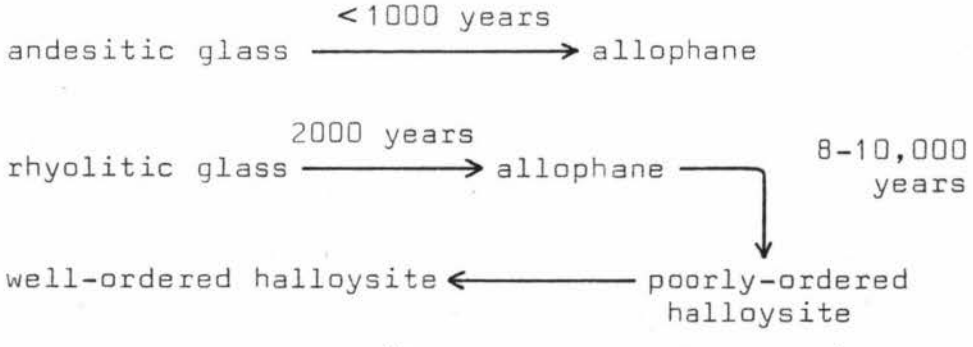

(Parfitt et al. in press)

Recent studies by Japanese and New Zealand workers suggest that the overall determining factor governing halloysite formation in soils is the equilibrium level of silica in solution. Furthermore, New Zealand studies confirm earlier conclusions of Aomine and Wada (1962), which suggested the rate of formation of crystalline clay minerals is affected by the intensity of pedological processes such as leaching and biotic aspects (Kirkman, 1980; Parfitt et al. 1980). Studies of Central North Island rhyolitic tephras have shown that allophane levels increased, and halloysite levels decreased, as rainfall increases from 1200 to 2000mm per annum (Birrell et al. 1977; Parfitt et al. 1980). Intense leaching of silica from rhyolitic tephra tends to perpetuate allophane and depress halloysite formation and this was attributed to lower levels of polymeric silica in solution (Parfitt et al. in press).

Chapter 3: MATERIALS AND METHODS

3.1. Field Techniques

To relate grain-size and mineralogical characteristics of ash and tephric loess deposits, this study was restricted to an investigation of sections in a transect upwind (prevailing wind; westerly to north-westerly) from Okareka Ash source, westwards across the Mamaku Plateau (Figure 3). Sites were selected where Okareka Ash bed thickness ensured accurate field recognition and the least possibility of contamination from underlying or overlying deposits. Changes in altitude, overburden depth and topography occur but all sections are free-draining.

Sections examined are located at eight sites on a transect commencing at a quarry near Lake Okareka and ending on the western side of the Mamaku Plateau 32 kilometres west of Rotorua (Figure 3). Tephra stratigraphy on this transect, shown in Figure 4, is already well established (Pullar and Birrell, 1973a). All sites, except Okareka Quarry and Lynmore, are located in road-side sections which facilitate accessibility and examination. Three additional sections, not on the above transect were also sampled. These include two well-documented sections; Gavin Rd (Pullar and Birrell, 1973b) and Te Ngae section (Soil Bureau, 1978), and a section located on Trunk Rd where Okareka Ash occurs at a thickness of 1.40 metres. Stratigraphy of these three sites is given in Figure 5. In all sections, Okareka Ash and overlying loess deposits immediately underlie Rerewhakaaitu Ash, and overlie Post-Te Rere or Post-Kawakawa loess deposits.

At Trunk Road, it is evident that the Okareka Ash eruption comprised multiple pulses of tephric material (Appendix 1A and 1B). The section shows laminated bedding of shower material ranging from coarse lapilli to fine sandy ash. The upper 1.10 metres of ash is dominated by rhyolitic material, pale yellow-grey in colour, although variations often occur between laminae

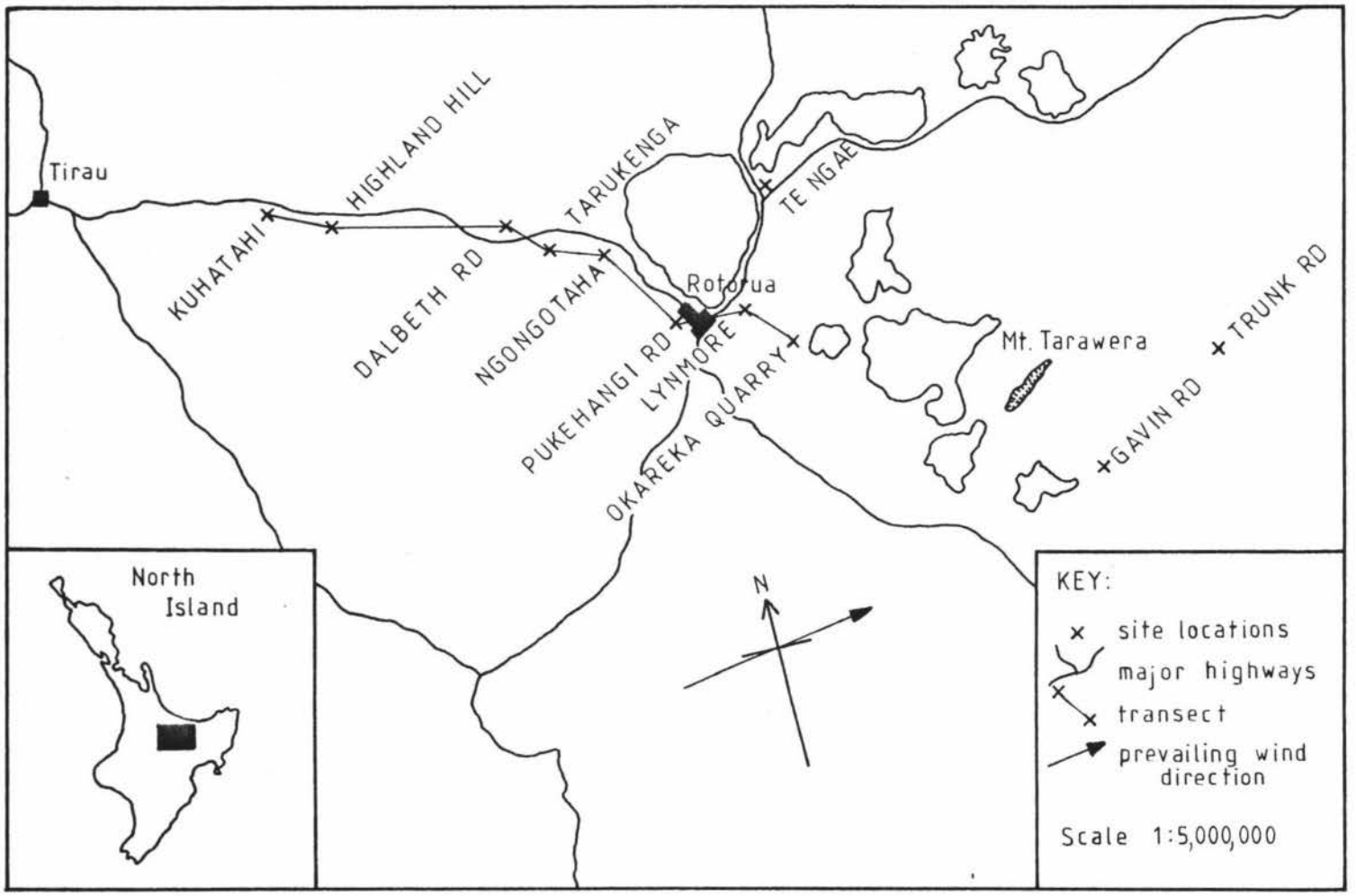

FIGURE 3 : Site locations, Rotorua district, Central North Island.

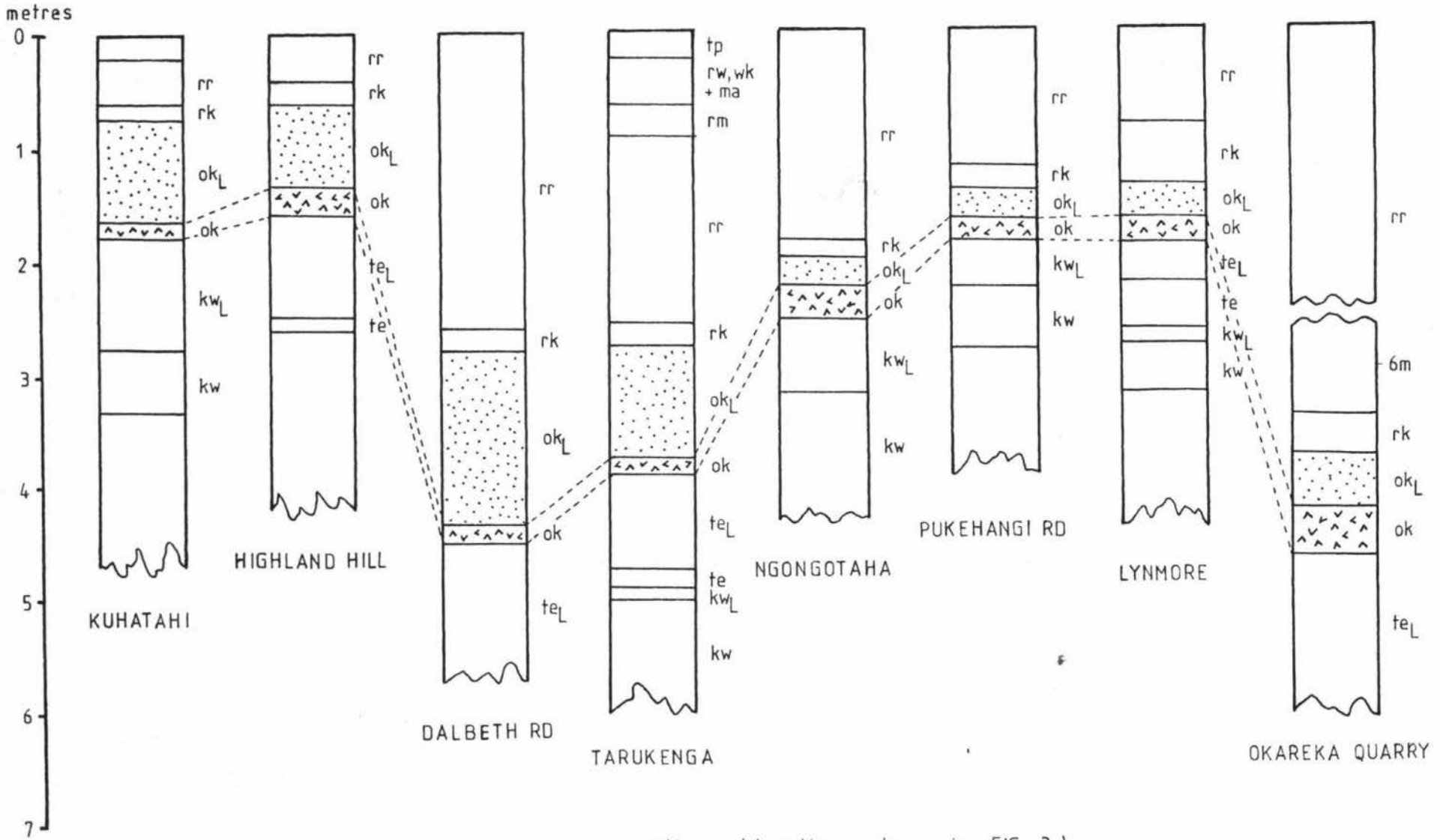

FIGURE 4: Stratigraphy of transect sections (Locations shown in FIG. 3)
Legend overleaf FIG. 5.

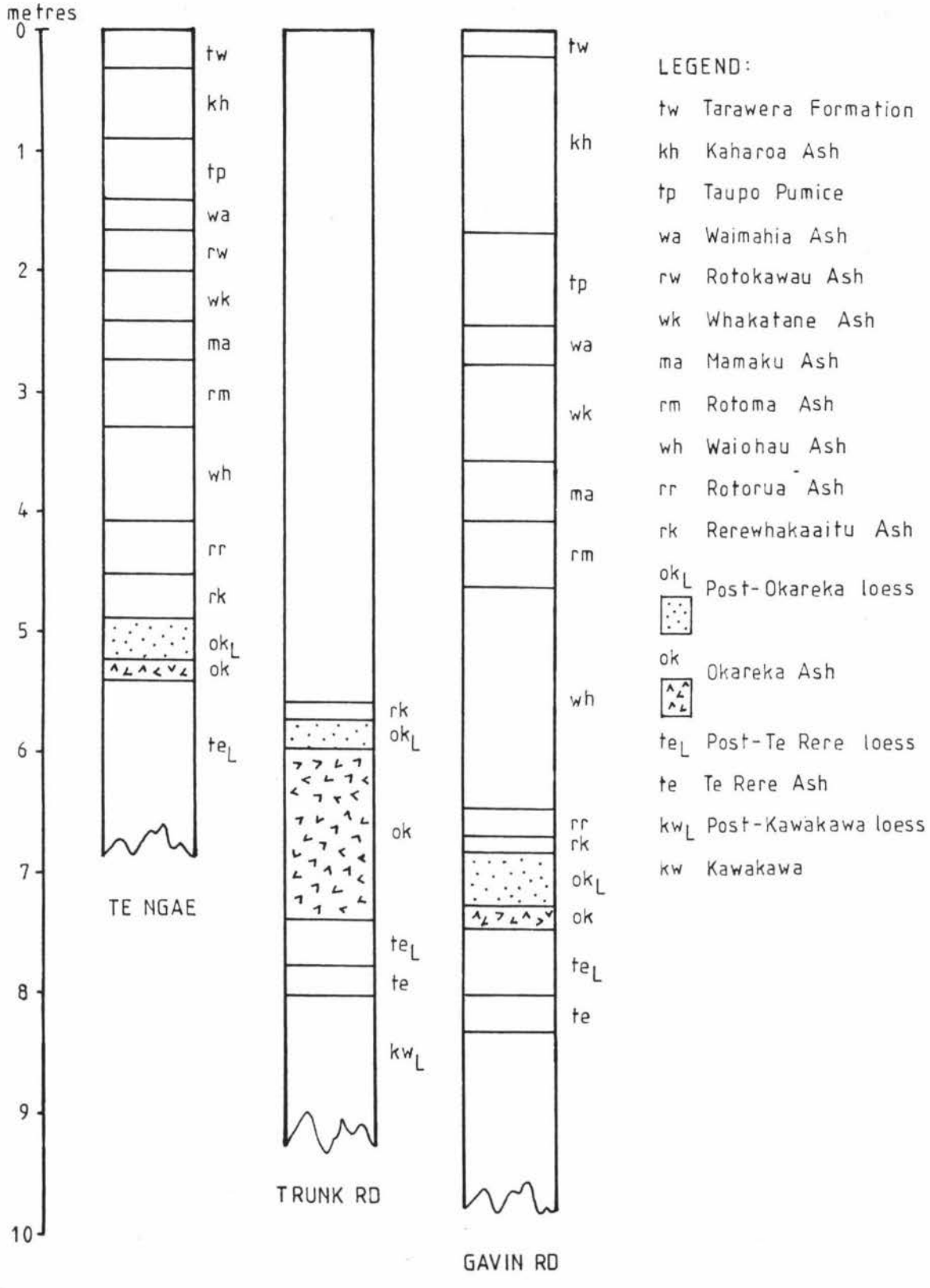

FIGURE 5: Stratigraphy of Te Ngae, Trunk Rd and Gavin Rd sections (Locations shown in FIG. 3).

due to staining by iron and possibly manganese. Five samples were taken from this upper part of Okareka Ash, and a further two samples taken from the basal 20-30cm of the section (Appendix 1B). The lower layers of ash at Trunk Rd are darker coloured with evidence of lithic fragments of more mafic composition than upper beds (Figure 6B).

At all sections, other than Trunk Rd, Okareka Ash beds were channel sampled, vertically, but due to the greater thickness of Post-Okareka loess, samples were taken at intervals determined by thickness of the bed. Soil samples were stored in polythene bags to maintain field moisture levels.

3.2 Instrumental Techniques

A 50g aliquot of field moist soil was suspended in distilled water, made alkaline to pH 10 with 1:1 NH_4OH, dispersed ultrasonically for two minutes (20kHz), and then wet sieved at 63μm. The >63μm fraction was dried at 55°C and then dry sieved at 500μm, 250μm, 125μm and 63μm grain-size intervals. The <63μm material was split into silt (63-1μm) and clay (<1μm) fractions by centrifugation. Normal laboratory procedure requires drying of soil samples at 105°C; however, to avoid changes in clays such as halloysite, and heavy caking of samples, throughout analytical work all fractions were dried at 55°C for a period of 2-3 days. Clay, silt and sand fractions received no further pretreatment prior to instrumental analyses.

The sand (250-63μm) and silt (63-1μm) fractions were lightly crushed, then scanned from 8° 2θ to 60° 2θ using a Co anode in a Philips (PW 1011) 2Kw X-ray diffractometer. To prevent possible dehydration and collapse of the halloysite component of clay fractions, aliquots of the <1μm suspension were placed on a glass slide and dried to a moist paste, prior to X-radiation. The clay pastes were scanned through 5° 2θ to 45°2θ, dried at 60°C, and then the scan repeated.

Infra-red spectroscopy (IR) and differential thermal analysis (DTA) determinations were made on aliquots of the clay ($< 1\mu m$) suspension after drying at $60^{o}C$ and gentle crushing to a fine powder. For IR analysis, potassium bromide discs were made by mixing 1mg of clay with 170mg potassium bromide. The discs were dried overnight at $60^{o}C$ then scanned through the 4000 to $200cm^{-1}$ region using a Pye Unicam SP3 - 200 infra-red spectrophotometer.

Differential thermal analyses were made on clays equilibriated at 56% relative humidity for 3 days. Thermal curves were obtained using 10mg aliquots of clay heated to $1000^{o}C$ at a heating rate of $10^{o}C$ / minute in a nitrogen atmosphere against an empty reference pan in a Stone (model 500) differential thermal analyser. In this study, use of open pan method for DTA was unable to differentiate between halloysitic and allophanic components by means of dehydration peaks at 80 - $90^{o}C$ and 120 - $130^{o}C$ respectively. This is reflected in all thermal curves which show a single dehydration peak between 50 - $80^{o}C$ for both minerals.

For electron optical studies specimens were prepared after suitable dilution of a $<1\mu m$ clay suspension and dispersion by sonication. One drop of the diluted suspension was placed on a carbon film supported by a 3mm copper grid and dried at $60^{o}C$. Morphological studies of clay fractions were made using a Phillips EM - 300 transmission electron microscope (TEM).

Scanning electron microscope studies were made on individual mineral grains handpicked from 500-63μm grain-size fractions under a light microscope, and then examined under polarizing conditions to ensure accurate mineral identification. Mineral and glass fragments of two selected grain size fractions (250 - 125μm and 63 - 20μm) were also investigated by scanning electron microscopy. Samples were mounted on aluminium stubs with silver conducting paint, sputter-coated with gold, and examined with a Quikscan / 100 field emission

scanning electron microscope (SEM).

Optical analysis included mineral identification and morphology studies of grain size fractions 250 - 125μm , 125 - 63μm and 63 - 20μm. Grains were mounted in Canada Balsam (RI 1.537), and grain counts obtained using a Nikon polarizing microscope and swift point counter. Grain counts of light and heavy minerals were also made of grain size fractions 250 - 125μm and 125 - 63μm after separation in bromoform.

Chapter 4: RESULTS

4.1. Sand and Silt Mineralogy

4.1.1 Okareka Ash Formation: Trunk Rd

In the present study, Okareka Ash Formation at Trunk Rd site, which occurs at a thickness of 1.40m was used as type section for mineralogical analysis. (Profile description - Appendix 6A and 6B). X-ray diffraction patterns of fine sand (63 - 250μm) and silt (1 - 63μm) fractions from the upper five ash layers at Trunk Rd indicate mineralogical composition comprises predominantly noncrystalline material, identified optically as rhyolitic volcanic glass. Crystalline minerals, present in Okareka Ash, consist of quartz, plagioclase feldspar (An 10 - 30%; oligoclase), and biotite in minor amounts, together with traces of cristobalite and alkali feldspar. X-ray diffraction analyses are confirmed by optical studies, which show a much greater abundance of vesicular glass particles than crystalline minerals (Table 2), together with a mafic mineral assemblage comprising hypersthene, hornblende, and a trace amount of titanomagnetite.

Although X-ray patterns and optical studies of basal Okareka Ash beds B_{AL} and B_{L} indicate that their sand and silt mineralogy is essentially similar to the overlying ash layers, total grain counts reveal volcanic glass and augite is in higher proportions in these lower layers (Table 2). In contrast to upper ash layers, volcanic glass comprises obsidian (brown volcanic glass), pumiceous particles with darkly coloured inclusions, and some transparent glass shards.

4.1.2 Okareka Ash: remaining sections

Okareka Ash deposits at sections other than Trunk Rd occur at thicknesses of 15 - 30cm (Figure 4). Close to source, at Okareka Quarry and Lynmore sections, Okareka Ash beds comprise shower-bedded lapilli and fine ash, while remaining sections are primarily of ash grade

63-125μm		VG	Qz	Fds	Bt	Opx	Cpx	Hb	FeO
Paleosol	P_T	68	9	14	<1	2	-	1	5
Loess	L_1	69	6	15	<1	5	-	1	4
	L_2	64	6	17	1	5	-	2	6
Ash									
ash/lapilli	R_{AL}	74	14	5	1	2	-	2	2
f/lapilli	R_{FL}	66	14	7	1	6	-	4	3
lapilli	R_L	-	-	-	-	-	-	-	-
ash	R_A	79	10	5	<1	2	-	2	2
c/lapilli	R_{CL}	-	-	-	-	-	-	-	-
ash/lapilli	B_{AL}	86	2	3	<1	2	2	1	3
lapilli	B_L	74	4	8	<1	4	2	1	5

125-250μm		VG	Qz	Fds	Bt	Opx	Cpx	Hb	FeO
Paleosol	P_T	53	10	20	<1	6	-	2	7
Loess	L_1	54	10	25	<1	3	-	1	7
	L_2	55	9	24	1	3	-	4	5
Ash									
	R_{AL}	74	13	6	1	2	-	1	3
	R_{FL}	60	21	9	1	4	-	2	4
	R_L	-	-	-	-	-	-	-	-
	R_A	65	18	10	<1	2	-	1	3
	R_{CL}	-	-	-	-	-	-	-	-
	B_{AL}	86	4	2	<1	3	1	1	3
	B_L	77	4	5	-	8	2	2	3

TABLE 2: Frequency of mineral species (percent) in the very fine sand (63 - 125μm) and fine sand (125 - 250μm) fractions from selected beds in Okareka Ash Formation, Trunk Rd section.

material.

X-ray diffraction and optical analyses (Total grain counts - Appendix 1) of sand and silt fractions indicate that mineralogical composition is similar to the Okareka Ash samples from Trunk Rd section. However, trace amounts of tridymite, high cristobalite and biotite-vermiculite are shown by XRD to occur in most ash beds. In silt (63 - 1/μm) fractions of Okareka Ash samples small quantities (≤5%) of halloysite are usually present, and gibbsite occurs in trace amount in silt fractions from ash samples at Lynmore, Ngongotaha, Dalbeth Rd and Highland Hill sections.

4.1.3 Post-Okareka Loess

Post-Okareka loess beds vary in thickness from 15cm at Trunk Rd section to 1.50m at Dalbeth Rd section (Figures 4 and 5). In the field, loess deposits have a silt loam to silty-clay texture, with massive structure, and often contain fine pores, and in most cases iron/manganese pinhead-size concretions. Mixing of lapilli and ash from underlying Okareka Ash with overlying finer loessial material is evident in basal sections of Post-Okareka loess beds.

Mineralogical composition of Post-Okareka loess is shown by XRD and optical studies to be similar to Okareka Ash. Total grain counts reveal sand fractions (63 - 125/μm and 125 - 250/μm) of loess deposits comprise a dominant amount of rhyolitic volcanic glass, including some obsidian, with feldspar (plagioclase and alkali), quartz, biotite, hypersthene, hornblende, titanomagnetite and augite occurring in minor amounts (Appendices 2 and 3). X-ray diffraction analyses indicate that high and/or low forms of cristobalite occur in small amounts in Post-Okareka loess beds at all sections. A trace amount of tridymite is also present in loess samples from Te Ngae, Lynmore, Ngongotaha and Highland Hill sections.

Changes in mineralogy are evident within a loess bed, and with distance along the transect. Whereas biotite

content decreases from lower to upper parts, augite is more common in upper layers of loess beds. Within a loess bed, feldspar and quartz occur in varying amounts, but, feldspar tends to occur in greater amount in upper layers. Feldspar is also present in higher amount in loess samples from Okareka Quarry, Highland Hill and Kuhatahi sections. Total grain counts show the fine sand (125 - 250μm) fractions of all loess samples contain a higher proportion of crystalline minerals, particularly quartz and feldspar, than the very fine sand (63 - 125μm) fraction (Appendices 2 and 3).

Compared with Okareka Ash samples, Post-Okareka loess sand and silt fractions contain greater amounts of feldspar and augite, and lesser amounts of quartz, biotite and titanomagnetite.

4.2 Sand and Silt Morphology

4.2.1 Okareka Ash

Scanning electron microscope and optical studies of Okareka Ash sand (250 - 63μm) and coarse silt (63 - 20μm) fractions reveal grains are generally angular. Volcanic glass particles appear relatively unweathered and shiny (Figure 6A), and comprise predominantly pumiceous fragments, as well as transparent shards. Quartz grains, which often show conchoidal fracture, are angular (Figure 7A) and occasionally of bipyramidal shape (Figure 7B). Albite (multiple) twinning and prismatic crystal habit are distinguishing features of plagioclase feldspar observed in scanning electron micrographs (Figure 6B).

In Okareka Ash beds mafic minerals, hypersthene and hornblende, occur as elongate prisms which often contain inclusions. Hypersthene grains, especially in finer size fractions exhibit surface pitting (Figure 8A), however, hornblende grains remain distinctly angular (Figure 9A). Biotite grains in ash samples are often pseudohexagonal (Figure 10A) while titanomagnetite grains generally

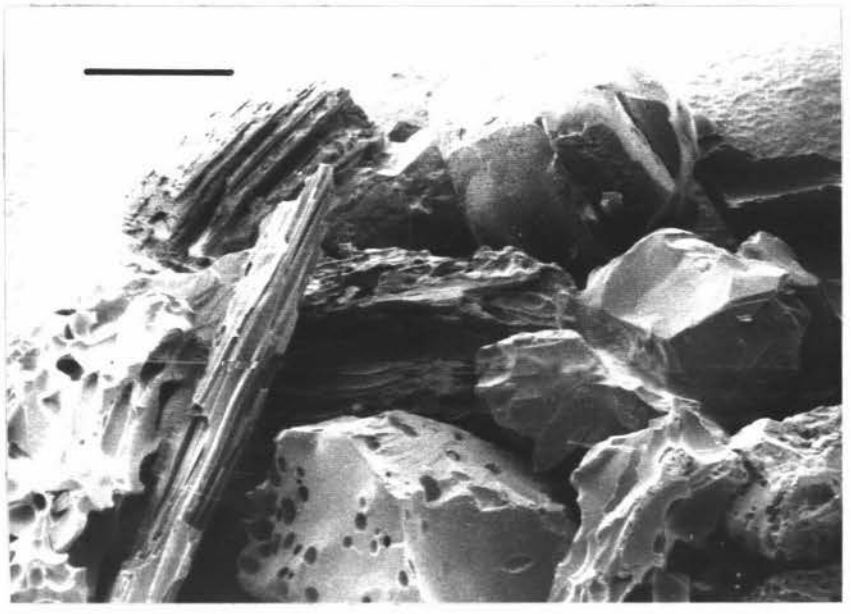

FIGURE 6A: Scanning electron micrograph of rhyolitic volcanic glass particles, separated from Okareka Ash samples (Bar = 500μm).

FIGURE 6B: Scanning electron micrograph of plagioclase feldspar grain exhibiting albite (multiple) twinning, separated from Okareka Ash samples (Bar = 250μm).

FIGURE 7A: Scanning electron micrograph of quartz grains separated from Okareka Ash samples (Bar = 200μm).

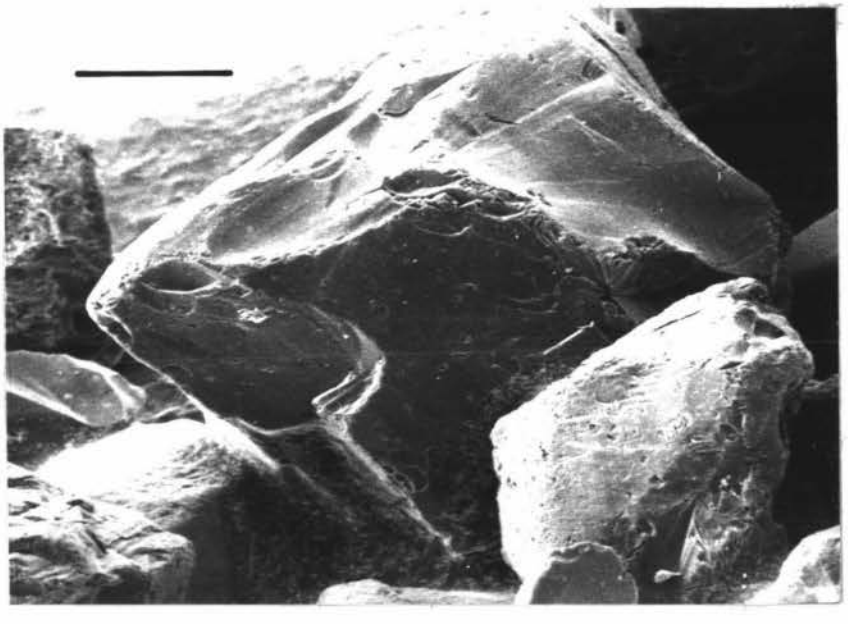

FIGURE 7B: Scanning electron micrograph of bipyramid-shaped quartz grain separated from Okareka Ash samples (Bar = 200μm).

A

B

FIGURE 8: Scanning electron micrographs of hypersthene grains separated from:

A - Okareka Ash (Bar = 100μm)

B - Post-Okareka loess (Bar = 250μm)

Surface pitting, and dissolution along cleavage planes is greater in grains from loess deposits.

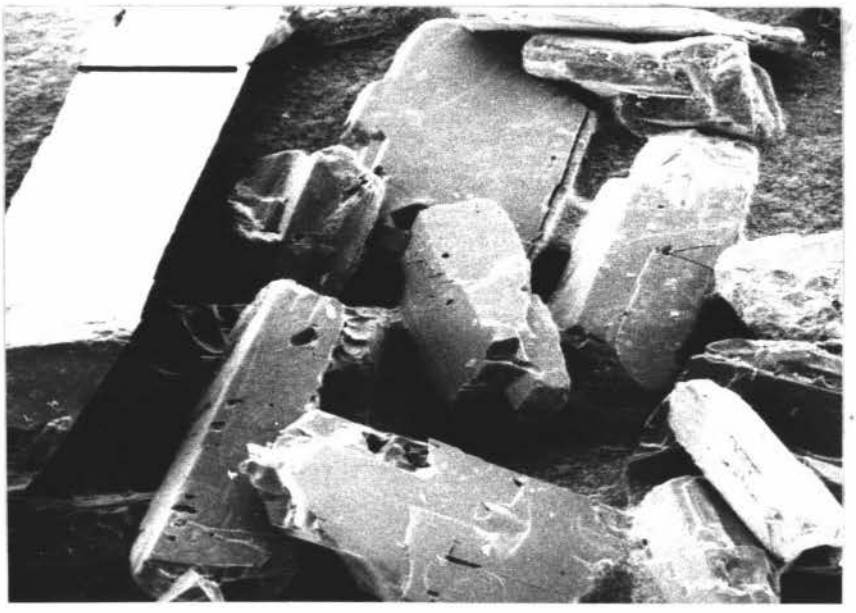

A

B

FIGURE 9: Scanning electron micrographs of hornblende grains separated from:

A - Okareka Ash (Bar = 200 µm)

B - Post-Okareka loess (Bar = 250 m)

Grains in both SEM's show only minimal evidence of weathering.

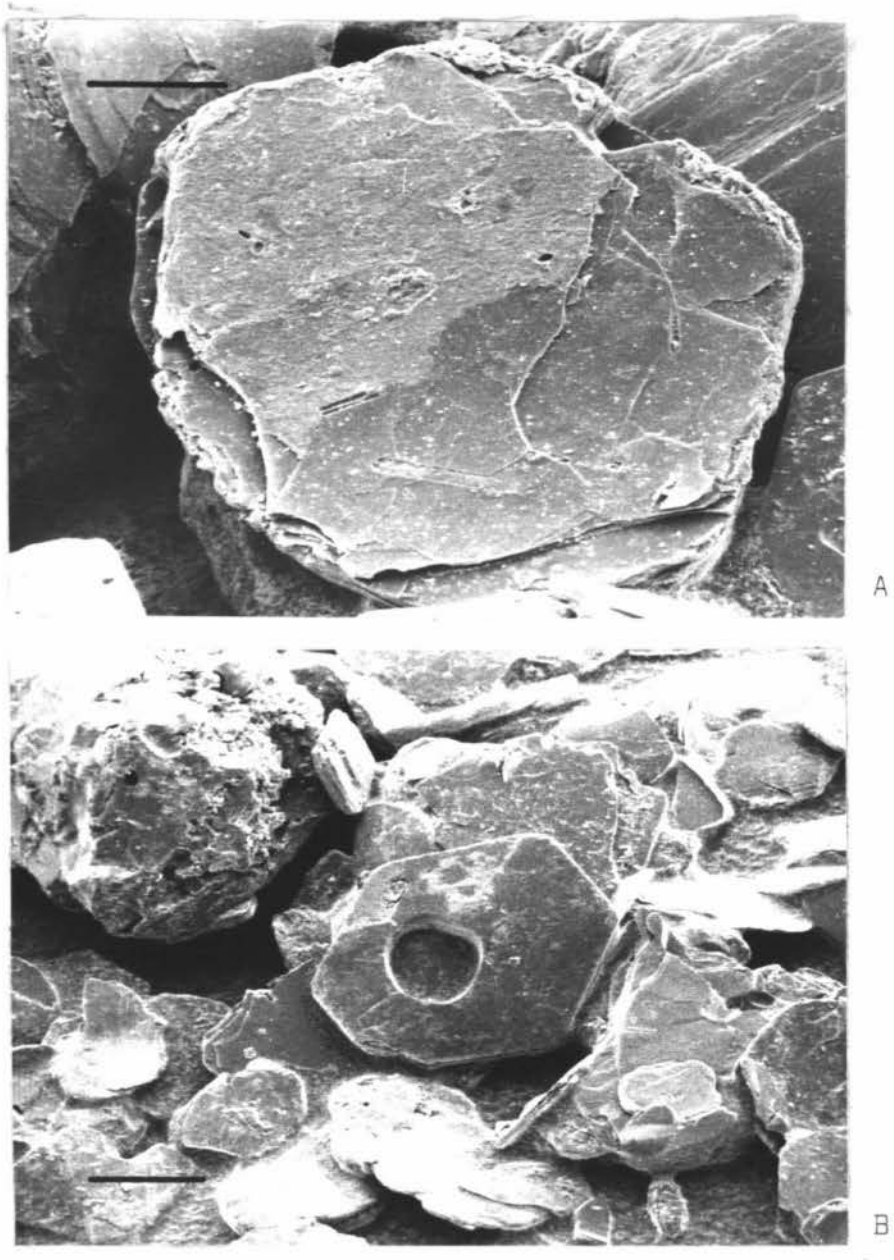

FIGURE 10: Scanning electron micrographs of biotite mica grains separated from:

A - Okareka Ash (Bar = 100μm)

B - Post-Okareka loess (Bar = 300μm)

Dissolution of biotite is greatest along cleavage planes, in both deposits.

assume an irregular cubic shape (Figure 11A). Electron micrographs indicate dissolution of these minerals in Okareka Ash sand and silt fractions occurs along cleavage planes (e.g. hypersthene - Figure 8A; biotite - Figure 10A), twin planes, and at prism edges (e.g. plagioclase feldspar - Figure 6B).

Scanning electron microscope studies reveal some changes in grain morphology occur with distance along the transect (Figure 12). Close to source, ash particles are extremely angular (Figure 12A). However, at the intermediate sections of Tarukenga and Dalbeth Rd, grain shape is tending angular to subangular, and less resistant grains show greater evidence of alteration by weathering (Figure 12B). Furthermost from source, at Highland Hill and Kuhatahi sections, solution of plagioclase feldspar, biotite and hypersthene grains is occurring to a greater extent in Okareka Ash samples (Figure 12C). This is particularly noticeable in finer fractions. Pumiceous particles, with cavities containing fine clay-size material, are evident in electron micrographs of these ash samples (Figure 12C).

4.2.2 Post-Okareka Loess

Electron optical investigation of Post-Okareka loess particles reveal quartz grains in sand and silt fractions are angular, and of similar appearance to quartz grains from ash samples. Plagioclase feldspar grains, particularly in finer fractions are more subangular than those of ash samples (Figure 13), and often exhibit surface coatings of clay-size material (Figures 14A and 14B) or etch marks (Figures 14C and 14D). These etch marks are due to preferential dissolution where a crystal dislocation meets the surface, and represent an initial phase in feldspar weathering (Wilson, 1975).

In Post-Okareka loess samples, hypersthene (Figure 8B) and to a lesser extent hornblende (Figure 9B) show increased alteration compared to those minerals in ash samples. Weathering is generally observed under the

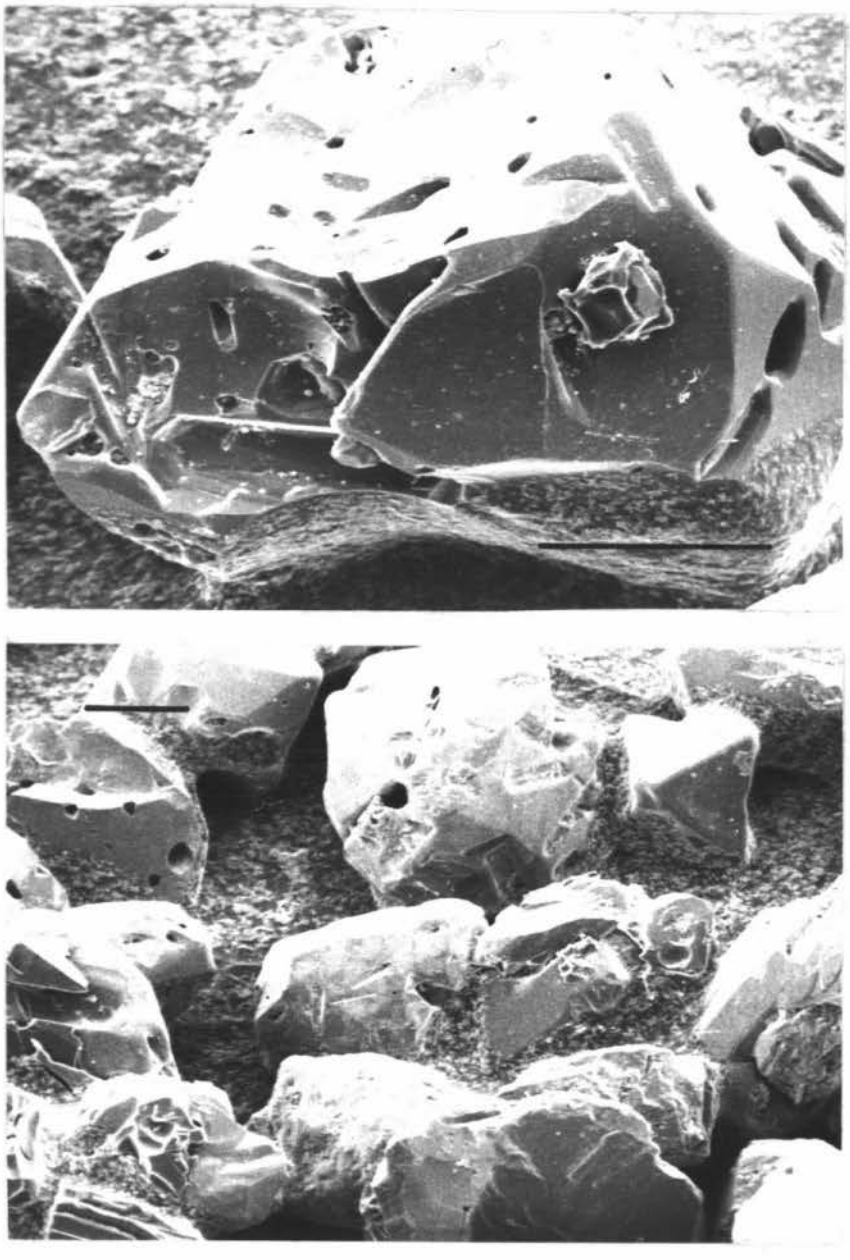

FIGURE 11: Scanning electron micrographs of titanomagnetite grains separated from:

A - Okareka Ash (Bar = 100μm)

B - Post-Okareka loess (Bar = 100μm)

Titanomagnetite grains generally exhibit surface pits which are visible in all grains above.

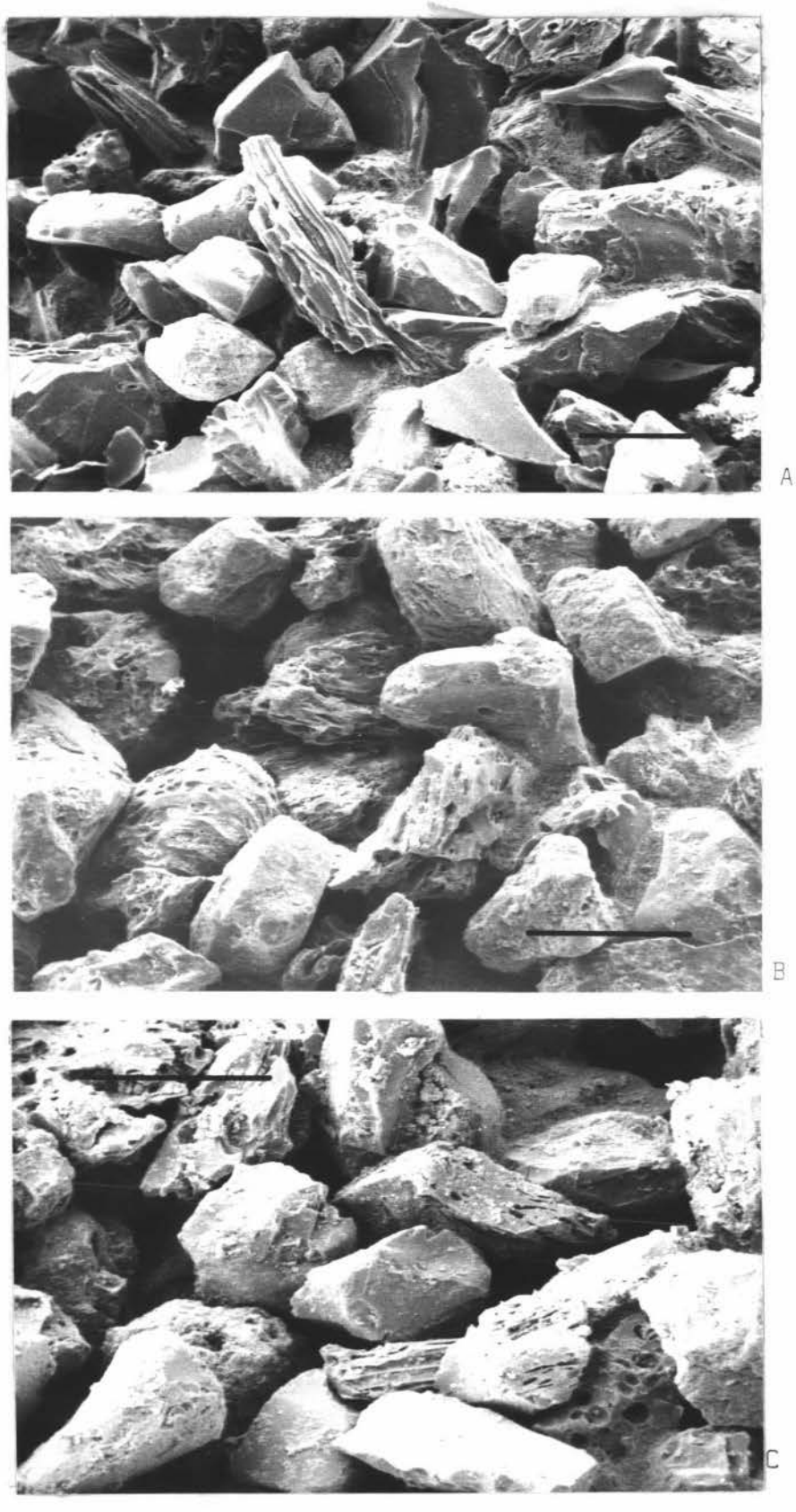

FIGURE 12: Scanning electron micrographs of Okareka Ash particles from sections: A - close (R_{AL}), B - intermediate (CA) and C - furtherest (EA) to ash source (Bars = 200μm). SEM's show decreasing grain angularity with increasing distance from source.

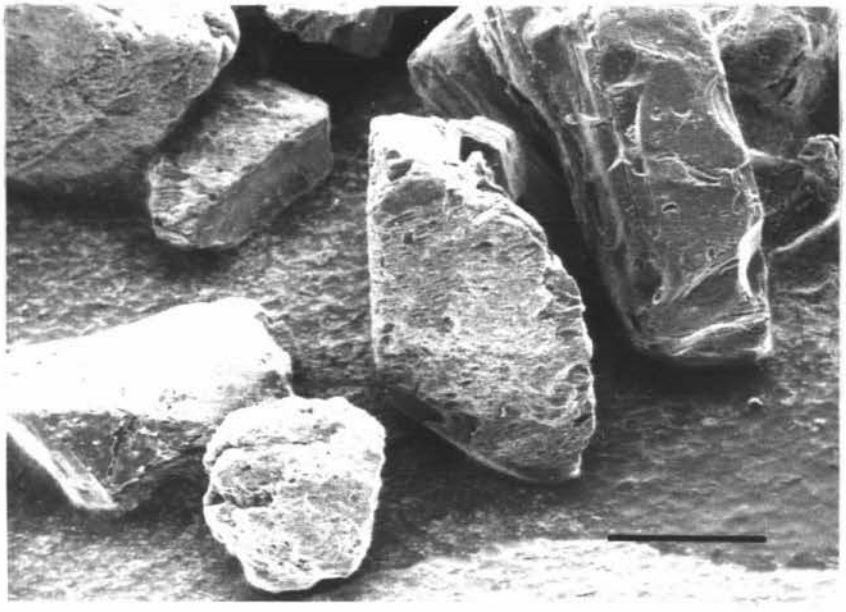

FIGURE 13: Scanning electron micrograph of plagioclase feldspar grains separated from Post-Okareka loess samples (Bar = 500μm).

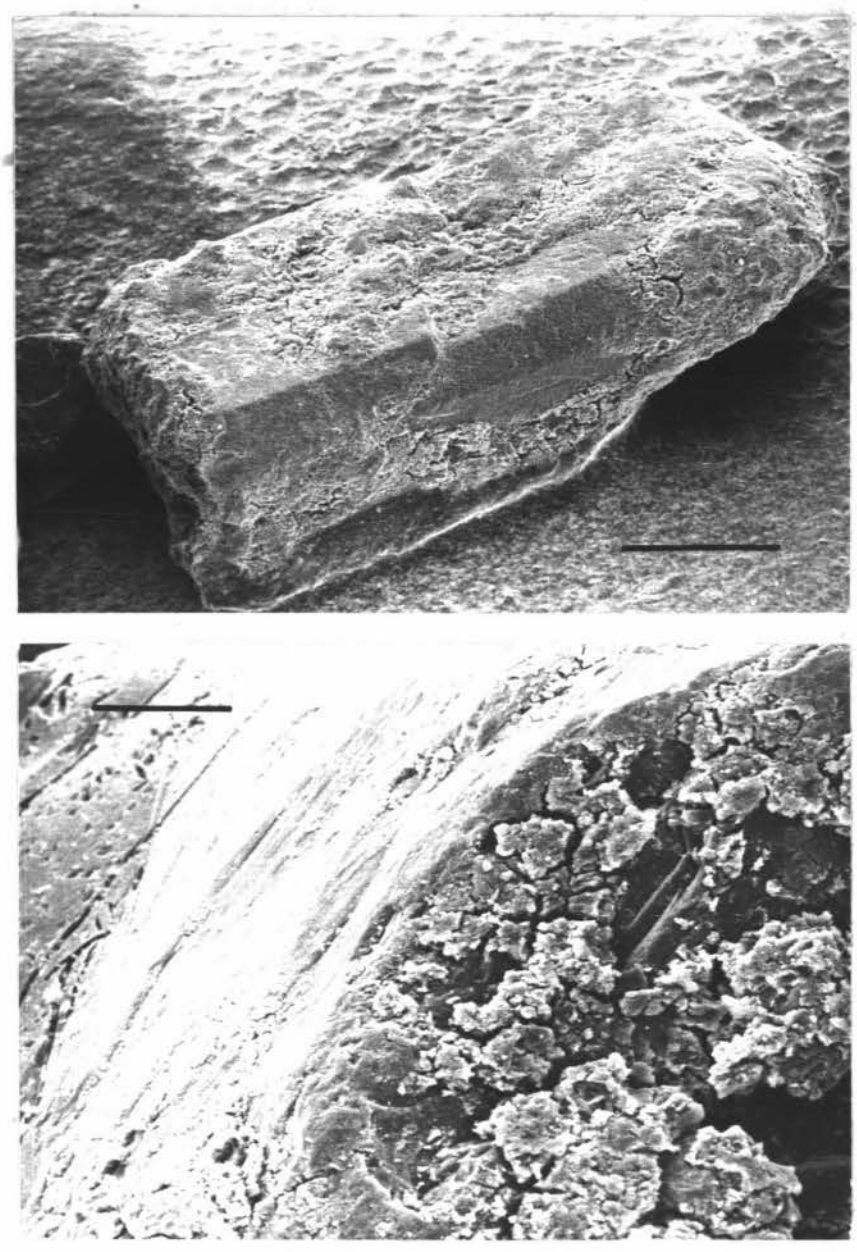

FIGURE 14: Scanning electron micrographs of a plagioclase feldspar grain separated from Post-Okareka loess:

A - feldspar prism coated with short-range order material (Bar = 200 µm)

B - short-range order material at higher magnification (Bar = 50 µm).

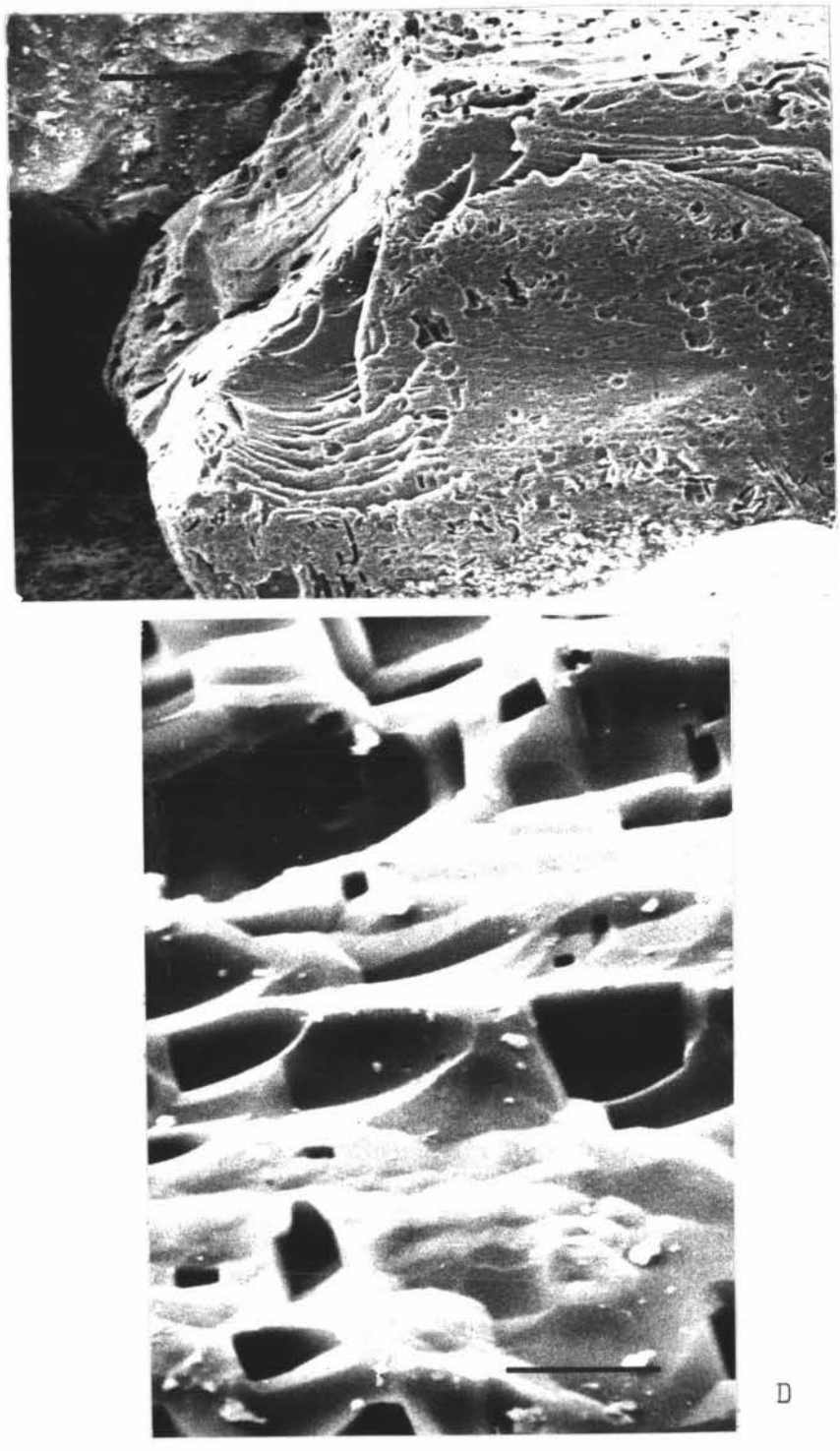

D

FIGURE 14: Scanning electron micrographs of a plagioclase feldspar grain separated from Post-Okareka loess:

C - feldspar prism showing solution etch marks (Bar = 100 μm)

D - etch marks at higher magnification (Bar = 5 μm).

light microscope as iron oxide rims or prism surfaces. Scanning electron micrographs reveal biotite (Figure 10B) and titanomagnetite (Figure 11B) grains in loess samples are less angular than those in ash samples.

In the present study, sodium dithionite treatment was not carried out on material $>63\mu m$, and therefore solution pits on titanomagnetite are probably the result of oxidation of ferrous iron (Fe^{2+}) on crystal surfaces (Wilson, 1975).

Optical and SEM studies indicate that compared to ash samples, loess particles, in particular volcanic glass, are subangular, duller, and more fragmented in Post-Okareka loess deposits. The dullness of most loess grains may be attributed to increased weathering resulting in surface etching which encourages dissolution along cleavage planes (e.g. Figure 8A and 15A), together with surface coatings of fine clay-size material (e.g. Figure 14A). Most vesicles of pumiceous glass shards in loess deposits are filled with possible weathering products in addition to fine-grained particles (Figure 15B).

The non-clay fraction in loess samples contains a higher proportion of silt-sized aggregates, which consist of pumiceous fragments, cemented by clay-size material (Figure 16A). Fine clay particles, possibly that of halloysite are visible on grain fragments (Figure 16B).

Variations in grain morphology are found to occur within loess beds. A greater proportion of grains in basal samples appear more angular and less weathered than those in upper beds, which is due to mixing of tephric and loessial components. A higher amount of silt-sized aggregates, together with more subangular to subrounded grains, are present in upper loess layer samples.

Post-Okareka loess particles, like those of Okareka Ash, show decreasing angularity and increasing weathering of grains with distance from source.

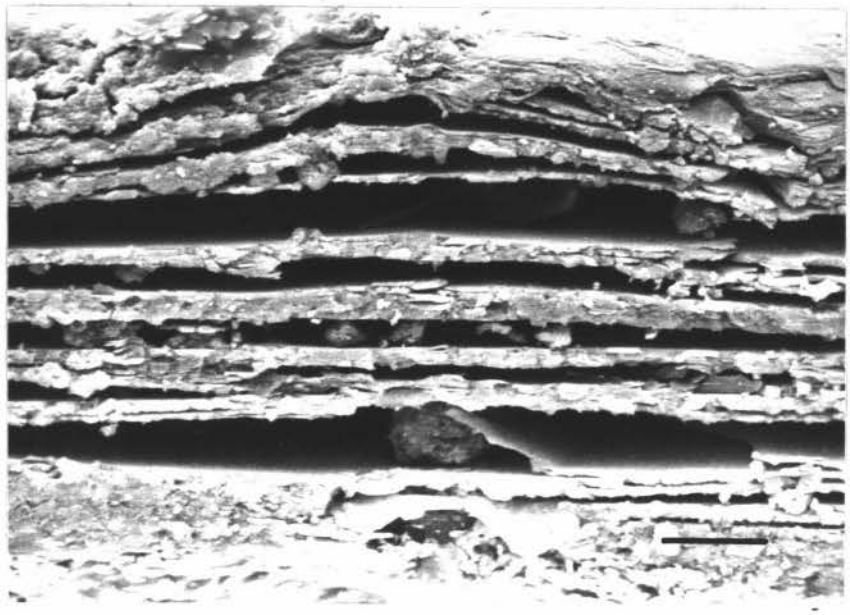

FIGURE 15A: Scanning electron micrograph of exposed cleavage planes in a biotite mica grain separated from Post-Okareka loess samples (Bar = 10μm).

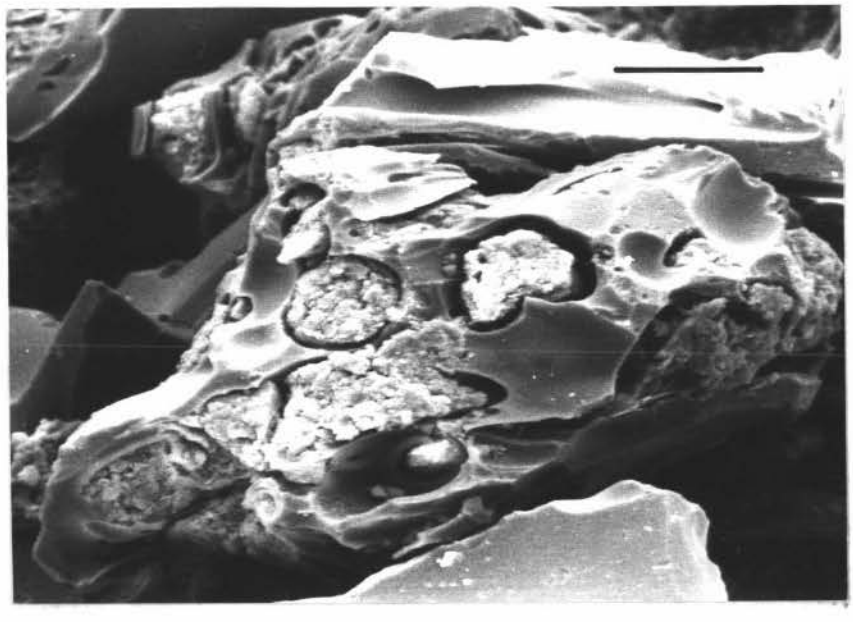

FIGURE 15B: Scanning electron micrograph of a pumiceous particle separated from Post-Okareka loess samples, the cavities of which are filled with possible short-range order material (Bar = 50μm).

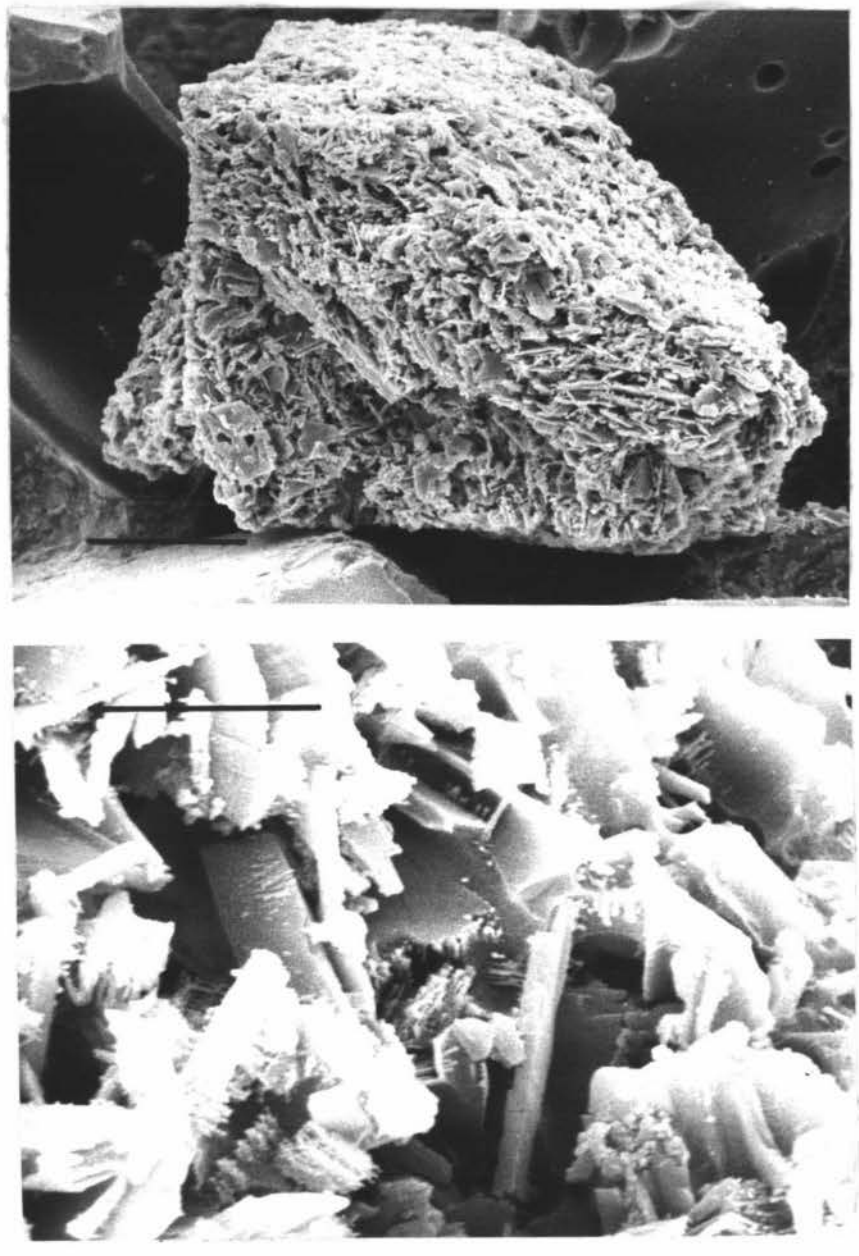

FIGURE 16: Scanning electron micrograph of:

A - a silt-size aggregate separated from Post-Okareka loess samples at Lynmore section (Bar = 50/µm)

B - clay minerals forming on small particles within the aggregate (Bar = 5/µm).

Compared to sections at close (Okareka Quarry and Lynmore (Figure 17A)) and intermediate (Tarukenga and Dalbeth Rd (Figure 17B)) distances from ash source, loess deposits from Highland Hill and Kohatahi section show grains which are distinctly subrounded and greatly altered (Figure 17C).

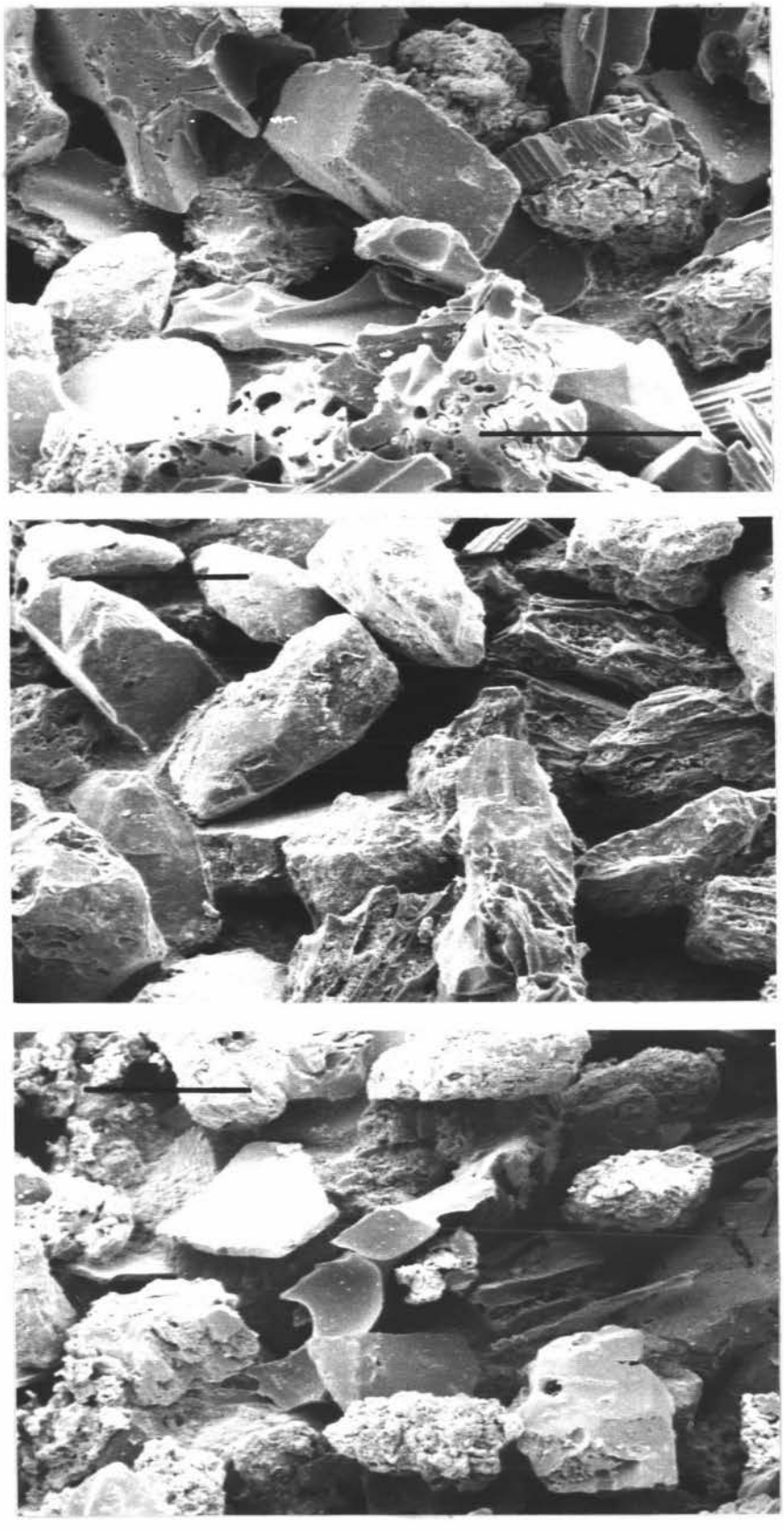

FIGURE 17: Scanning electron micrographs of Post-Okareka loess particles from sections: A - close (AL_1), B - intermediate (CL_2) and C - furtherest (EL_1) to ash source (Bars = 200 μm). With increasing distance from ash source, grain angularity decreases and the proportion of silt-size aggregates increases.

4.3 Clay Mineralogy

4.3.1 Okareka Ash: Trunk Rd

X-ray diffraction analysis reveals no distinct changes in clay mineralogy between Okareka Ash layers at Trunk Rd section. In all samples, the moist clay shows an intense 10.2Å peak (Figure 18A), which after drying shifts to 7.4Å (Figure 18B), and two further peaks at 4.4Å and 3.3Å, all due to halloysite. A broad plateau from 21° to 40° of 2θ for both moist and dry samples indicates short-range order material, which is confirmed by IR analysis to be allophane. Allophane is characterised by an absorption band at 3450cm^{-1} due to -OH stretching vibrations of either structural OH groups or adsorbed water, and a further major peak in 1050cm^{-1} region due to Si-O-Al stretching bonds within the mineral (Figure 19). Absorbance at different frequencies in the 1080 - 1100cm^{-1} region reflects differences in SiO_2 and Al_2O_3 content in allophane. Okareka Ash samples have a band at about 1050cm^{-1}, which indicates a phase containing much highly condensed silica.

Absorption peaks on IR spectra at 3696cm^{-1} and 3620cm^{-1} arise from -OH stretching bonds within the crystalline structure of halloysite. The peak at 3696cm^{-1} results from stretching motions of internal -OH bonds. The intensity and ratio of these two absorption bands indicate a degree of ordering within the halloysite structure. In Trunk Rd ash samples the 3620cm^{-1} peak is significantly stronger than the 3696cm^{-1} peak which suggests a moderate to poorly-ordered halloysite structure. An absorption band due to H-O-H deformation vibration of adsorbed water appears at 1630-1640cm^{-1}, and is characteristic of both allophane and halloysite. A phase containing highly condensed silica is indicated by a shoulder at 1120cm^{-1}, and absorbance at 915cm^{-1} due to in-plane bonding vibrations of inner Al-OH bonds of phyllosilicate minerals confirms that halloysite is present in moderate amount.

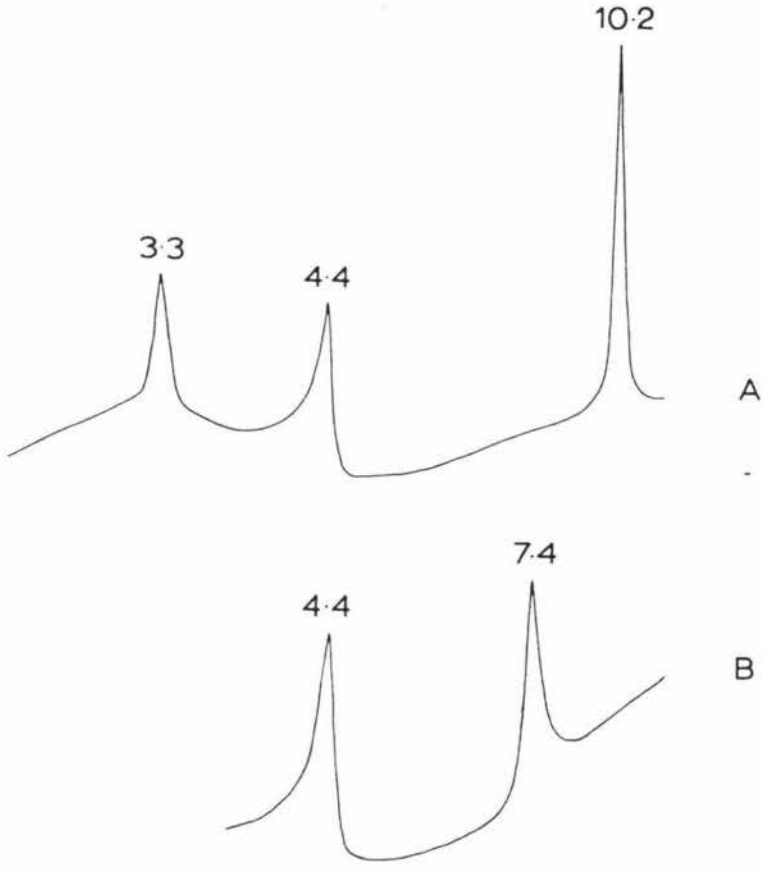

FIGURE 18: X-ray diffraction patterns (Å) of the clay (< 1.0 μm) fraction from Okareka Ash, Ngongotaha section:

A - moist (hydrated halloysite)

B - dried at 100°C for 10 minutes (dehydrated halloysite)

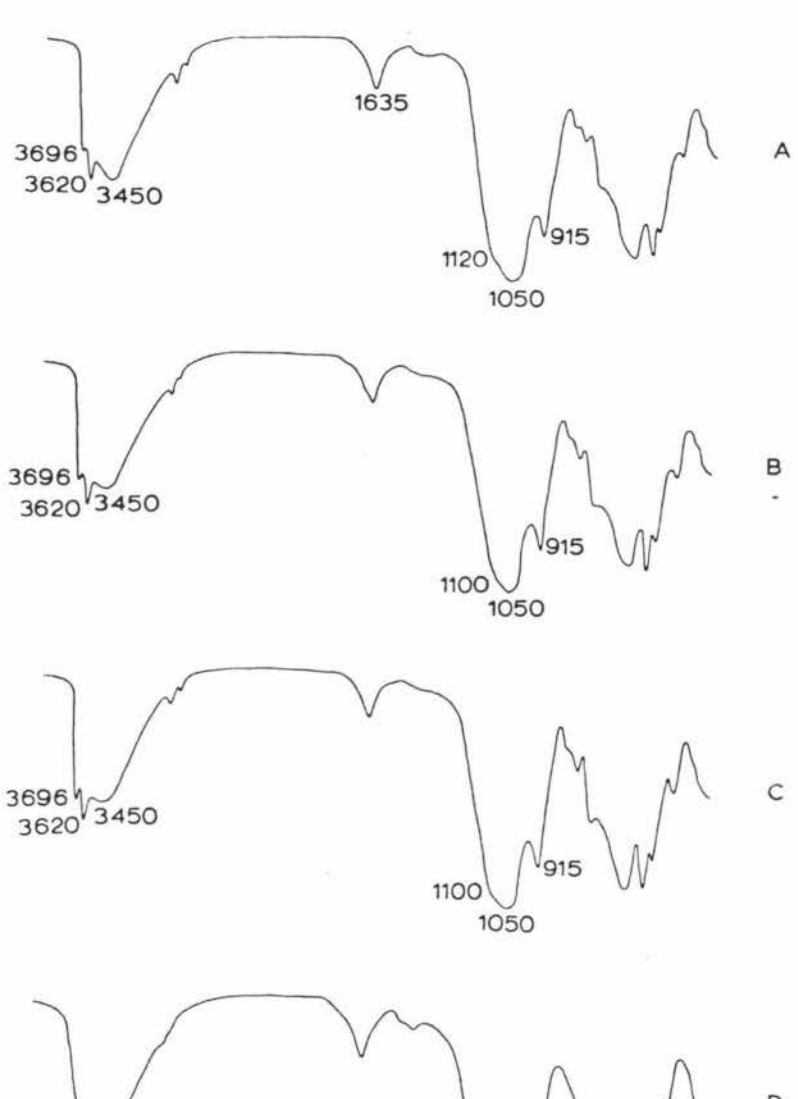

FIGURE 19: Infra-red spectra (cm^{-1}) of Okareka Ash clay (<1.0μm) from:

A - Trunk Rd (R_A)

B - Okareka Quarry (AA)

C - Ngongotaha (JA)

D - Tarukenga (CA)

sections, showing absorption due to halloysite (3696cm^{-1}, 3620cm^{-1} and 915cm^{-1}) and allophane (3450cm^{-1}).

Electron micrographs of Okareka Ash samples at Trunk Rd show halloysite morphology comprises predominantly squat ellipsoids, which have a circular appearance, with some curled flakes (Figures 20 and 21). A few halloysite tubes were observed in bed R_A, together with trace amounts of hexagonal-shaped material (Figure 22) that show surface boiling effects. Such effects are often observed on exterior surfaces of halloysite tubes after exposure for several minutes in the electron beam, and are apparent on tubes in Figure 22. Transmission electron microscope studies show allophane occurs as fine rounded particles which form irregular aggregates often associated with threads of imogolite, as well as particles of weathering glass (Figures 20 and 21). Within these 'grainy' weathering particles halloysite ellipsoids occur, often at an early stage of formation.

4.3.2 Okareka Ash: remaining sections

X-ray diffraction of Okareka Ash beds at sections closest to source, i.e. Gavin Rd, Okareka Quarry, Lynmore and Te Ngae, indicate a moderate amount of halloysite occurs, together with short-range order material, probably allophane. Trace amounts of feldspar, quartz, cristobalite and tridymite are also evident on XRD patterns. The ratio of absorption bands at 3696cm^{-1} and 3620cm^{-1} on IR spectra suggest that clay fractions of these ash samples contain moderate to poorly-ordered halloysite (Figure 19B). A sharp peak at 915cm^{-1} confirms the presence of halloysite, and absorbance at 3450cm^{-1} and 1050cm^{-1} indicates allophane is present, but only in small amount.

X-ray diffraction and IR evidence is confirmed by thermal curves of clays (Figure 23A) which show a moderate endothermic peak at 504^{o}C due to dehydroxylation of halloysite. Dehydration of both halloysitic and allophanic components results in an endotherm at 79^{o}C, and a high temperature exothermic peak at 985^{o}C is due to recrystallisation of products of the earlier dehydroxylation reaction, the new phase possibly being

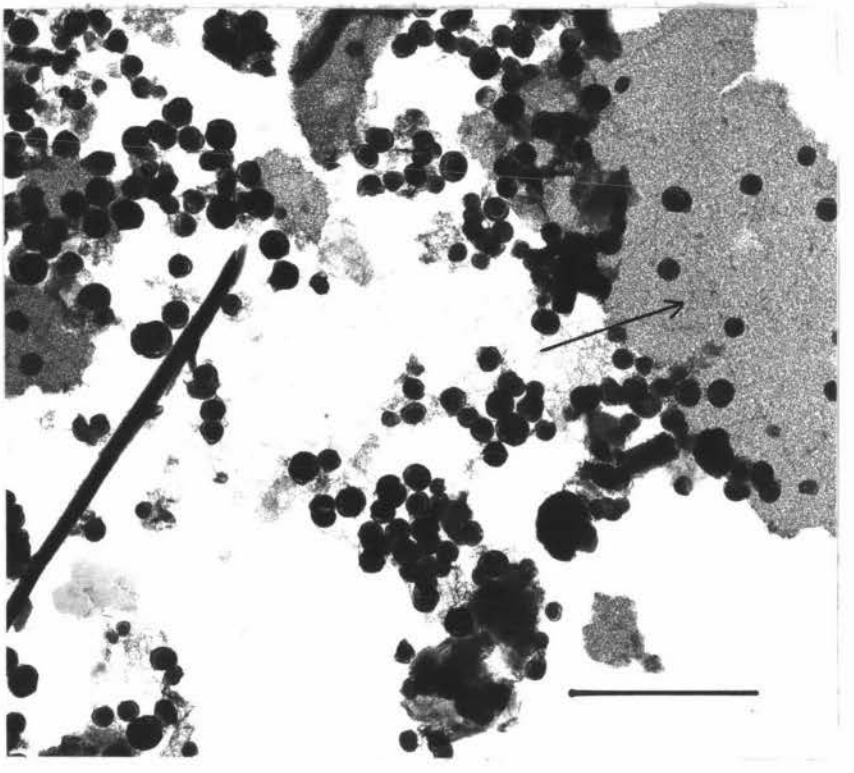

FIGURE 20: Transmission electron micrographs of $< 1.0\mu m$ size clay of Okareka Ash at Trunk Rd section.
The clay sample from R_A bed is composed mainly of halloysite ellipsoids, and particles of weathering glass (arrowed) (Bar = $1\mu m$).

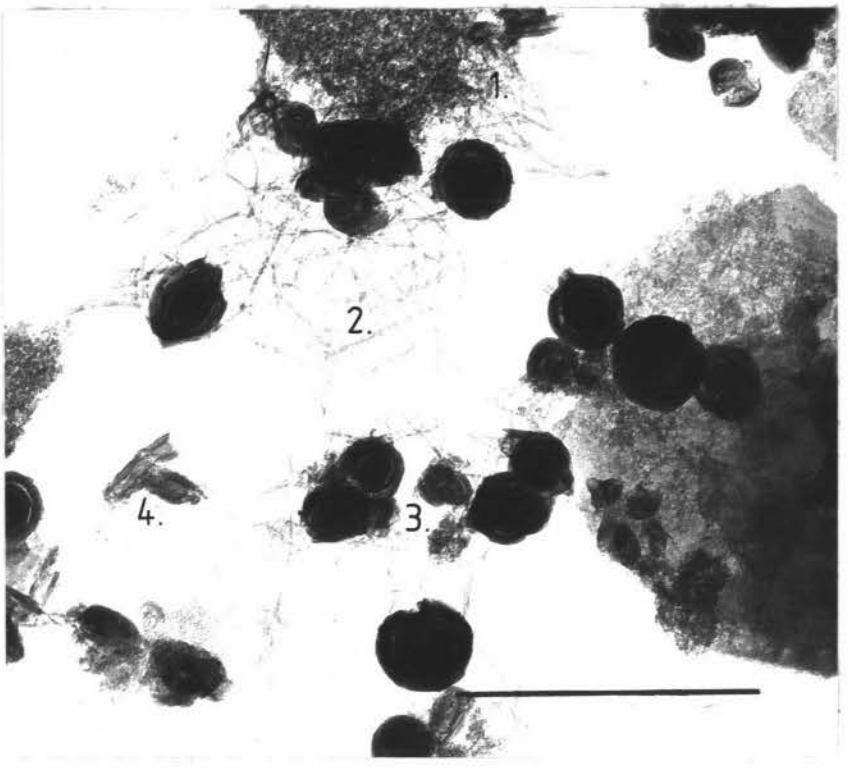

FIGURE 21: Transmission electron micrograph of $< 1.0\mu m$ size clay of Okareka Ash at Trunk Rd section.
Clay sample is from R_{AL} Bed, and at high magnification, shows:

1 - allophane
2 - imogolite
3 - halloysite ellipsoids
4 - curled flakes (Bar = $0.5\mu m$)

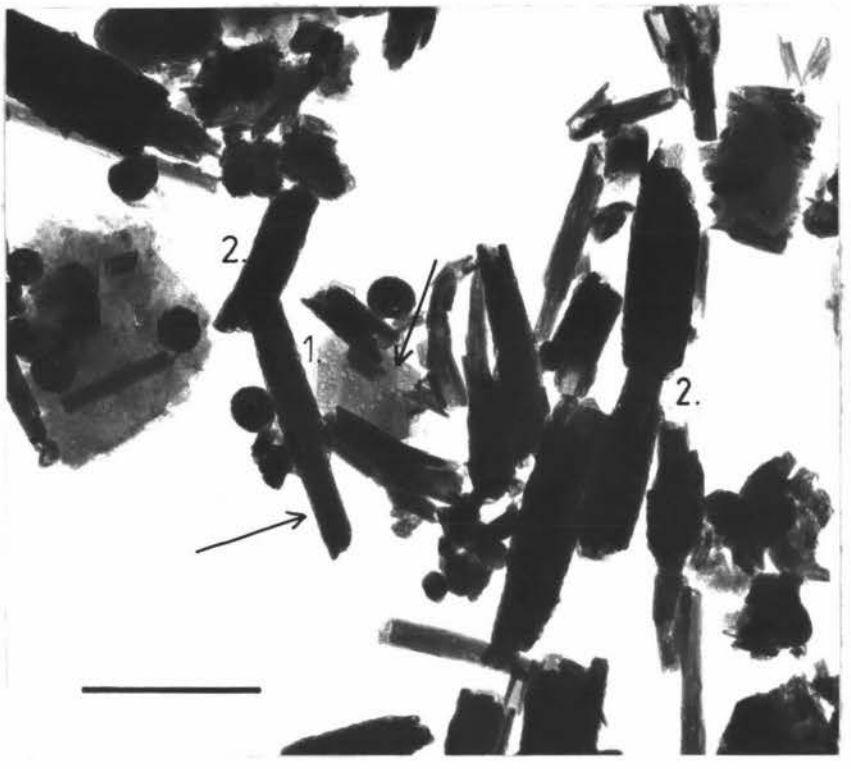

FIGURE 22: Transmission electron micrograph of <1.0μm size clay of Okareka Ash at Trunk Rd, showing surface boiling effect (arrowed) on:

1 - hexagonal-shaped material

2 - halloysite tubes (Bar = 0.5μm)

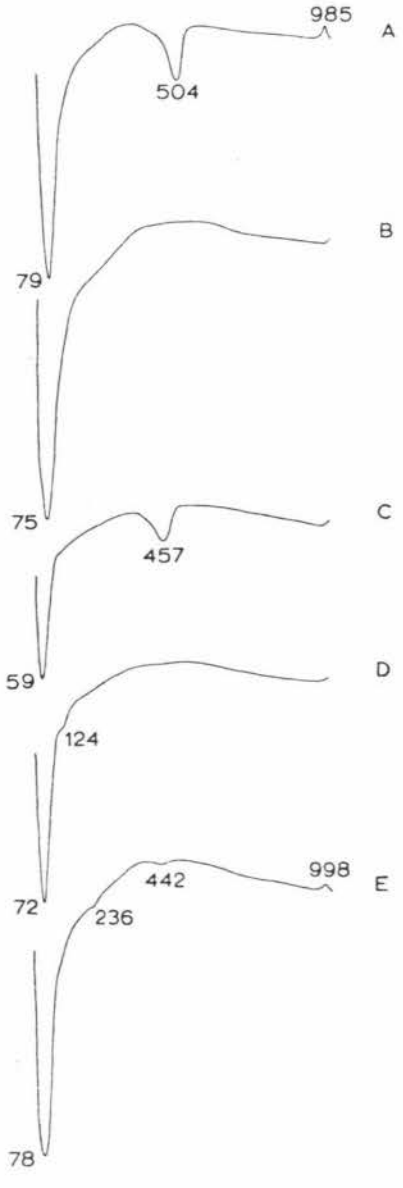

FIGURE 23: Differential thermal curves (^{o}C) of Okareka Ash clay (< 1.0 mm) from:

A - Okareka Quarry (AA)
B - Pukehangi Rd (BA)
C - Ngongotaha (JA)
D - Dalbeth Rd (DA)
E - Kuhatahi (EA) sections showing low temperature dehydration of halloysite and allophane (59-80^{o}C); dehydroxylation of gibbsite (236^{o}C); dehydroxylation of halloysite (442-504^{o}C), and high temperature exothermic recrystallisation (985-998^{o}C).

mullite or spinel (Yoshinaga and Aomine, 1962a). In clay samples from Okareka Ash deposits at Okareka Quarry, Lynmore and Te Ngae sections TEM studies show halloysite curled flakes occur in subordinate amount to squat ellipsoids. At Gavin Rd section, however, the clay fraction contains approximately equal amounts of each morphological form of halloysite. In electron micrographs of ash samples from all four sections allophane is observed as aggregated material or as fine particles associated with threads of imogolite (Figure 24).

At Pukehangi Rd site, XRD evidence indicates the clay sample of Okareka Ash consists solely of noncrystalline material. This is confirmed by a single well-defined peak at 3450cm^{-1}, and a further broad peak at 1050cm^{-1} on IR spectra. Furthermore, a large endothermic dehydration peak at 75^{o}C occurs on the thermal curve, and the absence of an endothermic reaction in the 500^{o}C region demonstrates a dominant amount of allophane is present (Figure 23B). Transmission electron microscope studies reveal allophane occurs as aggregates and as rounded particles associated with imogolite. Electron micrographs show that quite a significant amount of imogolite is present together with silica flakes, and trace amounts of halloysite ellipsoids and curled flakes (Figure 25).

In contrast to Pukehangi Rd section, XRD, DTA and IR analyses of Okareka Ash clay fraction from Ngongotaha section indicate halloysite is present in moderate amount. X-ray diffraction patterns show halloysite and short-range order material are dominant constituents of the clay fraction, with trace amounts of tridymite, cristobalite, feldspar and biotite-vermiculite. Absorption peaks at 3696cm^{-1} and 3620cm^{-1} on IR spectra reveal halloysite is quite well-ordered, with a small amount of allophane indicated by absorption at 3450cm^{-1} and 1050cm^{-1} (Figure 19C). X-ray diffraction and IR evidence is confirmed by DTA which shows a low temperature endotherm at 59^{o}C resulting from dehydration of allophane

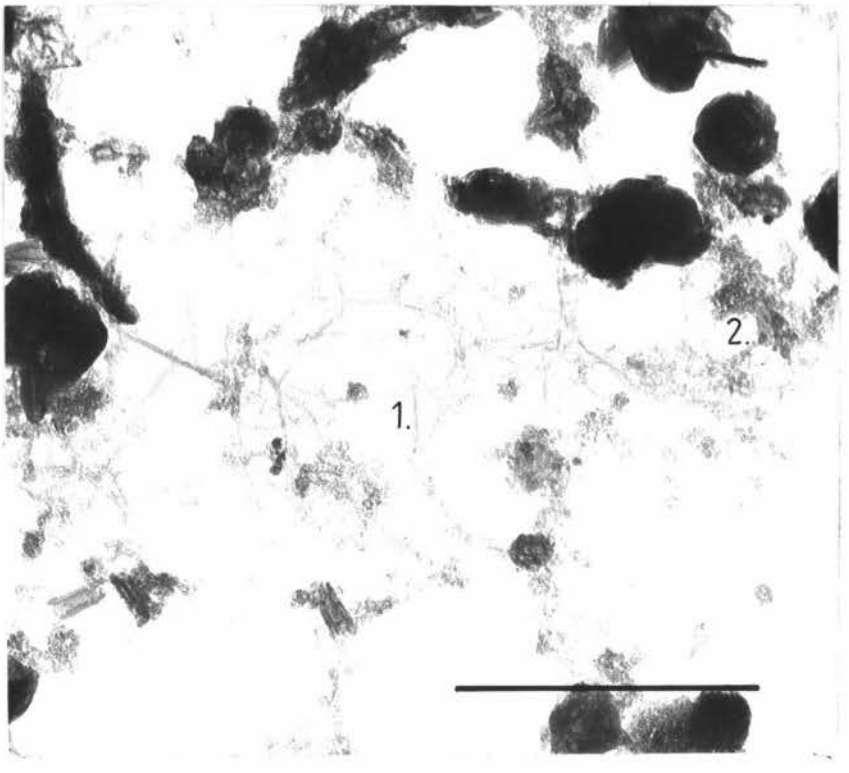

FIGURE 24: Transmission electron micrograph of $<1.0\mu m$ size clay of Okareka Ash at Te Ngae section showing:

1 - imogolite

2 - aggregates of allophane, and trace amounts of halloysite curled flakes and ellipsoids. (Bar = $0.5\mu m$)

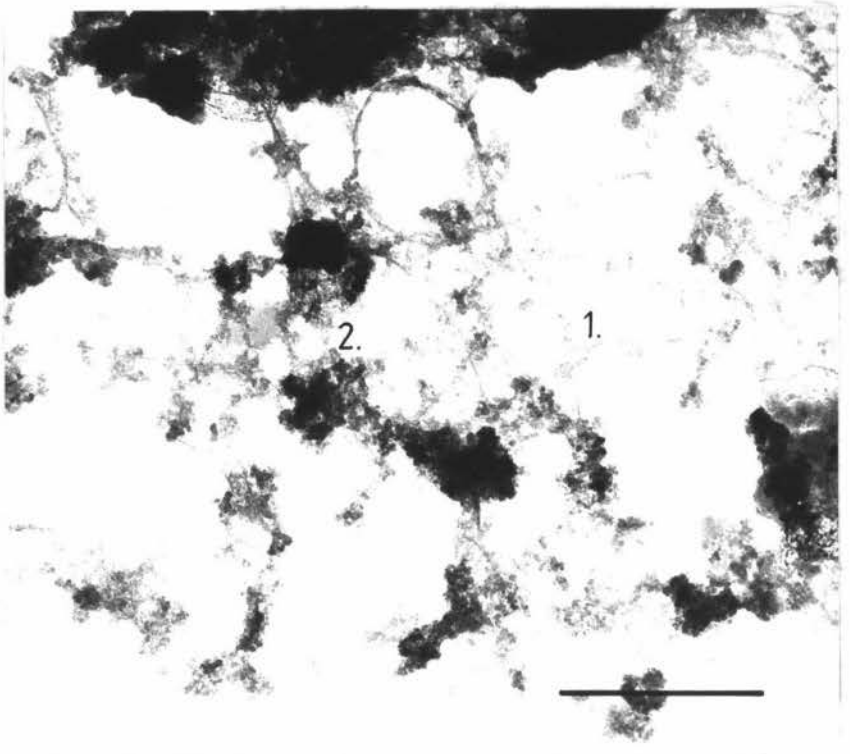

FIGURE 25 : Transmission electron micrograph of < 1.0 μm size clay of Okareka Ash at Pukehangi Rd section.
Clay sample consists predominantly of:
1 - imogolite
2 - allophane (Bar = 0.5 μm).

and halloysite, and a further endothermic peak at 457°C due to dehydroxylation of halloysite (Figure 23C). Electron optical studies reveal halloysite ellipsoids occur in greater amount than curled flakes, together with small amounts of imogolite and silica flakes. Allophane occurs as aggregates, or as finely dispersed particles.

Clay fractions of Okareka Ash samples from Tarukenga, Dalbeth Rd, Highland Hill and Kuhatahi sections are shown by XRD analysis to consist predominantly of short-range order material with no evidence of crystalline clay. However, the XRD pattern of the clay sample from Highland Hill section indicates feldspar, cristobalite, biotite-vermiculite, and quartz occur in trace amount. Absorbance at 3450cm^{-1} and 1045cm^{-1} on IR spectra confirms a dominant amount of allophane is present in all ash samples (Figure 19D). Differential thermal curves of ash clay fractions from Tarukenga and Dalbeth Rd sections show a single intense endothermic peak in the 70 - 75°C region, due to dehydration of allophane, with no further peaks indicative of crystalline material (Figure 23D). However, DTA patterns of Okareka Ash clay fractions from Highland Hill and Kuhatahi sections (Figure 23E) exhibit an endothermic peak in the range 230 - 240°C, due to a small amount of gibbsite. A shallow endothermic peak at 442°C due to a small amount of halloysite, as well as a high temperature exotherm at 998°C due to recrystallisation of products from the earlier dehydroxylation reaction, are also observed on the thermal curve of the Okareka Ash clay sample from Kuhatahi section.

Electron optical investigation of clay fractions confirms that noncrystalline material is the dominant constituent of Okareka Ash samples at these four sites. Aggregates of allophane are clearly evident, often in association with web-like strands of imogolite (Figures 26A and 26B). A small proportion of halloysite tubes, curled flakes, and squat ellipsoids

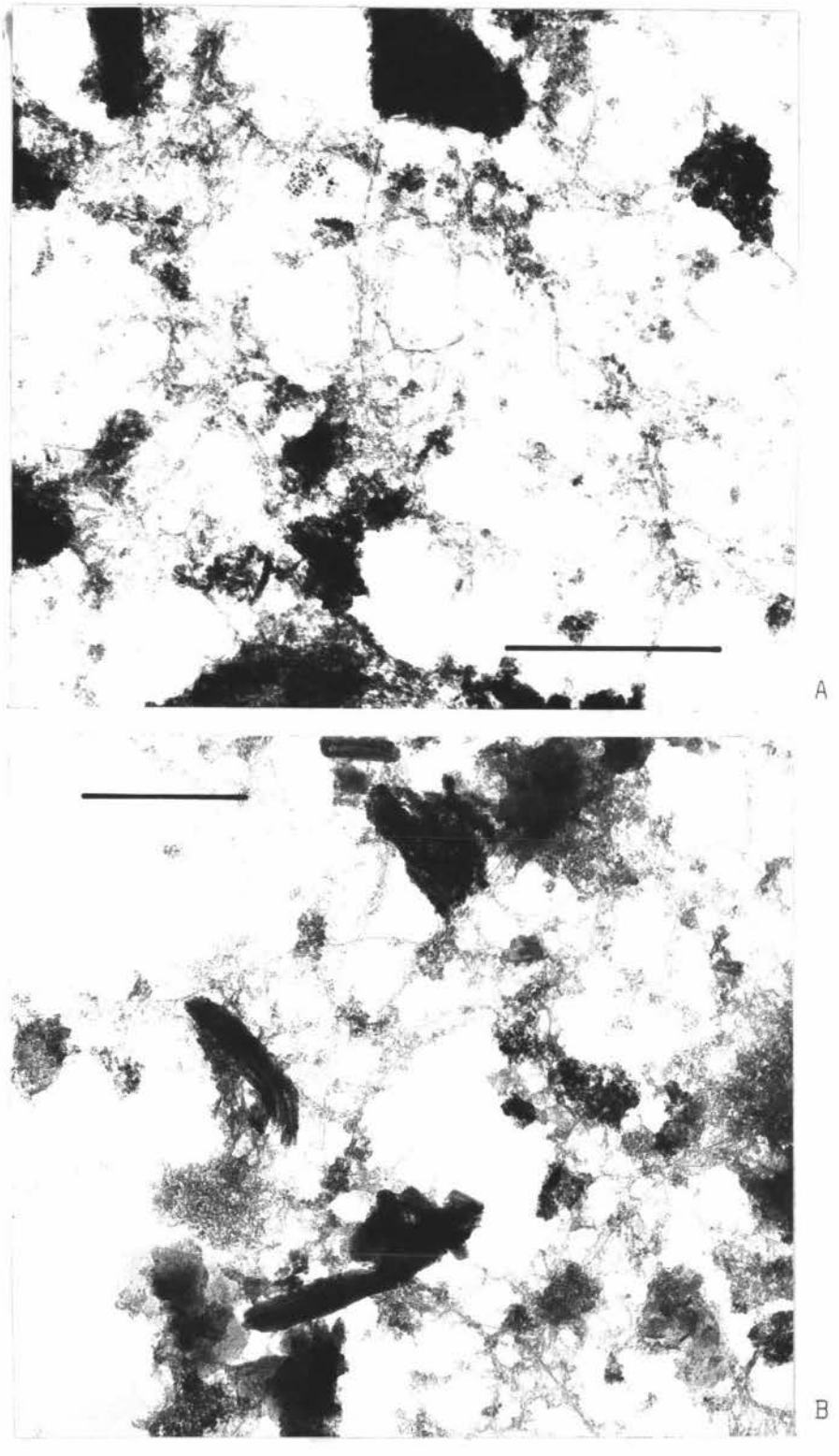

FIGURE 26: Transmission electron micrographs of <1.0μm size clay of Okareka Ash at:

A - Tarukenga section (Bar = 0.5μm)

B - Highland Hill section (Bar = 0.5μm)

Clay fractions consist predominantly of imogolite and allophane.

are also present, together with some silica flakes. Electron micrographs confirm XRD evidence, and show a small amount of crystalline material, together with weathering volcanic glass is present in the clay fraction of Okareka Ash from Highland Hill section (Figure 26B). A trace amount of hexagonal-shaped material is also observed in Okareka Ash samples from Tarukenga section.

4.3.3 Post-Okareka loess: Trunk Rd

Halloysite is the dominant clay mineral in the thin loess bed which overlies Okareka Ash at Trunk Rd. X-ray diffraction patterns show a moderate 10.1Å peak which reduced and shifted to 7.4Å upon drying. A broad rise in baseline between 21° and 40° of 2θ indicated short-range order material is present together with trace amounts of feldspar and quartz. The ratio of absorption bands $3696cm^{-1}$ and $3620cm^{-1}$ on IR spectra demonstrate halloysite is moderately to poorly-ordered, and in greater amount than allophane which absorbs at $3450cm^{-1}$ and $1050cm^{-1}$. The IR spectra of Post-Okareka loess samples at Trunk Rd section is similar to that of clay fractions from Okareka Quarry section shown in Figure 28A.

Electron optical studies reveal upper loess sample L_1 contains a dominant amount of halloysite curled flakes (Figure 27), which is in contrast to basal loess sample L_2 where halloysite ellipsoids predominate. Silica flakes, as well as allophane, often associated with web-like imogolite, or cementing aggregates of weathering glass are also apparent on electron micrographs.

4.3.4 Post-Okareka loess: Gavin Rd and Te Ngae sections

Post-Okareka loess clay fractions from Gavin Rd and Te Ngae sections consist of quite well-ordered halloysite together with minor amounts of allophane. X-ray diffraction analyses of moist clay samples show an intense first-order reflection at 10.1Å which after drying reduced in size and shifted to 7.4Å. Traces of feldspar and

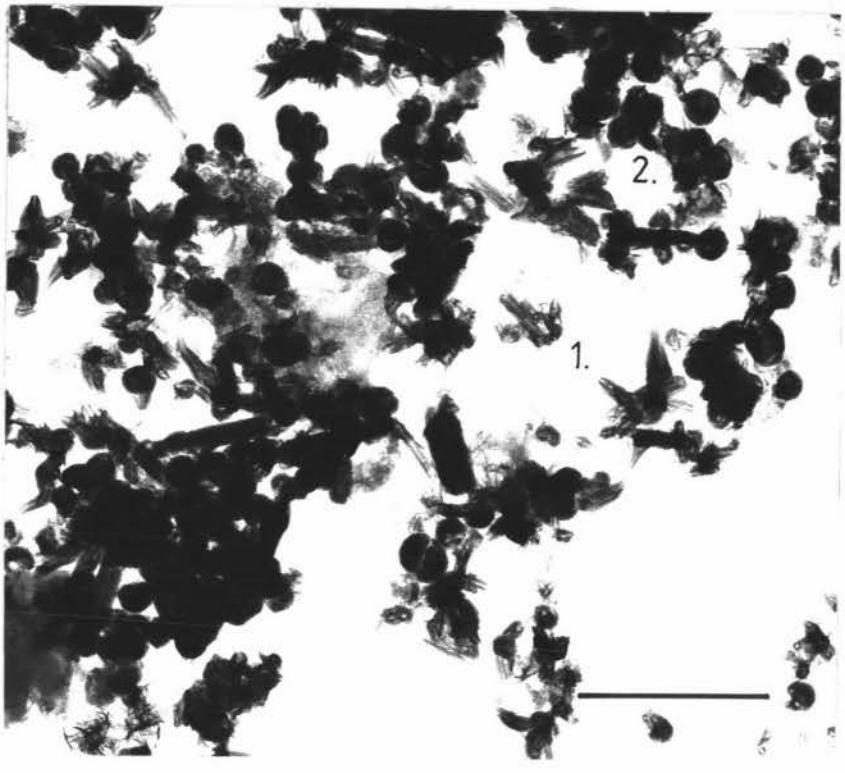

FIGURE 27: Transmission electron micrograph of <1.0μm size clay of Post-Okareka loess from Trunk Rd section.
Clay samples contain a greater proportion of: 1 - halloysite curled flakes
2 - halloysite ellipsoids
(Bar = 0.5μm).

tridymite are also evident on XRD patterns. Infra-red analyses confirm XRD evidence, and show halloysite is moderately well-ordered, particularly in upper loess samples. Absorption at 3450cm^{-1} due to allophane occurs on all IR spectra, but peak intensity varies between samples within loess beds. A greater amount of allophane is present in basal layers at each section, and absorption peaks in 3600cm^{-1} region indicate halloysite in these samples is less well-ordered. Small absorption peaks in 3600 - 3400cm^{-1} region due to gibbsite are also observed on IR patterns of the upper loess layer sample at Gavin Rd, and in clay fractions of loess samples from Te Ngae section. Electron-optical examination of clay samples indicate halloysite curled flakes are in greater amount than halloysite ellipsoids. Particles and aggregates of allophane are clearly evident, and in varying amounts in all clay fractions at both sites, together with imogolite and silica flakes.

4.3.5 Post-Okareka Loess: Transect sections

X-ray diffraction, DTA, IR, and electron optical studies demonstrate clay mineralogy of all Post-Okareka loess deposits sampled on the transect are similar, and vary only in amount and type of halloysite present. Moist clay samples of loess from all sections, except Pukehangi Rd, Highland Hill, and Kuhatahi, show a moderate peak at 10.2Å on XRD patterns, which upon drying shifts to 7.4Å, and is due to halloysite. A broad plateau between 21° and 40° of 2θ due to short-range order material, as well as trace amounts of crystalline material are also present in clay fractions from these sections. However, at Pukehangi Rd, Highland Hill and Kuhatahi section, XRD analyses of loess samples show halloysite is present in amounts subordinate to short-range order material.

Subtle differences in clay mineralogy of Post-Okareka loess deposits from each section are revealed by detailed investigation using IR, DTA and TEM methods.

OKAREKA QUARRY + LYNMORE sections:

Infra-red spectra of Post-Okareka loess deposits at Okareka Quarry and Lynmore sections confirm XRD analyses, and show absorption bands at 3696cm^{-1} and 3620cm^{-1} due to halloysite (Figure 28A). The intensity and ratio of these two peaks indicates halloysite is moderate to poorly-ordered, and in greater amount than allophane, which absorbs at 3450cm^{-1} and 1045cm^{-1}. Absorbance at 920cm^{-1} confirms crystalline clay material occurs in moderate to high amount. Dehydroxylation of halloysite results in an endothermic peak at 466^{o}C on thermal curves of clay fractions at both sections (Figure 29A). Differential thermal analyses also reveal a low temperature endotherm in 65 - 70^{o}C region due to dehydration of allophanic and halloysitic components, and a small endothermic peak at 238^{o}C which is attributed to a trace of gibbsite. Electron optical studies show halloysite morphology consists predominantly of curled flakes, but halloysite ellipsoids are present, the amount increasing with depth. Allophane is observed on electron micrographs as aggregates or as fine particles associated with web-like imogolite.

PUKEHANGI RD section:

The infra-red spectrum of the clay fraction from Post-Okareka loess at Pukehangi Rd section is similar to that of loess samples from Highland Hill shown in Figure 28D. In contrast to Figure 28D no absorption due to gibbsite appears on the IR spectrum, however, two small shoulders at 3696cm^{-1} and 3620cm^{-1} indicate a trace of poorly-ordered halloysite. A dominant amount of allophane is shown by absorption peaks at 3450cm^{-1} and 1060cm^{-1}. Endothermic peaks at 234^{o}C and 448^{o}C due to gibbsite and halloysite respectively are observed on the thermal curve of the loess sample at Pukehangi Rd (Figure 29B). Differential thermal analysis also reveals a dehydration peak at 64^{o}C, and recrystallisation of products from the earlier dehydroxylation reaction

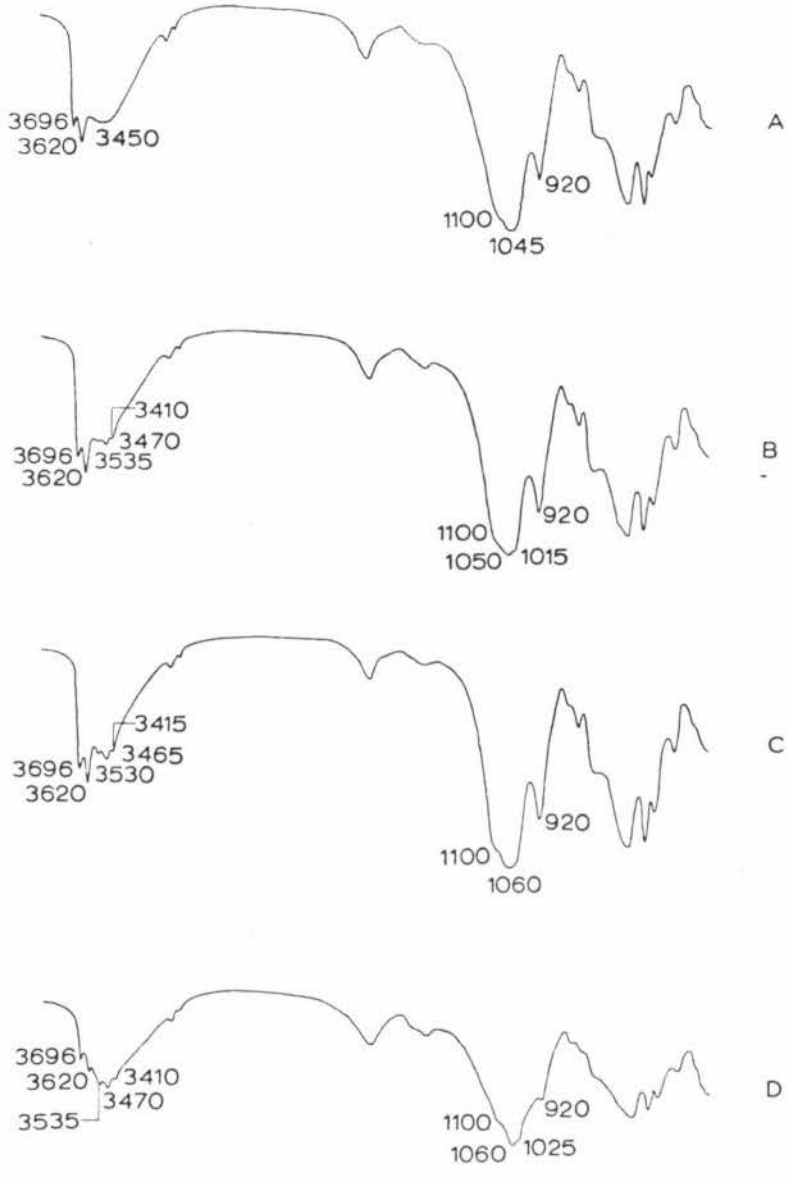

FIGURE 28: Infra-red spectra (cm^{-1}) of Post-Okareka loess clay (<1.0μm) from:

A - Okareka Quarry (AL_1)
B - Ngongotaha (JL_1)
C - Dalbeth Rd (DL_1)
D - Highland Hill (EL_1) sections showing absorption due to halloysite (3696cm^{-1}, 3620cm^{-1} and 920cm^{-1}), allophane (3450cm^{-1}), and gibbsite (3530-3410cm^{-1} region and 1015-1025cm^{-1} region).

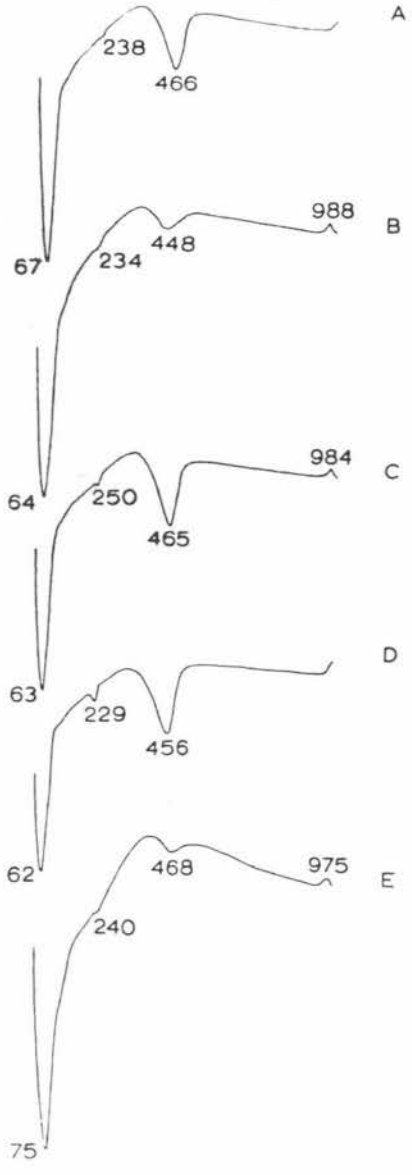

FIGURE 29: Differential thermal curves (^{o}C) of Post-Okareka loess clay (<1.0 µm) from:

A - Okareka Quarry (AL_1)

B - Pukehangi Rd (BL)

C - Ngongotaha (JL_1)

D - Dalbeth Rd (DL_1)

E - Kuhatahi (KL_1) sections, showing dehydration of halloysite and allophane (62-75^{o}C), dehydroxylation of gibbsite (229-250^{o}C), dehydroxylation of halloysite (448-468^{o}C) and high temperature exothermic recrystallisation (975-984^{o}C).

results in a high temperature exotherm at 988°C. Transmission electron microscope studies which confirm IR and DTA evidence, show the clay fraction comprises predominantly halloysite curled flakes together with some ellipsoids (Figure 30).

NGONGOTAHA section:

Infra-red, DTA and TEM studies of loess at Ngongotaha section, which is similar in altitude and aspect to Pukehangi Rd section, confirm halloysite is the dominant mineral of the clay fraction. Absorption bands at 3696cm^{-1} and 3620cm^{-1} on IR spectra (Figure 28B) indicate halloysite is quite well-ordered and in much greater amount than allophane. The presence of a significant amount of crystalline clay material is confirmed by a well-defined peak at 920cm^{-1}. Small absorption peaks at 3535cm^{-1}, 3470cm^{-1}, 3410cm^{-1}, and a further peak at 1015cm^{-1} show a trace amount of gibbsite is present. Investigation by DTA reveals dehydroxylation of a moderate to high amount of halloysite results in a peak at 465°C (Figure 29C). In addition to an endothermic dehydration reaction at 63°C, the thermal curve shows a small endothermic peak at 250°C, which confirms the presence of gibbsite, and a peak at 984°C due to a high temperature recrystallisation reaction. Electron optical studies of clay fractions from loess deposits at Ngongotaha section reveal allophane occurs in subordinate amount to quite well-developed halloysite (Figure 31). In upper loess samples halloysite curled flakes are more common than ellipsoids, but the two morphological forms occur in approximately equal amount in basal loess samples. Small amounts of imogolite and silica flakes are also present in the electron micrographs.

TARUKENGA + DALBETH RD sections:

Thick deposits of Post-Okareka loess overlie Okareka Ash at Tarukenga and Dalbeth Rd sections. X-ray diffraction analyses indicate a moderate amount of

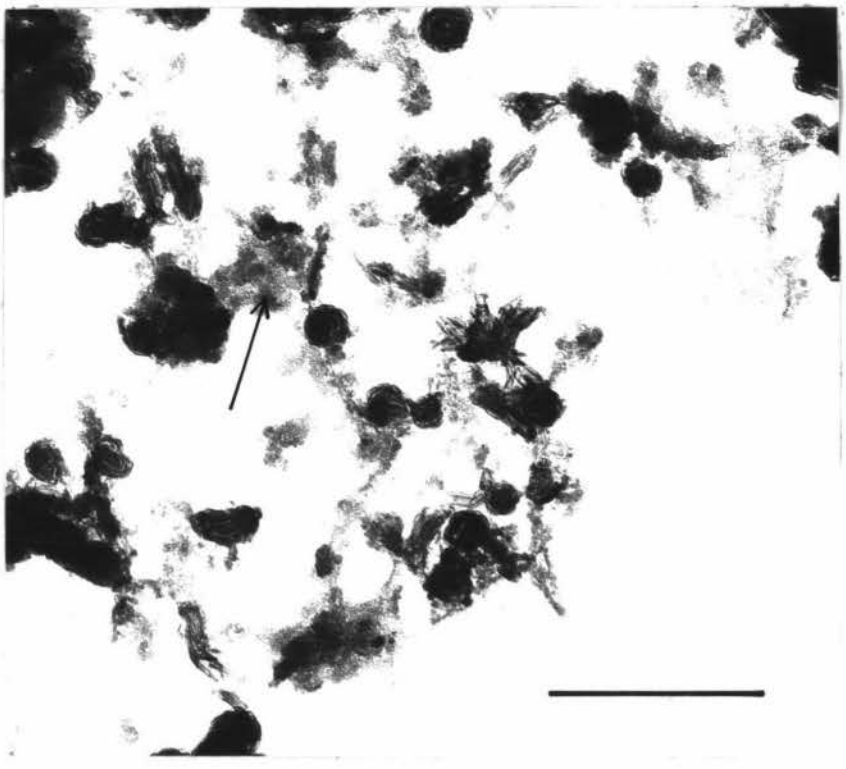

FIGURE 30: Transmission electron micrograph of <1.0μm size clay of Post-Okareka loess from Pukehangi Rd section, showing halloysite curled flakes and ellipsoids together with aggregates of allophane (arrowed) (Bar = 0.5μm).

halloysite is present in clay fractions, and this is confirmed by absorption peaks at 3696cm^{-1}, 3620cm^{-1} and a further intense peak at 920cm^{-1} on IR spectra, all due to halloysite (Figure 28C). The ratio of the former two bands show halloysite is moderate to poorly-ordered, and in greater amount than allophane which absorbs at 3450cm^{-1} and 1060cm^{-1}. Absorption peaks in the 3600 - 3400cm^{-1} region indicate gibbsite is also present in small amount in all loess samples. Infra-red analyses reveal basal loess layers at both sections contain slightly more allophane than upper layer samples.

Thermal curves of upper loess samples have a moderate endothermic peak due to dehydroxylation of halloysite in 450 - 460^{o}C region (Figure 29D), however, this peak is shallower and of lower temperature in basal samples. Dehydration of allophane and halloysite results in an endothermic peak in the range 59 - 70^{o}C, and gibbsite, indicated by a peak at 230^{o}C, occurs in varying amounts in all loess samples. Halloysite curled flakes in greater amount than squat ellipsoids are observed in electron micrographs of upper loess layers at both sections (Figures 32 and 33). This is in contrast to basal loess samples in which approximately equal amounts of ellipsoids and curled flakes occur. Transmission electron microscope studies show allophane, imogolite and silica flakes are present in all clay fractions. Tubular halloysite is also evident in basal loess samples of both sections. Hexagonal particles showing a surface boiling effect were seen in small amount in electron micrographs of clay fractions of loess deposits at Tarukenga section. Small electron-dense spheres, occurring in varying amount in clay samples from Dalbeth Rd section, are probably iron and/or manganese concretions (Figure 33).

HIGHLAND HILL + KUHATAHI sections:

Infra-red, DTA and EM studies of Post-Okareka loess deposits at Highland Hill and Kuhatahi sections confirm XRD evidence that clay fractions comprise halloysite in

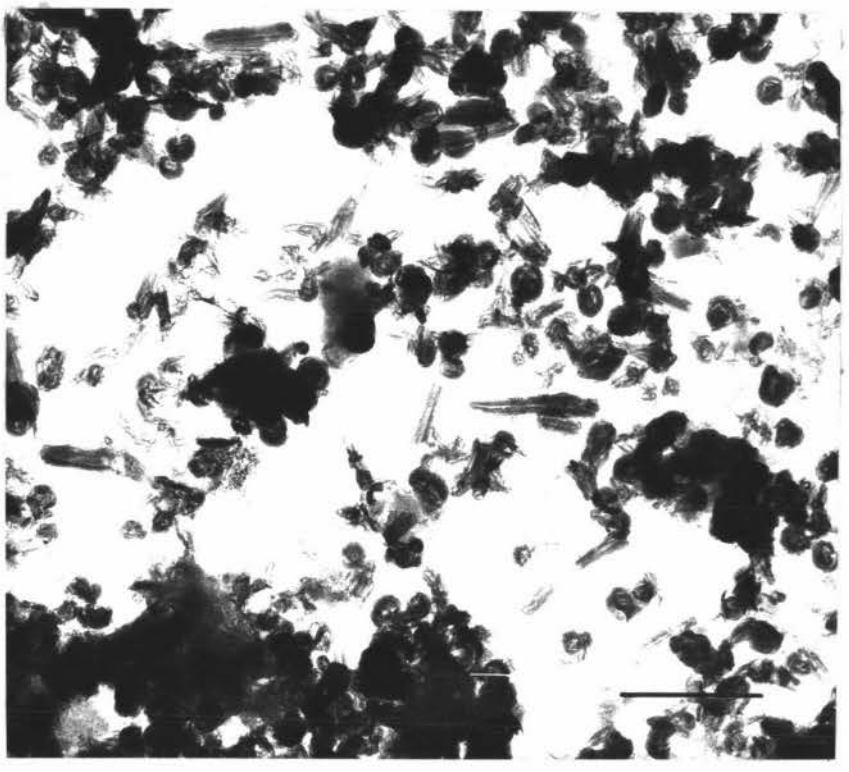

FIGURE 31: Transmission electron micrograph of <1.0μm size clay of Post-Okareka loess at Ngongotaha section. Clay fraction comprises halloysite ellipsoids and curled flakes, as well as a small amount of allophane (Bar = 0.5μm).

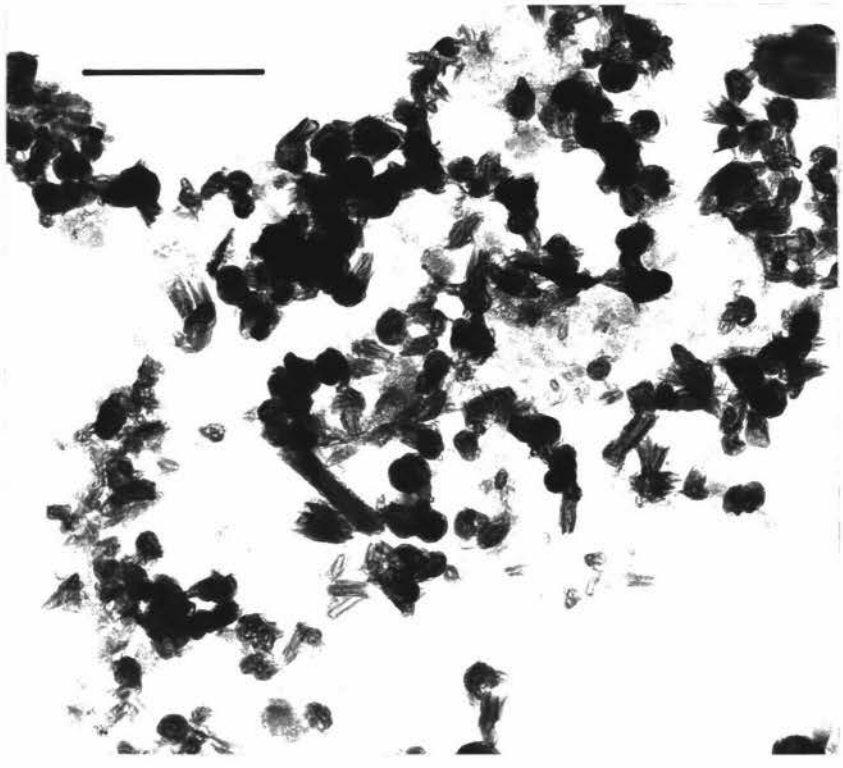

FIGURE 32: Transmission electron micrograph of <1.0μm size clay of Post-Okareka loess at Tarukenga section.
Halloysite curled flakes occur in greater amount than halloysite ellipsoids.
(Bar = 0.5μm)

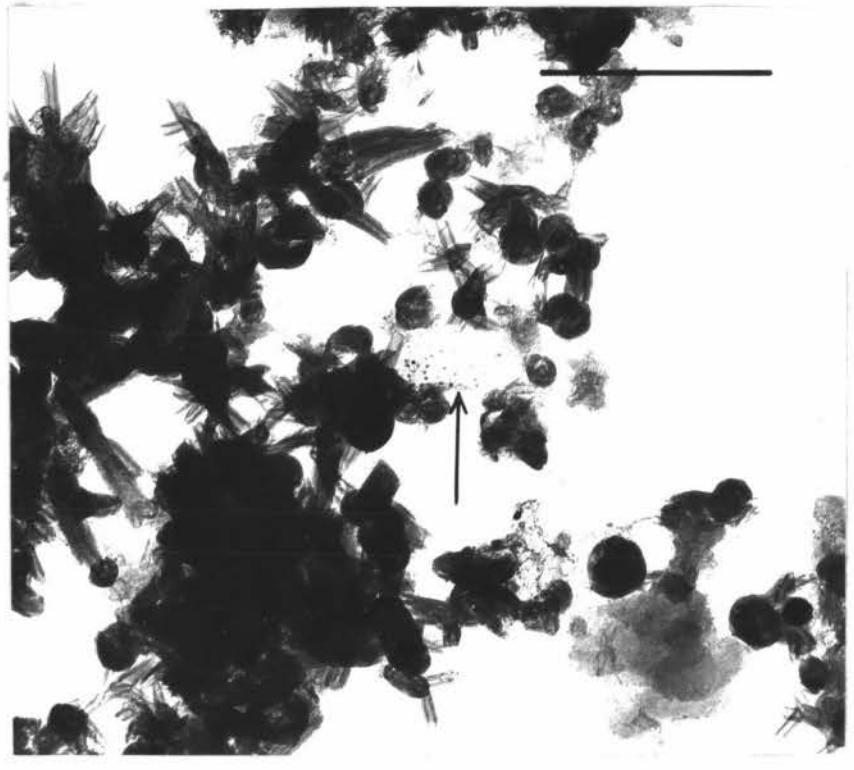

FIGURE 33: Transmission electron micrograph of <1.0μm size clay of Post-Okareka loess at Dalbeth Rd section, showing halloysite curled flakes in greater amount than halloysite ellipsoids. TEM also shows small electron-dense spheres (arrowed) which are probably iron and/or manganese concretions (Bar = 0.5μm).

amounts subordinate to noncrystalline material. Small peaks at 3696cm^{-1} and 3620cm^{-1} and 920cm^{-1} on IR spectra indicate a trace of halloysite (Figure 28D), but intense absorbance in the 3450cm^{-1} region and at 1060cm^{-1} show allophane is present in moderate to high amount. A small amount of gibbsite which absorbs at 3535cm^{-1}, 3470cm^{-1}, 3410cm^{-1} and 1025cm^{-1} is also revealed on IR spectra. Differential thermal analyses reveal a large dehydration peak in 70 - 75^{o}C region (Figure 29E), as well as a shallow endothermic peak at 468^{o}C due to a small amount of poorly-ordered halloysite. Thermal curves also show an endotherm at 240^{o}C due to gibbsite, and an exothermic peak at 970^{o}C which results from a recrystallisation reaction of dehydroxylation products. Infra-red and DTA analyses of loess deposits indicate allophane occurs in greater amount in basal layer samples than in upper loess layers. Investigation by TEM reveals allophane dominates clay fractions of all loess samples, with only trace amounts of halloysite ellipsoids and curled flakes, which are often observed between silica flakes (Figure 34). Allophane occurs as fine particles associated with thread-like imogolite, and as aggregates of weathering glass material.

4.3.6 Gibbsite in clay fractions of ash and loess deposits

X-ray diffraction, IR and DTA analyses show gibbsite is present in most ash and loess deposits sampled for this study. Gibbsite often occurs in amounts too low to be observed on XRD patterns, but such amounts are unmistakeably detected by IR, and particularly DTA methods.

In Okareka Ash and Post-Okareka loess deposits absorption peaks definitive of gibbsite are shown on IR spectra in the 3400 - 3600cm^{-1} region (Figure 28B). Furthermore DTA records an endothermic peak in the range 225 - 255^{o}C which may be attributed to gibbsite (Figure 35D). Well-ordered crystalline gibbsite, however, yields an endotherm in the 300 - 330^{o}C region (Hsu, 1977),

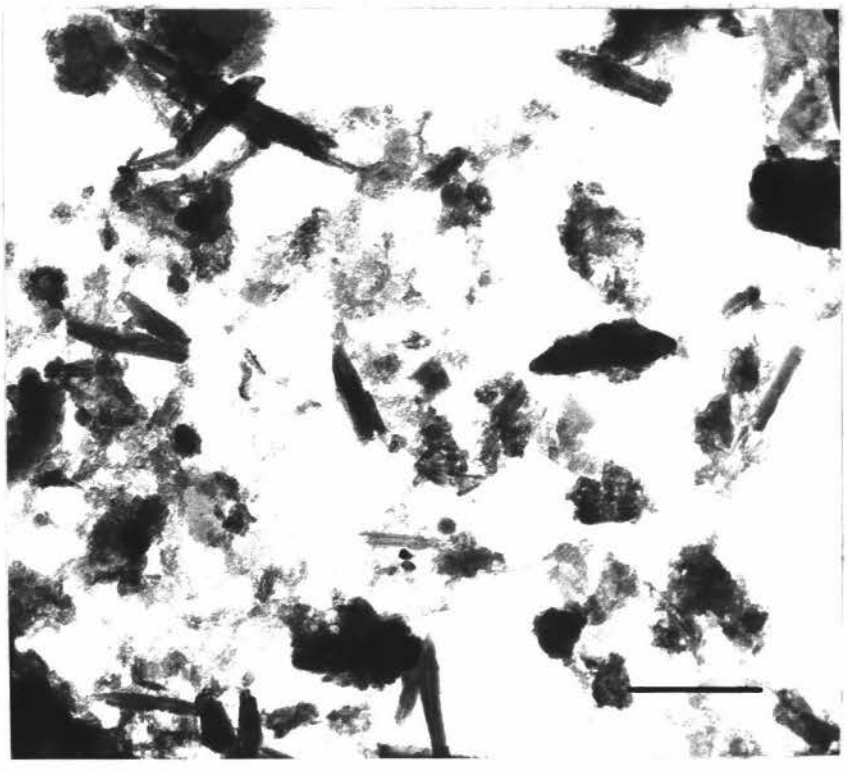

FIGURE 34: Transmission electron micrograph of <1.0μm size clay of Post-Okareka loess at Highland Hill section.
Clay samples consist predominantly of allophane, with some imogolite, and weathering glass and crystalline material (Bar = 0.5μm).

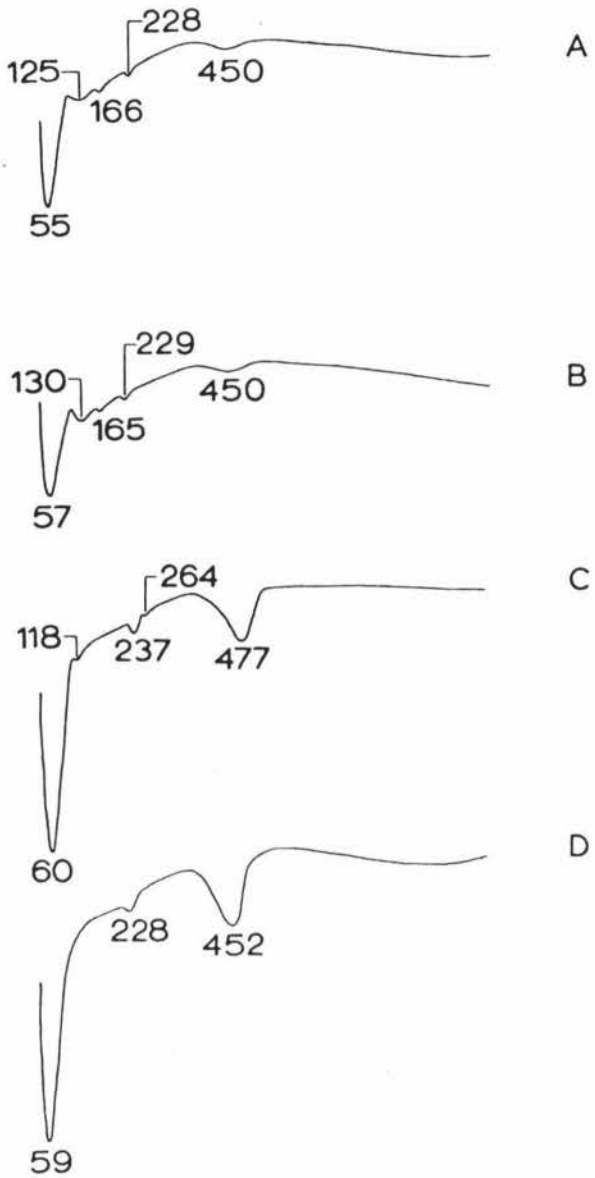

FIGURE 35: Differential thermal curves (^{o}C) of Post-Okareka loess (basal sample - DL_4) silt and clay fractions at Dalbeth Rd section:

A - 63-20 µm
B - 20-5 µm
C - 5-1 µm
D - < 1.0 µm

showing low endothermic peaks in 118-237^{o}C region due to gibbsite and/or cristobalite.

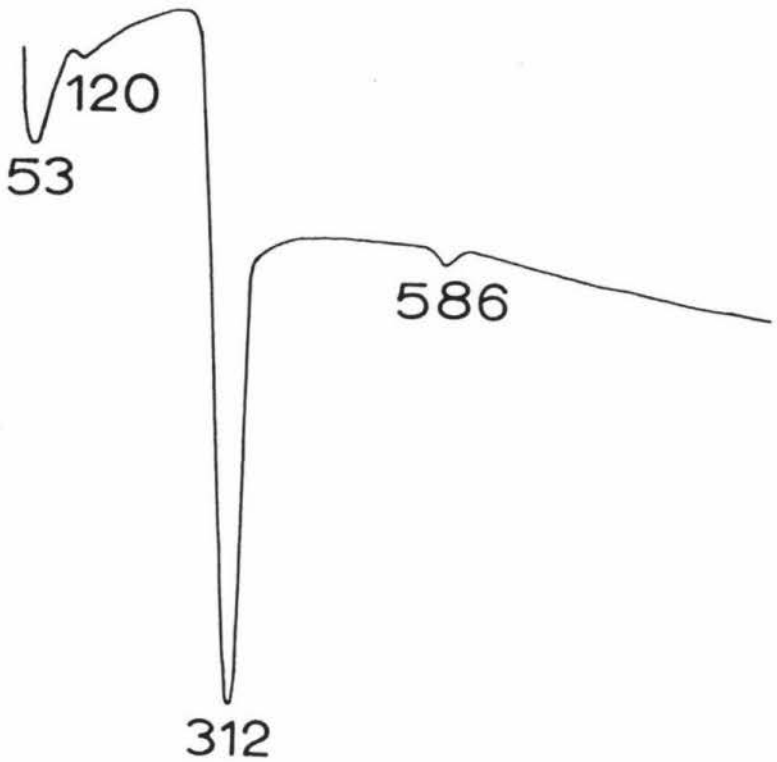

FIGURE 36: Differential thermal curve (^{o}C) of a well-ordered crystalline sample of gibbsite.

and this is considerably higher in temperature than any gibbsite observed in this study. This suggests that gibbsite occurring in Okareka Ash and Post-Okareka loess deposits is poorly-ordered and therefore gives an endothermic peak at lower temperatures.

To investigate gibbsite occurrence in silt fractions 1 - 5μm, 5 - 20μm and 20 - 63μm, two loess samples (upper and basal layer samples) from Dalbeth Rd section were analysed, using DTA and IR methods. A laboratory specimen of well-crystallised gibbsite was used as a reference mineral in both methods. The thermal curve for the reference mineral (Figure 36) shows a shallow endothermic peak at 129^{o}C, an intense peak at 310^{o}C, together with a small peak at 586^{o}C, all due to gibbsite. Absorption bands at 3540cm^{-1}, 3475cm^{-1} and 3420cm^{-1} were observed on the IR spectrum for the same mineral, with a

further definitive peak at 1015cm^{-1}.

Thermal curves of upper loess (DL_1 - Figure 28D), and basal loess (DL_4 - Figure 35D) clay (<1μm) fractions show peaks at 229°C and 228°C respectively, which are attributed to gibbsite. A trace amount of gibbsitic material is also indicated in DL_1 sample by a shallow endotherm at 118°C. Differential thermal analyses of 1 - 5μm, 20 - 5μm and 20 - 63μm (Figures 35D, 35C and 35B, respectively) fractions reveal curves are similar to that of the clay fraction with endothermic peaks in the 118 - 130°C and 228 - 240°C regions, due to gibbsite.

The thermal curve for cristobalite yields an endothermic peak in the range 120 - 130°C. It is possible that some reaction in this region, evident in both loess samples, could be due to this mineral, as IR spectra of all fractions greater than 1μm show an 800cm^{-1} absorption band, due to a highly siliceous mineral, possibly cristobalite or glass.

MINERALOGY	SAND / SILT	Okareka Ash %	Post-Ok. loess %	CLAY	
				Okareka Ash	Post-Okareka loess
	volcanic glass	±75	±80	variable amounts of	variable amounts of
	quartz	±10	±6	halloysite	halloysite
	feldspar	±12	±15	allophane	allophane
	biotite mica	<5	<2	imogolite	imogolite
	hypersthene	<3	<3	± gibbsite	gibbsite
	hornblende	<2	<2		
	augite	<1	<2		
	titanomagnetite	<6	<5		
	cristobalite	<5	<5		
	tridymite	<5	<5		
	N.B. feldspar and augite decreases, and biotite increases towards base of loess bed.				N.B. amount of halloysite in loess is usually greater than in the underlying ash.

MORPHOLOGY	SAND / SILT	CLAY
Okareka Ash	angular grains, relatively un-weathered, some surface weathering, especially feldspar, biotite, hypersthene and titanomagnetite	predominantly halloysite ellipsoids
Post-Okareka loess	subangular-subrounded grains, more weathered than ash, increased weathering with distance from ash source	greater proportion of halloysite curled flakes, increasing amount of halloysite ellipsoids towards base of loess bed

TABLE 3: Summary of Mineralogical and Morphological Results

Chapter 4: DISCUSSION

5.1 Okareka Ash Sand and Silt Mineralogy

Mineralogical results of Okareka Ash deposits sampled in the present study confirm that this ash is a biotite-bearing rhyolitic tephra. Studies by Birrell and Pullar (1973) showed that sand fractions of Okareka Ash contained augite and an increased amount of hypersthene, attributable to contamination by andesitic ash. Augite is present in trace amount in all Okareka Ash deposits, and in slightly greater quantities in the basal layer of Okareka Ash at Trunk Rd section. Several authors have found augite is a common constituent of Central North Island rhyolitic ashes (Ewart, 1963; Topping and Kohn, 1973), and it follows that the presence of this mineral may not necessarily indicate andesitic contaminants. Furthermore, hypersthene is present in consistent quantities (1 - 2%; Appendix 1) in all Okareka Ash deposits.

Okareka Ash samples also contain trace amounts of cristobalite and tridymite. These silica minerals are often found in spherulitic rhyolite, which is typical of rocks associated with Okataina Volcanic Centre, in particular, the Tarawera Complex (Cole, 1970b). Pullar and Birrell, 1973a and b) attributed the source of Okareka Ash to this area. Commonly, rhyolite with a biotite-dominated mineralogy is erupted from this volcanic centre (Ewart, 1963; Topping and Kohn, 1973). However, occasionally basaltic material has erupted explosively from vents in older rhyolitic rocks (Thompson, 1964), for example Tarawera Basalt Lapilli A.D.1886 (Cole, 1970a). The occurrence of a darkly coloured basal ash and lapilli layer in Okareka Ash Formation at Trunk Rd section suggests Okareka Ash eruption commenced with the emission of a small amount of basaltic material which was followed immediately by successive pulses of rhyolitic material. The basaltic layer was found at the base of thick deposits of Okareka Ash in a localised area, eastward and downwind

from source. The bulk of the rhyolitic material became distributed in an easterly direction from source, although a considerable amount was deposited upwind in western areas of Rotorua district (Figure 2).

Results from this study show that although Okareka Ash mineralogical composition is consistent between sections, considerable variation in the amounts of minerals is apparent. Such variations can be attributed to continued eruption of rhyolitic material at different intensities and directions from the vent, changes in wind direction, and depletion of coarser and heavier material from the ash cloud with increasing distance from source (Fisher, 1964, 1971; Walker, 1971).

5.2 Post-Okareka loess Sand and Silt Mineralogy

The mineralogical compostion of Post-Okareka loess deposits is similar to that of Okareka Ash deposits, which suggests the source area of this loessial material comprised predominantly rhyolitic material. Many Central North Island tephras erupted during late Pleistocene times contain a trace amount of biotite mica, but few are considered biotite-bearing as are Okareka Ash c.17,000 years B.P., and Rerewhakaaitu Ash c.14,700 ± 200 years B.P. (Topping and Kohn, 1973). Since Rerewhakaaitu Ash overlies Post-Okareka loess this clearly cannot be the source of loess, which suggests Okareka Ash is the major source material. Furthermore, biotite mica is present in greater amount in basal loess layers, and in lesser quantities in upper samples, which implies Okareka Ash became depleted towards later stages of Post-Okareka loess accumulation.

Cristobalite and tridymite are also present in Post-Okareka loess deposits, and are most probably derived from Okareka Ash. However, these minerals are constituents of Mamaku Ignimbrite c.220,000 years B.P., and also can be formed as secondary minerals in the weathering environment. X-ray diffraction results

indicate these silica minerals are not highly ordered, but are present in grain-size fractions coarser than fine silt. These data suggest cristobalite and tridymite were formed as late products of crystallisation or possibly as a result of reheating by hydrothermal processes (Hardjosoesastro, 1956; Cole, 1970b) rather than by neoformation from solution (Wilding et al. 1977). Tephras deposited prior to Rotorua Ash 13,450 ± 250 years B.P. have been eroded away down to and including weathered Mamaku Ignimbrite, for a distance 11km westwards along state highway No.5 between Rotorua and Tirau (Figure 3: Pullar and Birrell, 1973a). Small quantities of eroded ignimbrite material containing cristobalite and tridymite may have been derived from this source.

Augite, plagioclase feldspar and rhyolitic volcanic glass occur in greater amounts in Post-Okareka loess deposits than in Okareka Ash deposits. Increased quantities of these minerals may be due to differential transport or sorting of particles prior to deposition of loess, as well as to the occasional additions of wind-blown material from sources other than Okareka Ash. During Post-Okareka loess accumulation, particularly in peripheral areas, where ash beds are thinnest, Okareka Ash deposits would have provided only a limited supply of tephric material. Post-Te Rere loess or Post-Kawakawa loess deposits underlie Okareka Ash, and it is conceivable variable amounts of these materials, especially in erosion-prone areas such as valley sides, may have become eroded, reworked and redeposited. Furthermore, ignimbrite plateaus, likened to cold mini-deserts (Kennedy and Pullar, 1977), may have also contributed an appreciable portion of material to Post-Okareka loess deposits.

Differences in mineralogy between Post-Okareka loess and Okareka Ash are most evident in the upper parts of loess beds. This implies a greater variation in source material during the later stages of loess accumulation

when Okareka Ash deposits were either buried beneath loess, or had been completely eroded. Variation in local topography, near-surface turbulent winds, and prevailing wind directions, would also result in changes in a localised source area, and is evident by mineralogical changes in Post-Okareka loess deposits between sections. Such variability was noted in the present study because several sections were sampled, rather than one or two as is frequently the case.

5.3 Okareka Ash Sand and Silt Morphology

Tephra is defined as "all pyroclastic materials which, during an eruption, are transported from the crater through the air" (Thorarinsson, 1954). Pyroclastic fragments are formed by either magmatic, phreatomagmatic or combinations of these two types of eruptions. The shape and texture of pyroclastic particles, can therefore be related to the type of eruption, and magma composition (Heiken, 1972).

In magmatic eruptions of high viscosity lava such as rhyolite, the shape of volcanic glass particles is dependent on vesicle shape and the density of the glass (Heiken, 1972). Such characteristics, which are inherited from the eruption, are evident in volcanic glass fragments within Okareka Ash deposits, particularly at sections closest to source. Okareka Ash glass particles exhibit a morphology typical of a magmatic eruption of rhyolitic ash, which comprises fragments of vesicular glass, flat glass plates, and fibrous pumice fragments.

In contrast to volcanic glass, the morphology of crystalline fragments within ash deposits largely reflect the mechanical properties of the parent rock, and are dependent upon the amount of interparticular abrasion within the conduit during eruption (Heiken, 1972). In Okareka Ash deposits, especially at sections close to source, crystalline minerals are equant and slightly subangular. However, with increasing

distance from source, Okareka Ash particles exhibit features typical of wind sorting and abrasion, and post-depositional weathering processes. These processes have resulted in subangular to subrounded grain morphology. The surfaces of volcanic glass fragments in Okareka Ash deposits at distance from source have remained relatively smooth and unweathered, although pumiceous particles contain a greater amount of presumed short-range order material in vesicles, and some weathering cavities. With increasing distance from ash source, susceptible crystalline minerals such as feldspar, hypersthene and titanomagnetite, show increased alteration by weathering, and are tending to be more subrounded. Grain morphologies of glass and crystalline fragments in Okareka Ash deposits at sections furthest from source closely resemble those of tephric loess particles.

5.4 Post-Okareka loess Sand and Silt Morphology

The shape and surface texture of a loess grain can provide clues as to its origin and depositional history, and to chemical processes within its immediate environment (Allen, 1970; Smalley and Cabrera, 1970). Morphological studies of Post-Okareka loess particles, indicate that although fragments were originally derived from tephric material, they have been reworked and redeposited by aeolian processes.

Sand grains in aeolian deposits are moved primarily by saltation, and silt-sized particles are carried in suspension by wind (Selby, 1976). In Post-Okareka loess deposits, particularly at sections close to Okareka Ash source, sand grains are angular, which suggests a relatively short period of saltation, and, therefore, a short travelling distance. Loess deposits furthest from ash source, contain less sand-sized material, with many fractured edges on grains indicative of longer periods of saltation. Silt-sized grains are lifted to greater heights than sand grains,

and, therefore, are carried much greater distances (Embleton and King, 1975).

Post-Okareka loess silt grains are more rounded than sand grains, the trend becoming more apparent with distance from Okareka Ash source. Clay and very fine silt-sized material, possibly created by abrasion and attrition of aeolian grains during reworking and transportation, are observed covering grain surfaces, or are aggregated into coarse silt and fine sand-sized particles. Aggregates, together with material adhering on grain surfaces, are common in Post-Okareka loess deposits. Similar features have also been observed for aeolian deposits found in Long Island, USA (Margolis and Krinsley, 1971: Nieter and Krinsley, 1976). However, aggregates of fine clay-sized material are also present in Okareka Ash deposits from sections furthest from source, which indicates they were produced by aeolian processes, or formed by post-depositional processes.

5.5 Weathering in Okareka Ash and Post-Okareka loess deposits

Studies by Aomine and Wada (1962); Fieldes and Furkert (1966); Kirkman (1975, 1980); Birrell *et al.* (1977); Parfitt *et al.* (in press) have demonstrated that weathering of tephra and tephra-derived soils is dependent upon several inter-related pedogenic factors. Most of these investigations compared several ash deposits of varying age, but commonly individual beds were sampled once only, usually at the 'best' site (e.g. Birrell and Pullar, 1973; Kirkman, 1975; Mizota, 1976). This type of study has been used to elucidate the weathering of primary and secondary minerals, including glass, feldspar and allophane, under a wide range of pedogenic conditions. While such studies have shown that formation of halloysite, gibbsite, imogolite and allophane are interdependent within weathering environments of tephra and tephra-derived soils, the mechanisms and processes involved in

their formation are less well understood (Farmer et al. 1978; Parfitt, et al. in press). The present investigation was designed so that detailed mineralogical analysis of a particular deposit at several locations could be made in order to compare weathering processes and products. This study attempts to relate the formation and abundance of clay minerals to local variations in environmental factors, such as topography, altitude, overburden depth, rainfall, and drainage within two types of deposit of similar age and composition.

Investigations of Central North Island tephras and tephric loess deposits (Vucetich and Pullar, 1969; Pullar and Birrell, 1973a; Birrell and Pullar, 1973; Cowie and Milne, 1973), have shown weathering differences occur between tephras deposited prior to deposition of Rerewhakaaitu Ash 14,700 $\pm$ 200 years B.P. and those ashes deposited subsequent to that eruption. Despite a higher amount of halloysite in clay fractions of late Pleistocene tephras Okareka Ash, Te Rere Ash and Kawakawa Tephra, sand fractions of these tephras were found to be more weakly weathered than younger ashes which were dominated by allophane (Birrell and Pullar, 1973). Results from this study confirm observations by Birrell and Pullar (1973) that sand and silt particles of Okareka Ash remain angular. Furthermore, it is only at sites of high rainfall and altitude that grains become more subangular, and coated with weathered material. This evidence supports the view that Okareka Ash accumulated during a glacial period when cool, semi-arid conditions inhibited soil development (Birrell and Pullar, 1973).

Within Post-Okareka loess, deposited in the period c.17,000 - 15,000 years, weathering is more advanced, especially in upper loess layers. This may be attributed to a finer particle-size, and possibly warmer conditions encouraging plant growth, particularly towards later stages of loess accumulation. The

absence of paleosol features in upper Post-Okareka loess layers at all sections except Trunk Rd indicates, either paleosols which had developed were subsequently eroded away, or that climatic conditions were such that insufficient vegetation was present for soil development. Nevertheless, a warmer climate, and, therefore, a more luxuriant vegetation is implied by an absence of loessial material overlying Rerewhakaaitu Ash. This suggests loess accumulation continued but was gradually diminishing prior to eruption of Rerewhakaaitu Ash. A minor amount of loess deposited after this eruption may have become incorporated into the tephric material, possibly by pedogenic processes. Since eruption of Rerewhakaaitu Ash, a more temperate climate has encouraged vegetative growth, which has facilitated weathering of younger ash deposits, and resulted in obvious paleosol development (Kennedy, 1980).

In the present study, weathering of primary minerals is more advanced in Post-Okareka loess deposits, particularly at sections experiencing high rainfall conditions, i.e. Highland Hill and Kuhatahi. However no distinctive differences in degree of weathering are observed within either deposit at all other sections. In Okareka Ash and Post-Okareka loess deposits it is the less-resistant minerals, such as plagioclase feldspar, biotite mica and mafic minerals, which are most weathered.

Alteration of plagioclase feldspar and, to a lesser extent volcanic glass in Okareka Ash and Post-Okareka loess deposits, is revealed by surface coatings of short-range order material, and solution pits. In silt fractions, particularly within silt-sized aggregates, halloysite tubes were observed on grain surfaces, which suggests these aggregates comprise predominantly fine particles of feldspar and possibly glass (Figure 16A and 16B).

Biotite-vermiculite is generally formed in an environment where efficient leaching causes hydrated ions to replace potassium at fracture edges and crystallographic dislocations (Douglas, 1977), resulting in expansion of interlayer spaces of biotite flakes (Figure 15A). Biotite and biotite-vermiculite increase in amount towards the base of Post-Okareka loess deposits, which implies either differential weathering of this mineral in upper loess layers, or a decrease in amount of biotite-rich source material during later stages of loess accumulation. Mineralogical data suggests the latter is more likely, as in basal loess layers the amount of biotite is not proportional to that of biotite-vermiculite, or vermiculite found in upper layers.

The factors that determine the nature of weathering processes, i.e. parent material composition, climate and other pedogenic conditions, and are particularly relevant to ferromagnesium minerals, whose weathering products are determined by oxidation, acidity and drainage status of the soil environment (Wilson, 1975). The ferromagnesium minerals hypersthene, augite, titano-magnetite, and to a lesser extent hornblende, are widely regarded as easily weatherable but details of the mechanisms of degradation are unknown (Wilson, 1975). Alteration of these minerals in Okareka Ash and Post-Okareka loess samples are revealed by iron oxide rims, solution pits and weathering along cleavage planes. The weathering products of these minerals often result in iron/manganese pinhead-size concretions, which commonly are disseminated through Post-Okareka loess, and sometimes Okareka Ash deposits. These concretions result from precipitation of iron when an enriched solution encounters oxidizing conditions in a highly leached environment (Aomine and Wada, 1962).

In contrast to plagioclase feldspar and mafic minerals, cristobalite, tridymite and quartz remain resistant to weathering processes in Okareka Ash and

Post-Okareka loess deposits, even under highly leached conditions.

The dissolution of a highly siliceous parent material under well-drained conditions, and subsequent desilication of alumino-silicate minerals and glass, results in silica enrichment of the soil solution (Kirkman and McHardy, 1980). Recent studies suggest that in this situation the concentration of silica in solution determines the type and abundance of secondary minerals (Birrell et al. 1977; Kirkman, 1978; Parfitt et al. in press).

In the present study, despite wide variation in environmental factors such as overburden depth, topography, altitude and rainfall, Okareka Ash clay fractions from sections closest to source, i.e. Trunk Rd, Te Ngae, Gavin Rd, Okareka Quarry and Lynmore, and at Ngongotaha section, are dominated by halloysite. However, clay samples from Okareka Ash deposits at Pukehangi Rd, Tarukenga, Dalbeth Rd, Highland Hill and Kuhatahi sections, contain a much greater amount of allophane and imogolite than halloysite. Except for Pukehangi Rd, these sections are furthest from ash source, are at relatively high altitudes ($>$ 380m), and receive a high amount of moisture from rainfall, fog and low cloud. Under these conditions, intense leaching of silica from rhyolitic ash tends to perpetuate allophane and depress halloysite formation (Parfitt et al. in press). However, at present, Pukehangi Rd section has similar environmental conditions to that of Ngongotaha and Lynmore sections which contain a dominant amount of halloysite. This suggests, therefore, that past conditions, in particular drainage, have changed and subsequently altered the course of weathering in one or other of these sections.

It has been suggested that imogolite forms only where depositional overburden of volcanic ash, which serves as a silica source, is relatively thin (Aomine and Mizota, 1973). At Tarukenga and Dalbeth Rd

sections depositional overburden is much greater than at other sections, and based on the observation of Aomine and Mizota (1973), imogolite would not be expected to occur in appreciable amount. Nevertheless, mineralogical results indicate Okareka Ash clay fractions at these sections contain quite a high proportion of imogolite compared to allophane (Figure 21B). Imogolite is also present in lesser amount at Highland Hill and Kuhatahi sections, where depostional overburden is thinnest. Weathered Mamaku Ignimbrite (c.220,000 years B.P.) which would act as an impervious layer to percolating soil solutions, is present at a shallow depth beneath Okareka Ash deposits at these sections. In contrast to what is normally expected in cases of impeded drainage, little weathering of primary minerals, and formation of crystalline clay minerals such as halloysite has occurred.

Birrell et al. (1977) and Parfitt et al. (in press) have suggested that in clay fractions of rhyolitic tephras of Central North Island, the amount of allophane increases and halloysite decreases as rainfall changes from 1200mm to 2600mm. Such trends, however, were not observed in Okareka Ash clay fractions. As well as Pukehangi Rd and Lynmore sections, Ngongotaha and Tarukenga sections also show contrasting clay mineralogies despite similar rainfall and altitude conditions at each site. Okareka Ash clay samples from Lynmore and Ngongotaha sections contain less allophane than halloysite, and the reverse is true of Pukehangi Rd and Tarukenga sections. These differences in clay mineralogy between sections further suggest that past pedogenic conditions have directed clay mineral formation.

Despite wide variation in amount of halloysite in Okareka Ash clay fractions at all sections, the halloysite that is present consists predominantly of squat ellipsoids. The presence of halloysite ellipsoids indicates derivation from highly siliceous volcanic glass, via a short-range order intermediate, probably

allophane (Kirkman, 1977). Halloysite ellipsoids are found to occur, and often appear to be forming, possibly by spiral mechanism (Kirkman, 1977), between silica flakes, and within weathering aggregates of pumiceous glass (Figure 17B). In coarser fractions feldspar grains remain quite angular, and in clay fractions only a few halloysite curled flakes or tubes were observed, which implies little weathering of plagioclase feldspar to halloysite.

Weathering studies in Central North Island suggest that whereas tephra deposits contain more allophane than halloysite, the order of abundance is reversed in clay fractions of the overlying tephric loess deposits (Pullar and Birrell, 1973a; Birrell and Pullar, 1973; Birrell, 1974). These conclusions were confirmed by Russell et al. (1981) who, when working on a largely andesitic-derived tephric loess, and an overlying tephra unit of similar composition in Taranaki, showed that loess deposits contain less allophane, and more halloysite and gibbsite than does the ash. Results of the present study confirm these conclusions. Irrespective of pedogenic factors such as topography, altitude, rainfall and overburden depth, Post-Okareka loess clay fractions contain a greater amount of halloysite and gibbsite than those of Okareka Ash. However, Post-Okareka loess deposits do not always contain a dominant amount of halloysite.

At Pukehangi Rd, Highland Hill and Kuhatahi sections, Post-Okareka loess clay fractions contain less halloysite than allophane. Loess clay samples from these sections are similar to those of Okareka Ash, and contain a significant amount of allophane and imogolite, which suggests processes impeding formation of halloysite occurred in both ash and loess deposits. Except for Tarukenga and Dalbeth Rd sections, loess clay samples exhibit similar mineralogies to those of Okareka Ash. This suggests also that pedogenic processes governing clay mineral formation were

operative in both ash and loess deposits. However, although Okareka Ash clay fractions at Tarukenga and Dalbeth Rd sections are dominated by imogolite and allophane, the overlying Post-Okareka loess clay samples have a greater amount of halloysite.

In contrast to Okareka Ash clay fractions, those of Post-Okareka loess, particularly upper samples, consist predominantly of halloysite curled flakes. This implies plagioclase feldspar is weathering to a greater extent than rhyolitic glass. However, in basal loess layers, a greater amount of halloysite ellipsoids was observed in electron micrographs, which suggests mixing of loessial and tephric components, and increased weathering of tephric (glass-rich) material.

Post-Okareka loess deposits, together with Okareka Ash deposits at Highland Hill and Kuhatahi sections contain gibbsite in clay and silt fractions. A moderate to high amount of gibbsite in both deposits at Highland Hill and Kuhatahi sections is probably due to high rainfall, or possibly poor drainage conditions. The former has been found to be a prerequisite for gibbsite formation in some young ash soils (Sherman et al. 1967). Gibbsite forms under these conditions by reaction of permeating solutions with disordered thin layers on plagioclase feldspar surfaces, during initial stages of weathering in an acid environment (Tazaki, 1979). This process could explain the occurrence of gibbsite in silt fractions in ash and loess deposits, as gibbsite would occur most probably as pseudomorphs of feldspar rather than crystallising from solution (Sherman et al. 1967).

Gibbsite is present in all other Post-Okareka loess deposits, but does not occur in the underlying Okareka Ash deposits. However, plagioclase feldspar is present in greater amounts in loess than ash, and this, together with a warmer climate during later stages of loess accumulation, could encourage gibbsite formation in loess, and not in Okareka Ash. Some gibbsite may arise

from weathering of andesitic glass, a possible contaminant of Post-Okareka loess deposits. However, such glass, if it were ever present, has been completely weathered, since it was not revealed by mineralogical study of the sand and silt fractions.

The present work illustrates the difficulties of sampling techniques in weathering studies. Mineralogical results reveal no consistent trends in weathering of tephra and tephra-derived soils, even when several samples of one or more deposits were taken. The variation in occurrence and abundance of clay minerals in ash and loess deposits between sections, clearly indicates local changes in environment have influenced the course of weathering. This is pertinent to weathering studies, as a detailed knowledge of past and present environmental factors is essential for interpretation of data. However, such detailed information is not always obtainable, nor within the scope of these investigations.

SECTION B:

GRAIN-SIZE ANALYSIS

Chapter 6: LITERATURE REVIEW

6.1 Textural Studies

During the 1930's and 1940's sedimentologists placed much emphasis on the use of grain-size analysis to characterise sediment textures in specific sedimentary environments (e.g. Krumbein, 1938, Doeglas, 1946; Pettijohn, 1949). These studies led to an increased knowledge of grain-size characteristics of a wide range of deposits, but few evaluations were made in terms of depositional processes. Inman (1949) recognised three fundamental modes of sediment transport; surface creep, saltation and suspension. Utilizing existing knowledge of fluid mechanics (Bagnold, 1942; Kalinske, 1943), Inman (1949) derived certain relationships between environments and mean grain-size, sorting and skewness. This work formed the basis for later grain-size distribution investigations which led to development of the essential ideas relating sedimentary processes to textural responses (Visher, 1969). Several studies have used statistical measures of grain size (e.g. Inman, 1952, Bagnold, 1956, Folk and Ward, 1957, Moss, 1962, 1963) to define descriptive features of a sedimentary deposit.

Textural parameters such as mean grain-size, sorting, skewness and kurtosis were used to separate deposits within beach, dune, aeolian and fluvial environments, which has enabled correlation between sediment types, their mode of deposition, and their environment in many locations. These investigations have shown that textural parameters may not always be sufficiently accurate to characterise a deposit formed by a specific depositional process. However, grain-size studies do facilitate differentiation of deposits within which sediments possess textural characteristics inherited from several sedimentary processes. Loess deposits of this nature have been reported in Argentina, where a greater part of the Pampean sediments consist of reworked or secondary loess (Teruggi, 1957). These deposits have

a mineralogical composition of volcanic-pyroclastic origin, and are similar to wind-deposited volcaniclastic material analysed by Fisher (1966). Such aeolian deposits comprise predominantly reworked tephric material, although they exhibit grain-size characteristics which are similar to primary loess deposits found in Europe and North America (Teruggi, 1957; Fisher, 1966). Although tehpric loess deposits analysed by Teruggi (1957) and Fisher (1966) are of older age, loessial deposits found overlying several late Pleistocene tephras in Central North Island also consist of reworked and redeposited pyroclastic material. However, in contrast to these deposits, Central North Island loess deposits bear close resemblance to the underlying airfall tephra (Vucetich and Pullar, 1969). It is necessary, therefore, to consider the variables that affect the textural characteristics of loess and airfall tephra, in order to evaluate tephric loess deposits in these different environments.

Loess deposits were first recognised in the Northern Hemisphere, particularly Europe and USA, where deposits formed important agricultural land (Selby, 1976). Although several European authors (e.g. Russell, 1944a, 1944b; Berg, 1964) debated the aeolian origin of loess, it was generally accepted by the early 1970's that loess was a result of glacial action, and had accumulated in regions peripheral to continental ice sheets in areas of periglacial conditions (Smalley, 1966; Smalley and Vita-Finzi, 1968). Textural studies evaluated loess characteristics using variables such as particle size, loess thickness, distance from source, wind direction and strength. Early grain-size investigations of loess (e.g. Krumbein, 1937; Smith, 1942; Swineford and Frye, 1945, 1955) used changes in loess distribution and thickness with distance from source to propose models, which were later refined by researchers such as Waggoner and Bingham (1961), and Frazee et al. (1970). Subsequently these models have been developed to demonstrate relationships between aeolian sediments in

many different locations (Franzmeier, 1970; Fehrenbacher, 1972; Ives, 1973; Handy, 1976).

Textural studies of tephra are similar to that of loess, and have involved consideration of variables such as wind strength and direction, distance from source, and thickness of deposit (Fisher, 1964, 1971; Walker, 1971). The importance of textural parameters to pyroclastic deposits was first established by Moore (1934), who differentiated airfall and airflow tephra by mechanical analysis. During the ensuing forty years, investigations of many pyroclastic deposits resulted in data which have facilitated correlation of grain-size characteristics with factors such as mechanisms of eruption, magma composition and dispersal (e.g. Thorarinsson, 1954; Murai, 1963; Fisher, 1971; Walker, 1971; Walker and Croasdale, 1971, 1972; Watkins and Huang, 1977). Characterisation of volcaniclastic deposits according to these criteria has, therefore, assisted comparison between these deposits and other aeolian deposits (e.g. Fisher, 1966).

In a study of John Day Formation of eastern Oregon, Fisher (1966) compared textural characteristics of tuff and loess. Using Inman sorting coefficients, loess derived from volcaniclastic material was shown to be better sorted than airfall tephra deposits. Loess deposits, in general, are better sorted than airfall tephra, as wind is highly effective in separating silt-size grains, which are uplifted and carried long distances greater than a metre from the surface, and sand particles, that travel by saltation close to the ground for shorter distances (Fisher, 1964; Allen, 1970; Embleton and King, 1975). In contrast to loess, volcanic ash particles are continually sorted by wind within the ash cloud, and studies by Fisher (1964, 1971) and Walker(1971) have found that with distance from source, airfall tephra deposits tend to become better sorted, and loess deposits more poorly-sorted. However, compared to loess, ash deposits are more poorly-sorted when deposited, and with time, post-depositional

processes further increase sorting coefficients of the original deposits (Fisher, 1966).

Both tephra and loess deposits exhibit an exponential decrease in thickness downwind from source, and a corresponding decrease in mean grain-size (Fisher, 1964; Scheidigger and Potter, 1968). The greatest variability in mean grain-size in both deposits occurs close to source, but the causes of such variability differ between them (Walker, 1971; Frazee et al. 1970). Deposits of coarse and fine-grained tephric material found near the vent may be attributed to variation in strength and direction of the eruption, as well as increased turbulence due to interaction of airfall and airflow material (Walker, 1971). In contrast to airfall tephra, loess particles close to source are affected to a greater extent by turbulent winds, variable wind velocities, and bluff topography. These variables have an important effect upon particle size changes with distance from source (Frazee et al. 1970; Handy, 1976). With increasing distance from source, both tephra and loess distribution is controlled predominantly by wind direction and strength. Consequently, in peripheral areas of deposition grain-size characteristics tend to become similar, making the differentiation of two sediments more difficult. Other factors influencing the thin distal deposits are worms (bioturbation), vegetation, and with time, pedogenesis (Fisher, 1966).

In this study an attempt was made to gauge the effectiveness of grain-size parameters in distinguishing between tephra and tephric loess deposits in Central North Island. A single tephra, Okareka Ash, and its associated overlying tephric loess, Post-Okareka loess, were analysed at several locations at varying distances from ash source. Weathering effects upon the textural parameters (graphic mean grain-size - Mz, inclusive graphic standard deviation - σ_I, inclusive graphic skewness - SK_I, and graphic kurtosis - K_G; Folk, 1968) were also evaluated during the course of this study.

Chapter 7: MATERIALS AND METHODS

7.1 Analytical Techniques

For grain-size analysis, a 50g aliquot of field moist soil was suspended in distilled water, dispersed and wet sieved as for mineralogical analysis. The $>63\mu m$ fraction was dried at $55^{o}C$, dry sieved at 1mm, $500\mu m$, $250\mu m$, $125\mu m$ and $63\mu m$ grain intervals, and the fractions weighed. Any material passing through the $63\mu m$ sieve was added to the $<63\mu m$ suspension. An untreated 20g aliquot of field moist soil was dried at $55^{o}C$ for 2-3 days for determination of moisture content.

Sodium dithionite (Mitchell *et al.* 1971) was used to remove free Fe_2O_3 and associated silica and alumina from the $<63\mu m$ fraction, prior to grain-size analysis by pipette (Folk, 1968). For grain-size analysis the clay fraction ($<2\mu m$) was assumed to be of secondary origin, and therefore grain-size curves were calculated on a clay-free basis.

Grain-size data was analysed using a computer program designed by Adams (1977).

Chapter 8: RESULTS AND DISCUSSION

8.1 Grain-size parameters

8.1.1 Mean grain-size (Mz): Okareka Ash

Initially, the particle size and quantity of pyroclastic material erupted from a volcano is dependent upon magnitude and direction of eruption. After ejection from the vent pyroclastic fragments are carried through the air, and may settle out or be sorted according to their fall velocities (Walker, 1971). Important factors influencing airborne pyroclastic material are wind direction and strength. The former determines the direction the major amount of material is carried, and the latter determines the sorting efficiency of particles (Fisher, 1964; Walker, 1971).

Field observations and grain-size results of Okareka Ash Formation at Trunk Rd indicate pulses of tephric material were erupted in closely spaced succession. The Trunk Rd site is located directly downwind in an eastward direction and in close proximity to Okareka Ash source, but, except for Gavin Rd site, all remaining sections are located immediately upwind from source (Figure 3). Okareka Ash samples from Trunk Rd have a much coarser mean grain-size than other sections, and comprise laminated beds of ash and lapilli (Mz $<3\emptyset$ ($>125\mu m$) medium-coarse sand). At all other sections sampled in this study Okareka Ash deposits show no evidence of separate phases of erupted material. This suggests many of the eruptives recorded at Trunk Rd were not carried far, or that pyroclastic fragments became mixed by turbulent winds while still airborne.

Okareka Ash deposits exhibit mean grain-size characteristics typical of airfall tephra (Fisher, 1964; Scheidigger and Potter, 1968; Walker, 1971). Ash samples show a wide range of mean grain-size values (1.5 - $4\emptyset$: (350 - $60\mu m$), medium-very fine sand - Appendix 4), with coarsest and most variable values from sections closest to source, i.e. Trunk Rd, Gavin Rd, Okareka Quarry, Lynmore and Te Ngae sections (Figure 37).

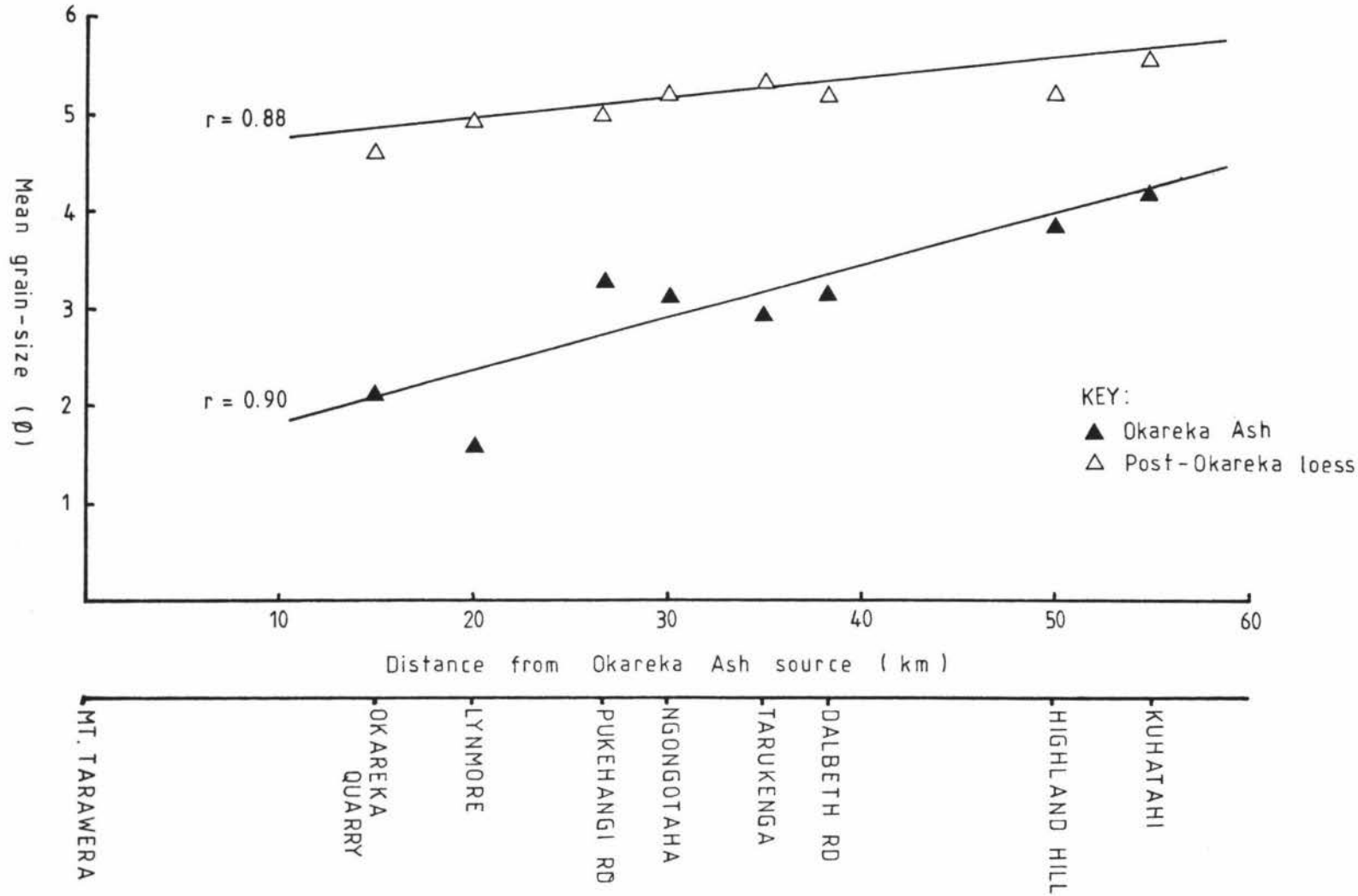

FIGURE 37: Mean grain-size of Okareka Ash and Post-Okareka loess in relation to distance from ash source.

At these sections, Okareka Ash deposits contain a high percentage of material in the coarse sand fraction as well as a considerable amount of material greater than 2mm (Figure 38). Okareka Ash deposits show a progressively finer mean grain-size with increasing distance from source (Figures 37 and 38). After eruption of Okareka Ash, the ash cloud, with increasing distance from source, became depleted gradually in coarse-grained material. This is also reflected by a decreasing sand content, and an increase in the proportion of silt in ash deposits at sections furthest from source (Figure 39.)

8.1.1 Mean grain-size (Mz): Post-Okareka loess

The amount of sand-sized material in airfall tephra deposits is higher than in loess as coarse fragments are ejected into the air by the energy of eruption and become airborne irrespective of wind strength and direction (Fisher, 1964). In contrast, uplift and deposition of loess grains is entirely dependent upon wind conditions. Two factors of transportation; lift and carry, affect particle size mode of loess deposits. Silt-size particles in the range 50 - 10μm are lifted and carried most efficiently in suspension by wind (Selby, 1976). However, sand grains move by a combination of creep and saltation within a metre of the ground surface, and travel much shorter distances than suspended silt grains (Embleton and King, 1975).

Mean grain-size values of Post-Okareka loess deposits occur in the narrow range 4.0 - 5.5Ø (63 - 20μm) coarse silt (Appendices 5A and 5B), and are consistently finer than Okareka Ash (Figure 40). Mean grain-size of Post-Okareka loess deposits tends to increase towards the base of loess beds due to mixing of tephric loess with the underlying tephra (Figure 41).

In contrast to Okareka Ash, Post-Okareka loess deposits contain a small amount of sand-sized material, which decreases in amount with increasing distance from source (Figure 39). This suggests source material was finer at distance from ash source, and could also

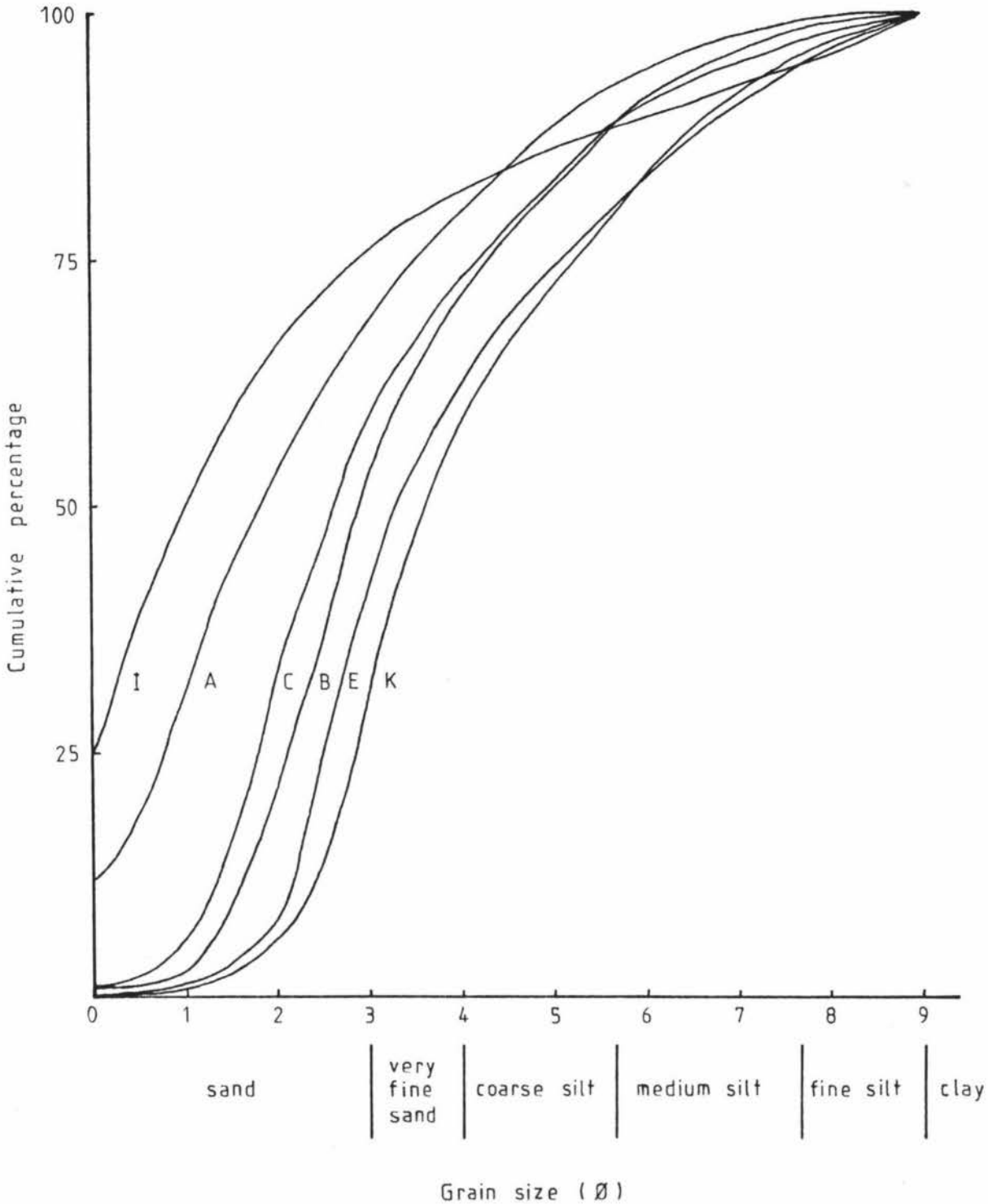

FIGURE 38: Grain-size cumulative curves for Okareka Ash deposits at: A, Okareka Quarry; I, Lynmore; B, Pukehangi Rd; C, Tarukenga; E, Highland Hill; and K, Kuhatahi sections, showing grain-size distribution changes with increasing distance from source.

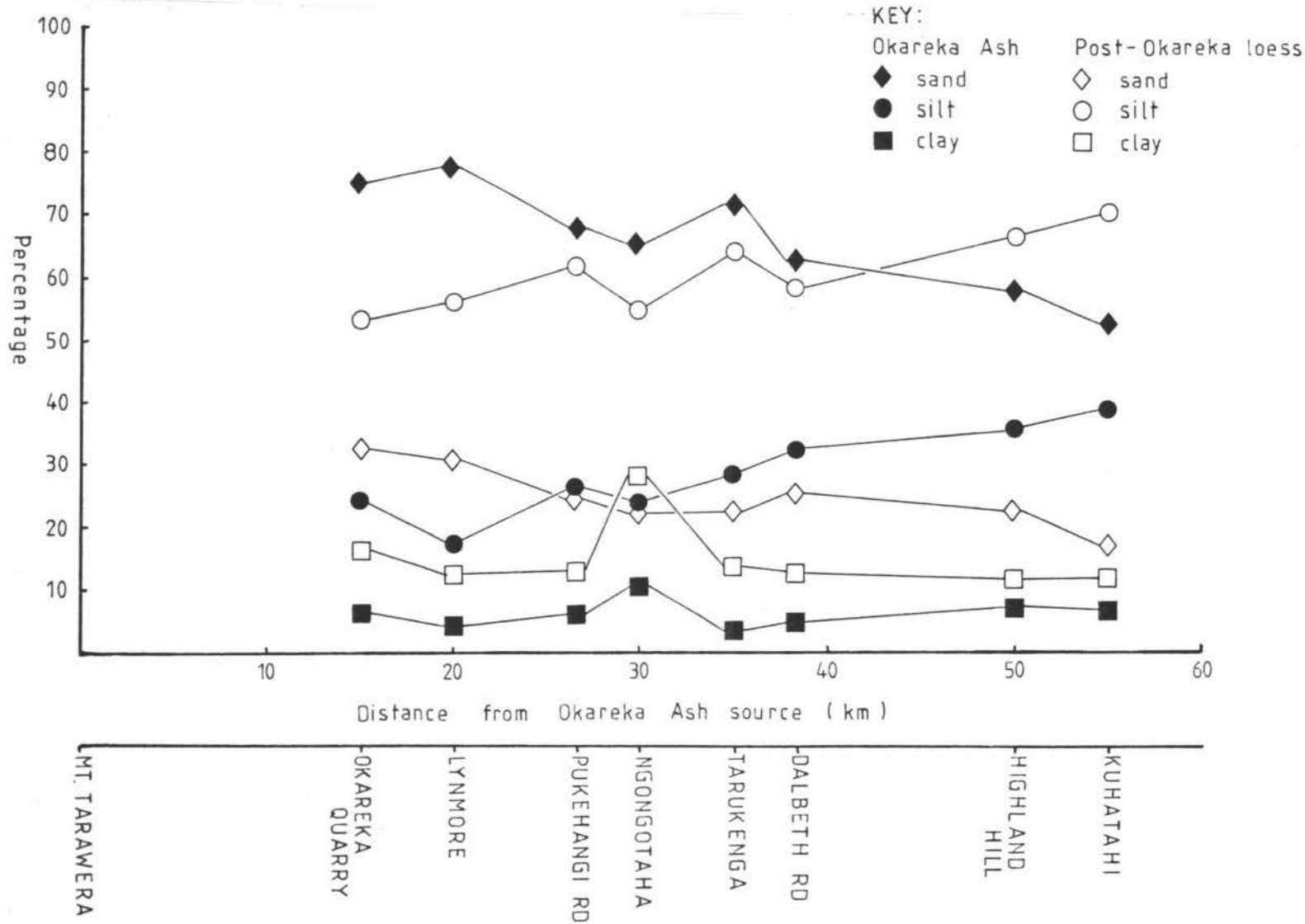

FIGURE 39: Variation in sand, silt and clay percent in Okareka Ash and Post-Okareka loess deposits in relation to distance from ash source.

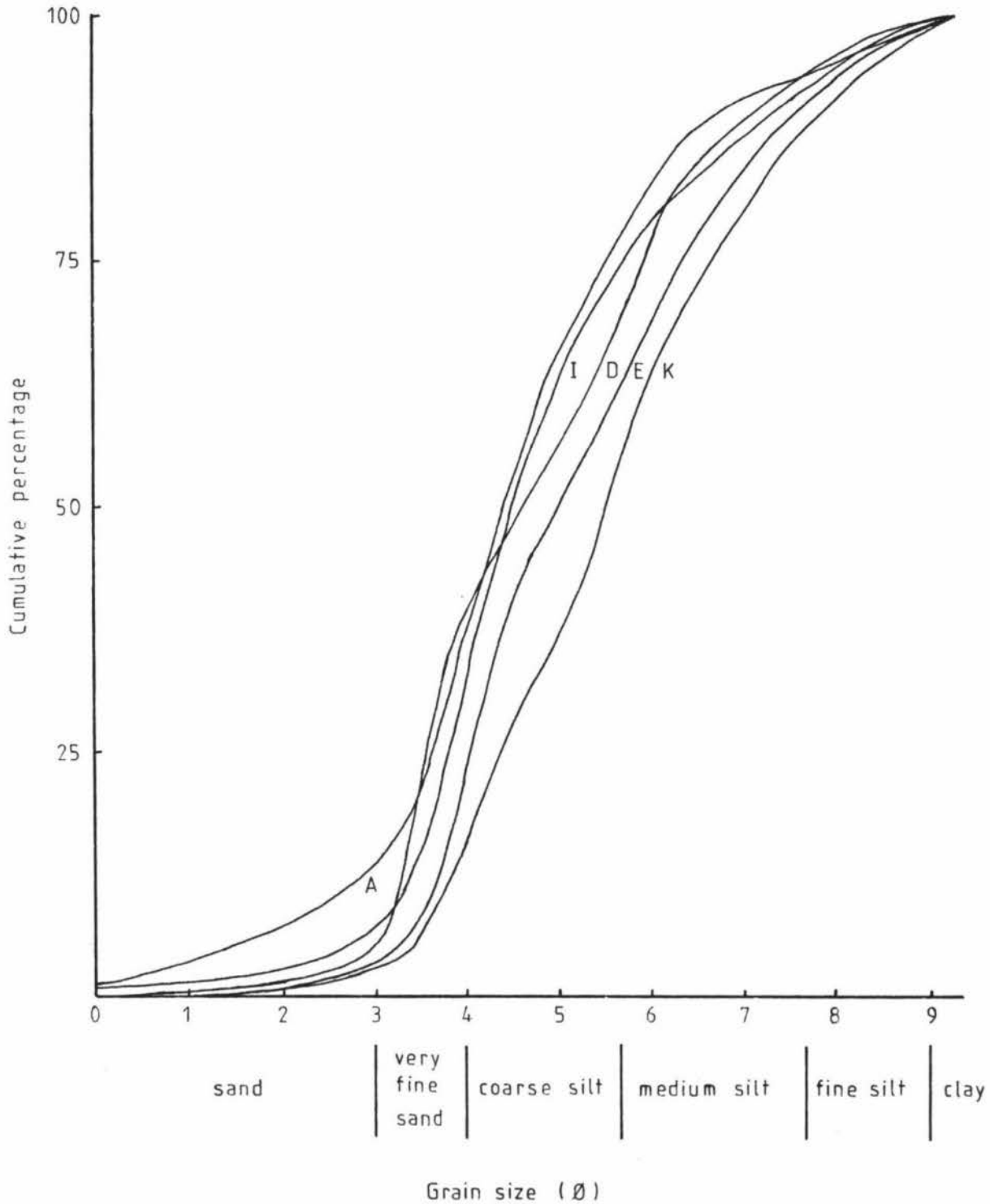

FIGURE 40: Grain-size cumulative curves for Post-Okareka loess deposits at: A, Okareka Quarry; I, Lynmore; D, Dalbeth Rd; E, Highland Hill; and K, Kuhatahi sections, showing grain-size distribution changes with increasing distance from Okareka Ash source.

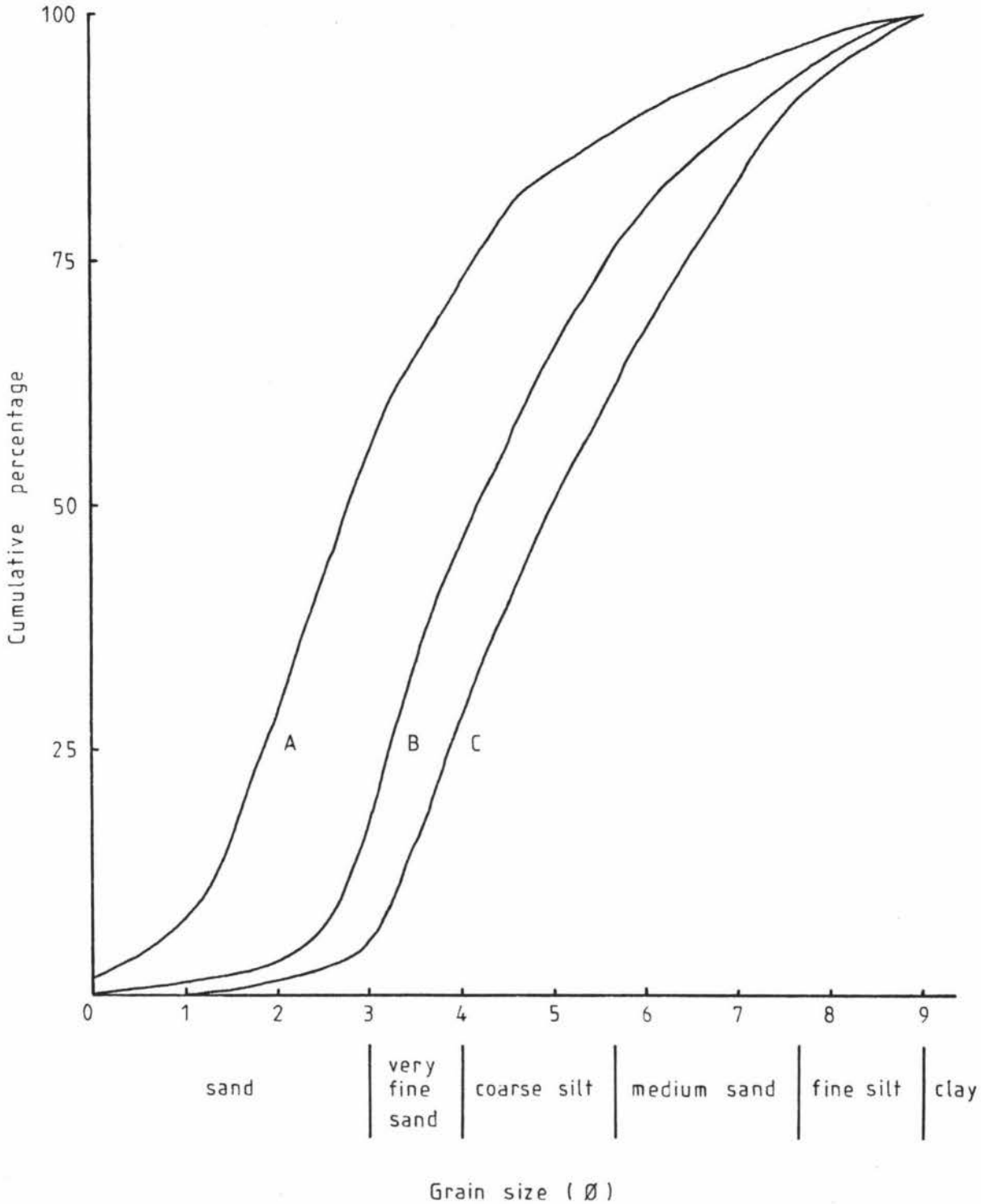

FIGURE 41: Grain-size cumulative curves for: A, Okareka Ash; B, lower and; C, upper Post-Okareka loess samples from Ngongotaha section.

indicate sand-size material was transported shorter distances than silt particles. An increase in silt content in Post-Okareka loess deposits with distance from source (Figure 39) can be attributed to preferential sorting, or additives of silt-sized material from sources further afield than Okareka Ash, Alternatively, processes of reworking, i.e. attrition and abrasion, during transportation and deposition of this tephra, especially in areas peripheral to ash source, would have resulted in the formation of a certain amount of finer-sized material. Sand and silt percentages of Post-Okareka loess closely parallel those of Okareka Ash which suggests that loessial material is most probably derived from this airfall tephra, and that source is essentially localised.

8.1.2 Sorting (σ_I)

Variables which affect sorting coefficients of pyroclastic particles include magnitude and direction of eruption, composition of the initial material ejected from the vent, and wind strength (Fisher, 1964; Walker, 1971). Okareka Ash deposits at all sections are poorly-sorted to very poorly-sorted, with sorting tending to improve with distance from source (Figure 42). Greatest variability and poorest sorting occurs in Okareka Ash samples from sections closest to source. This may be attributed to variable eruption directions close to the vent, in addition to the emission of many pulses of material at different intensities. Coarse-grained deposits are usually considered indicative of close proximity to vent, but fine-grained material may also be present (Walker, 1971). Okareka Ash deposits at sections close to source contain a moderate amount of fine material, which may be due to small amounts of smaller and lighter particles falling early in the eruption accumulating with larger and heavier fragments (Walker, 1971). However, the bulk of fine particles are carried greater distances from the vent, and are therefore subjected to some sorting by wind (Fisher, 1964). At a critical distance from source, wind strength exceeds diminishing eruptive energy, pyroclastic particles are

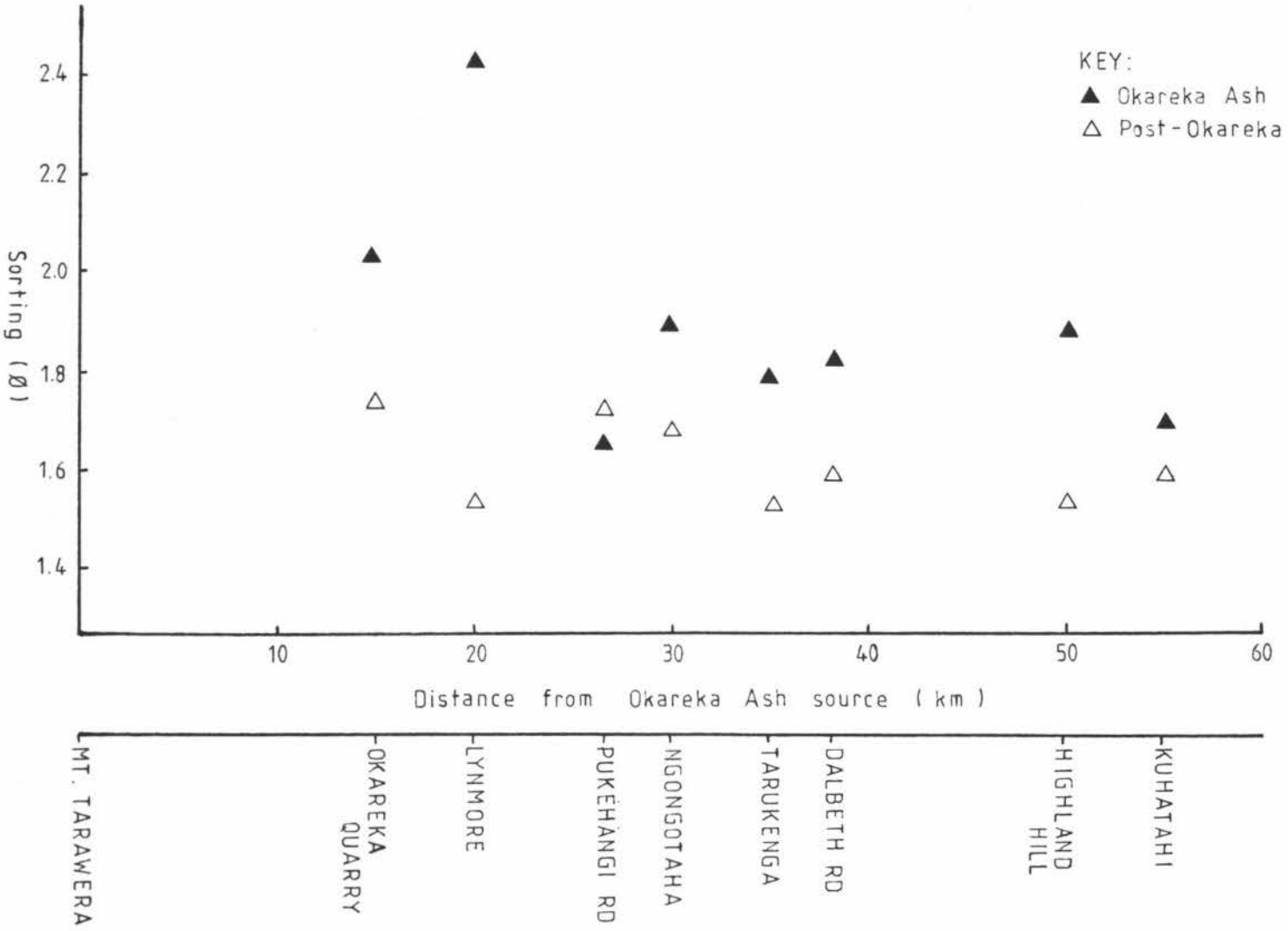

FIGURE 42: Sorting of Okareka Ash and Post-Okareka loess deposits in relation to distance from ash source.

sorted and carried thereafter by prevailing winds. Okareka Ash deposits show considerable variability in sorting values with distance from source, which may be a function of change in intensity and periodicity of volcanic activity or wind (Huang et al. 1975).

Post-Okareka loess deposits exhibit similar sorting characteristics to Okareka Ash, however, loess deposits are, in general, slightly better sorted than ash (Figure 42). Accumulation of silt-sized particles, together with saltating sand grains, has resulted in poorest sorting in Post-Okareka loess deposits at sections closest to ash source (Figure 42). With distance along the transect, the source material of Post-Okareka loess deposits has become progressively finer, and therefore, loess deposits show a slight increase in sorting values. During loess accumulation a sparsely vegetated landscape (Kennedy and Pullar, 1977) would have facilitated processes such as cryoturbation (frost-churning; Embleton and King, 1975), near-surface wind turbulence, and possibly bioturbation (e.g. worms). These processes, together with the accumulation of fine loessial material above a coarser sandy tephra has resulted in some of the finer material penetrating down into the interstices, and thus becoming mixed with the coarse material (Walker, 1971). Grain-size results show that coarsest mean grain-size and poorest sorting of loess samples occurs at the base of each Post-Okareka loess bed, which indicates some or all of the above processes have caused mixing of the two components during initial stages of loess accumulation.

8.1.3 Skewness (SK_I)

Skewness values indicate Okareka Ash beds at all sections are more strongly fine-skewed than overlying Post-Okareka loess deposits. Whereas ash samples exhibit a narrow range of skewness (0.26 - 0.46), skewness values of loess samples range from nearly symmetrical to strongly fine-skewed (0.00 - 0.40)

(Appendices 4 and 5). Although grain-size data was calculated on a clay-free basis, positive skewness values indicate both deposits have excess fine material. The narrow range of Okareka Ash skewness values illustrates that these deposits have a dominant sand mode, particularly at sections close to source. However, in Post-Okareka loess, the greater variability in skewness suggests that these deposits are more bimodal, and therefore, more negatively skewed (Folk and Ward, 1957). The reworking of the original tephric material from a localised source area is reflected by Post-Okareka loess skewness values which are consistently more fine-skewed than those of Okareka Ash. In basal loess samples, where mixing of tephric and loessial material has occurred, loess deposits are more negatively skewed. Neither Okareka Ash nor Post-Okareka loess deposits exhibit a consistent change with distance from source (Figure 43). However, values are most variable in both deposits at sections close to Okareka Ash source, particularly within loess beds.

8.1.4 Kurtosis (K_G)

At sections close to Okareka Ash source, ash deposits are meso/leptokurtic (1.02 - 1.35) indicating that better sorting occurs in the central portions of grain-size distributions. With increasing distance from source, kurtosis values of ash samples are more platykurtic (0.86 - 0.97), poorer sorting now evident in central portions (Appendix 4). Post-Okareka loess deposits exhibit similar kurtosis values to ash samples (0.81 - 1.23; platy/leptokurtic) (Appendices 5A and 5B). However, with distance from ash source loess deposits tend to be more platykurtic than Okareka Ash deposits (Figure 44).

The addition of small amounts of another mode in basal loess layers results in poorer sorting in the tails of the grain-size distribution, while sorting in the central remains good (Folk and Ward, 1957).

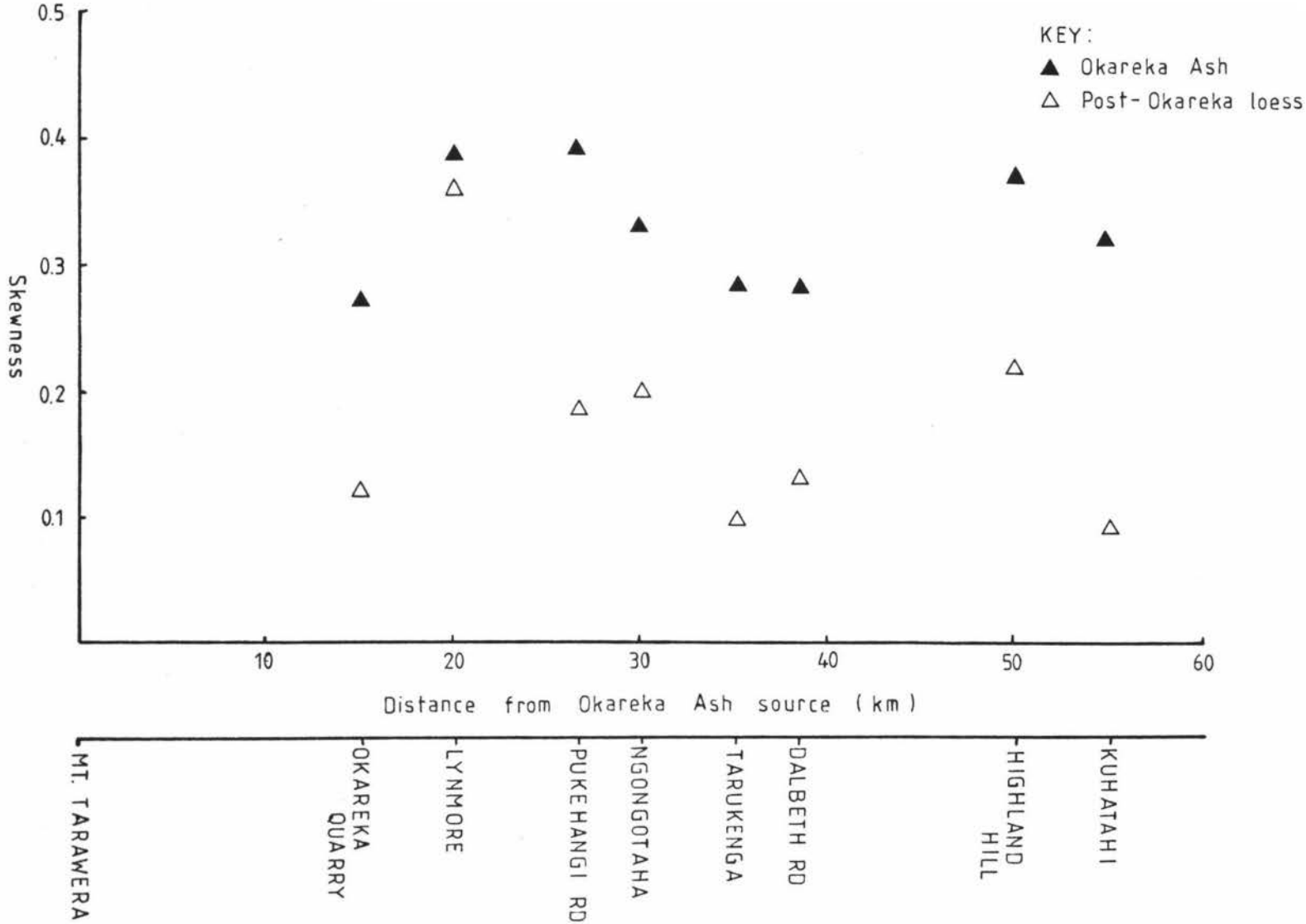

FIGURE 43: Skewness of Okareka Ash and Post-Okareka loess deposits in relation to distance from ash source.

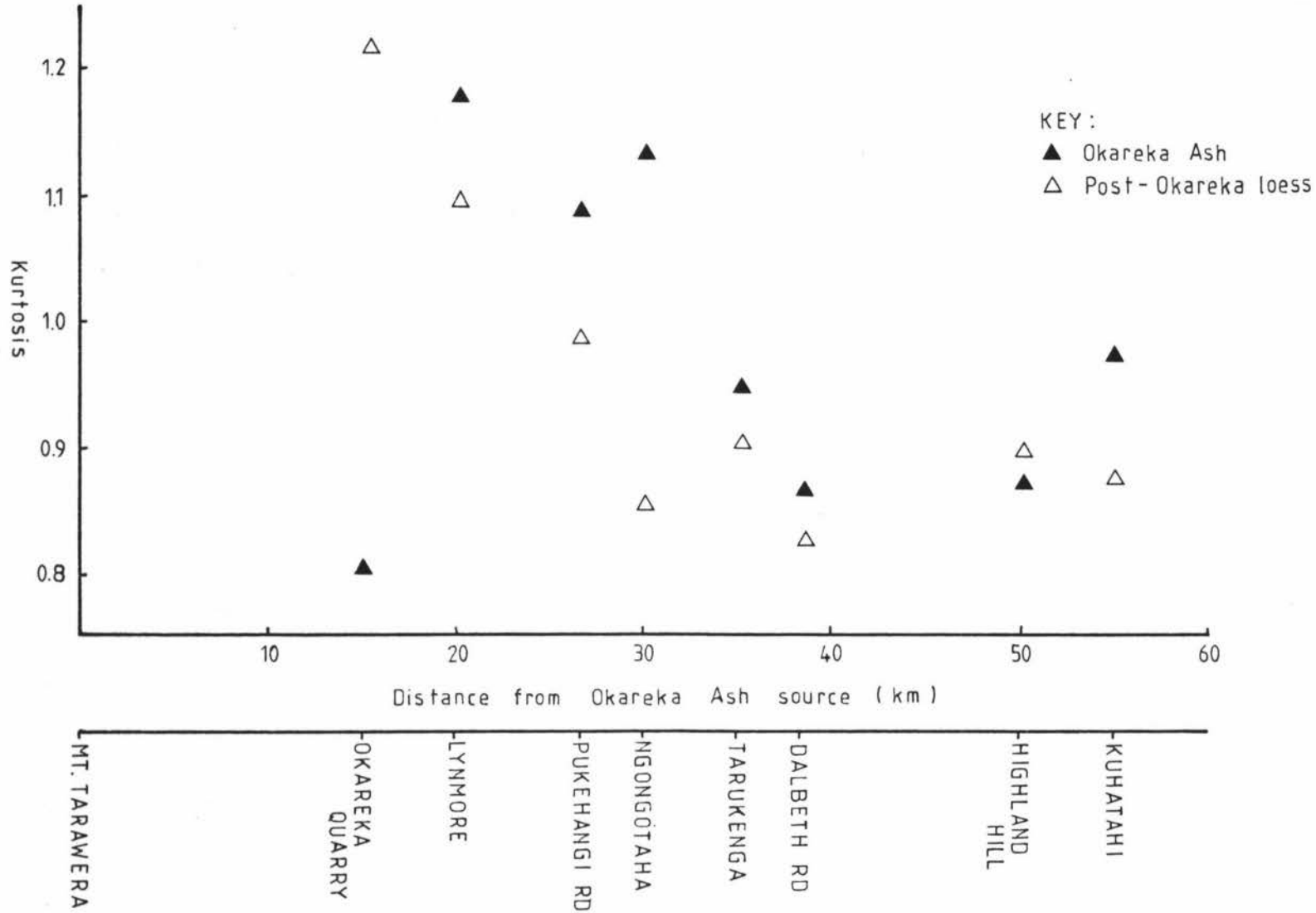

FIGURE 44: Kurtosis of Okareka Ash and Post-Okareka loess deposits in relation to distance from ash source.

The more platykurtic behaviour of Okareka Ash and Post-Okareka loess deposits with increasing distance from source suggests both deposits comprise two component modes of subequal proportion. Ash deposits tend to be dominated by a greater amount of silt and less sand with increasing distance from source. Although Post-Okareka loess deposits consist predominantly of silt, at distance from Okareka Ash source they comprise much less sand, and more fine silt.

8.1.5 Mean grain-size versus Sorting

Plots of Mz versus σ_I for Okareka Ash samples demonstrate that deposits are progressively better sorted with decreasing mean particle-size, i.e. with increasing distance from source (Figure 45). However, comparison of Mz values with sorting coefficients of Post-Okareka loess deposits reveals no relationship exists between these two parameters with distance from ash source (Figure 45). This suggests that during reworking and redeposition, the tephric material became sufficiently better sorted than the original tephra for there to be little association between sorting and mean grain-size (Folk and Ward, 1957). Examination of the graph Mz versus σ_I for loess deposits close to ash source confirms earlier conclusions in this study that coarsest mean grain-size and poorest sorting occurs in basal samples, and is consistent with mixing of tephric and loessial components.

Fisher (1966) found that with increasing distance from source ash deposits tend to become better sorted as mean grain-size decreased, and the reverse is true of loess deposits. However, this study reveals that both Okareka Ash and Post-Okareka loess deposits exhibit better sorting with increasing distance from ash source. This may be attributed to the localised source area, and minimal weathering of the loessial material.

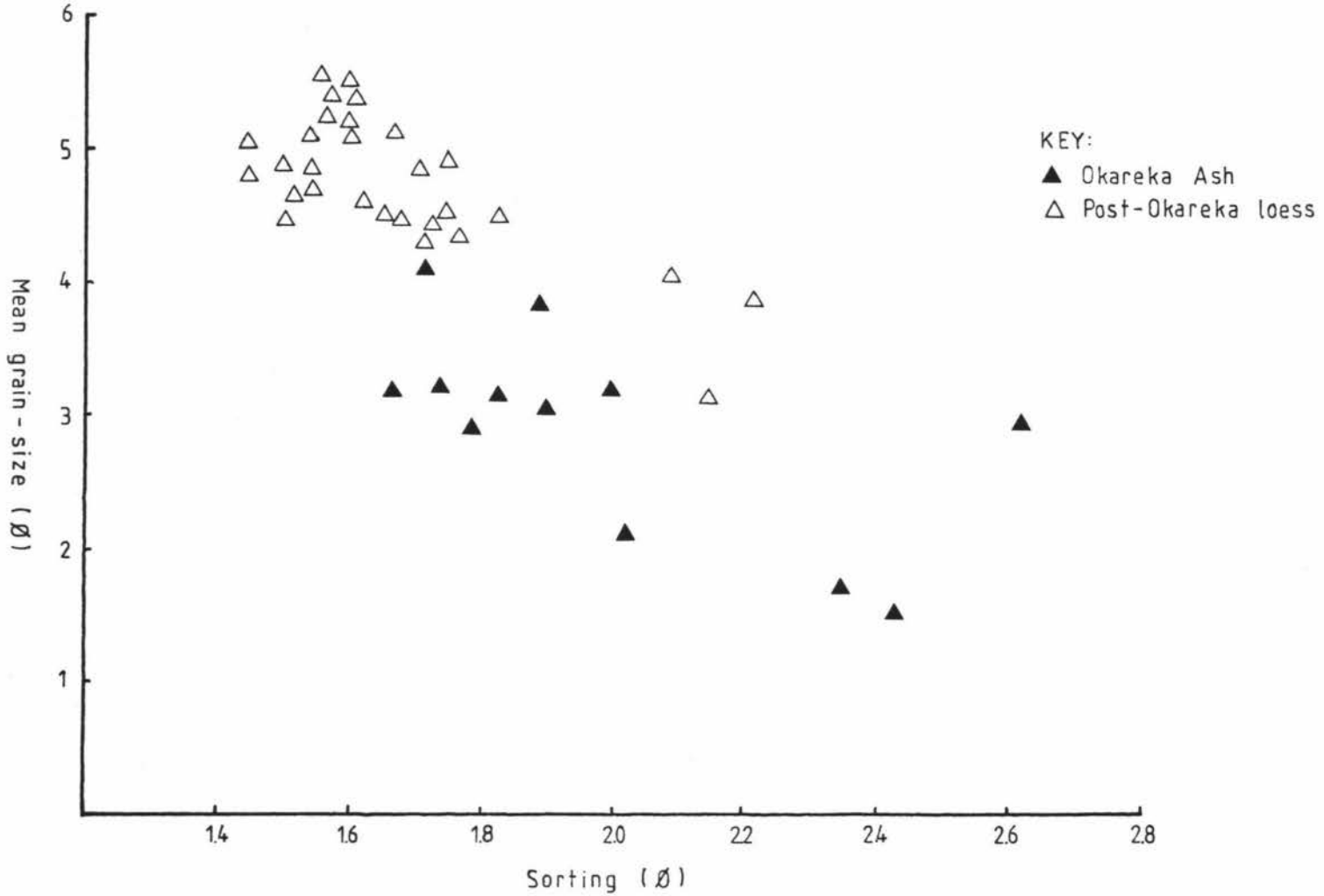

FIGURE 45: Mean grain-size versus sorting plots for Okareka Ash and Post-Okareka loess deposits.

8.1.6 Mean grain-size versus Skewness and Kurtosis

Plots of mean grain-size versus skewness (Figure 46), and mean grain-size versus kurtosis (Figure 47) reveal no correlation between these parameters in Okareka Ash or Post-Okareka loess deposits, with distance from ash source.

8.1.7 Mean grain-size versus $\frac{Mz}{Mz + \sigma I}$

In a study of volcaniclastic deposits of loessial origin, and airfall tephra, Fisher (1966) used a plot of Inman coefficients, mean grain-size (MdØ) against the mean grain-size - sorting coefficient ratio $\frac{Md\emptyset}{Md\emptyset + \sigma\emptyset}$ to distinguish between the two deposits. He found the ratio values tended to become larger as sorting coefficients and MdØ values decrease, and smaller as they increase. Fisher (1966), therefore, suggested this parameter distinguishes tephra from 'tephric loess' on the basis ash becomes better sorted as mean grain-size decreases. The reverse is true of loess. The ratio is used for convenience of plotting values that approach 1 as an upper limit, and to show relative increase and decrease of grain-size parameters with mean grain-size (Fisher, 1966).

In the present study, the parameters used were those defined by Folk (1968), and therefore the equivalent to Fisher's ratio (1966) becomes $\frac{Mz}{Mz + \sigma I}$. In order to compare this data with that of Fisher's, calculated values included material in the clay fraction.

Okareka Ash samples demonstrate a consistent relationship between mean grain-size and this ratio with distance from ash source (Figure 48). This is also true of Post-Okareka loess, but the relationship is less distinct because loess deposits exhibit a narrow Mz range (4.5 - 5.5Ø) and only a slight increase in Mz values with distance from source. Both ash and loess deposits show increasing ratio values with decreasing mean grain-size and sorting coefficients. A positive slope shown by Okareka Ash deposits correlates closely

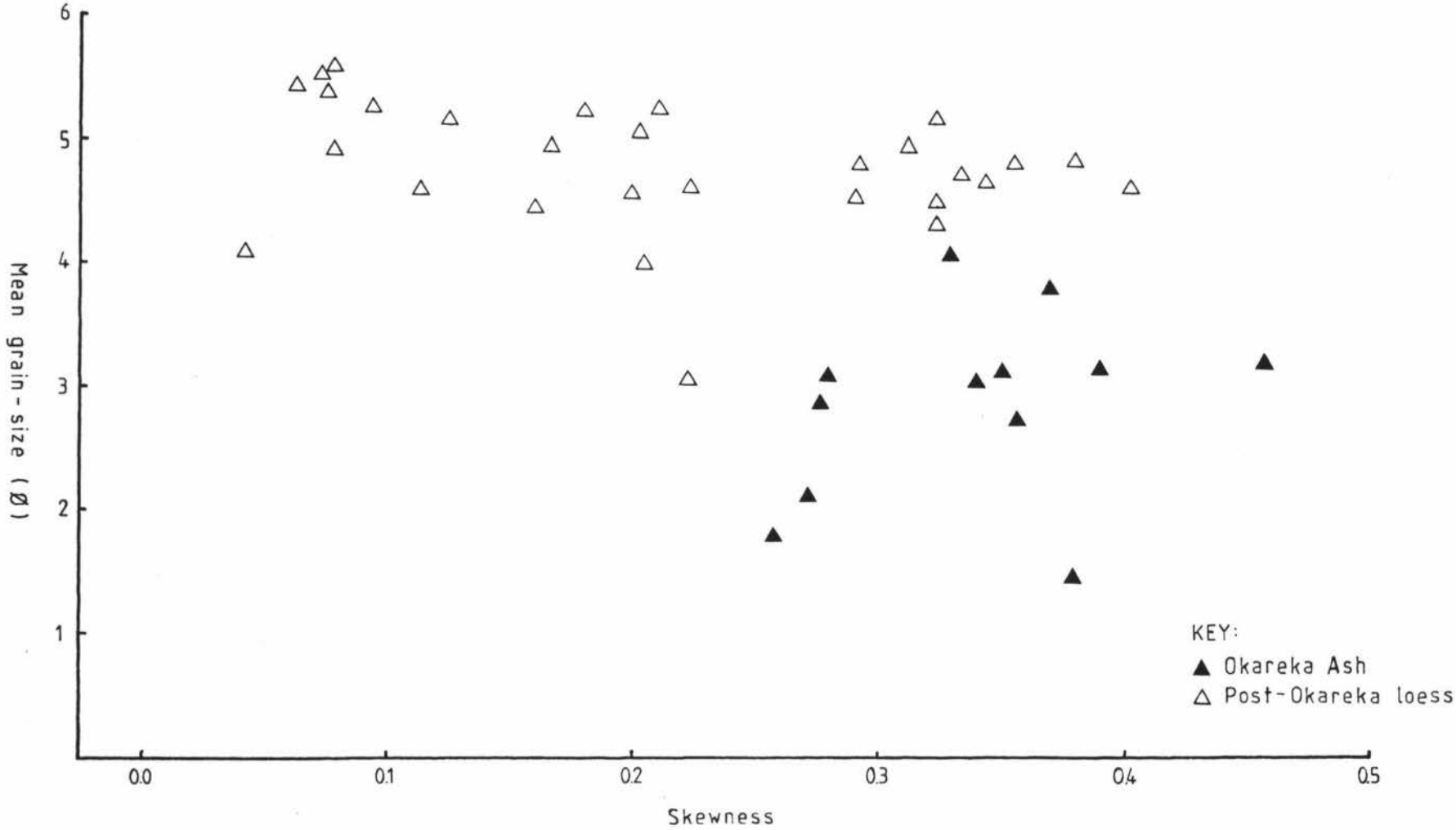

FIGURE 46: Mean grain-size versus skewness plots for Okareka Ash and Post-Okareka loess deposits.

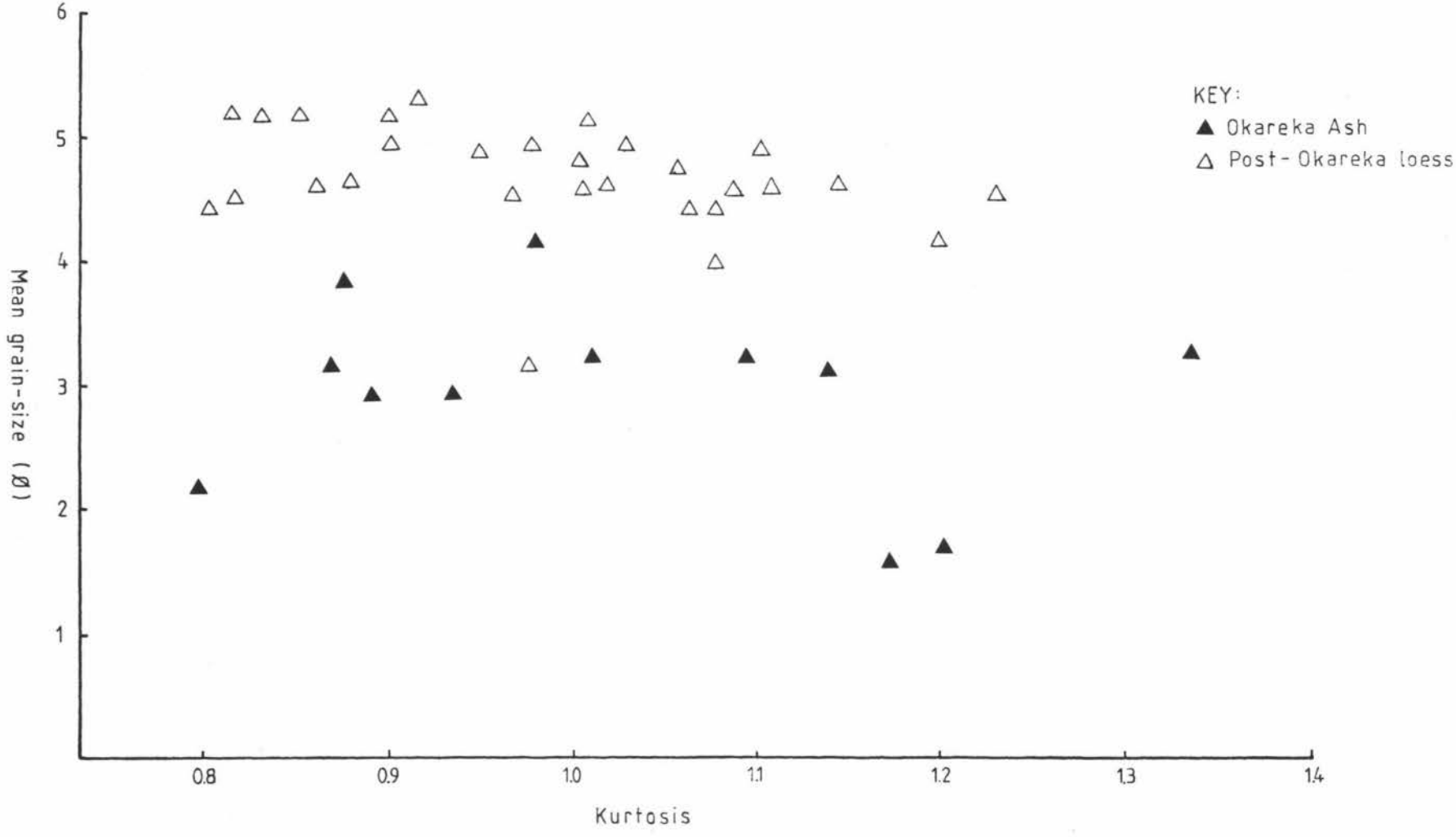

FIGURE 47: Mean grain-size versus kurtosis plots for Okareka Ash and Post-Okareka loess deposits.

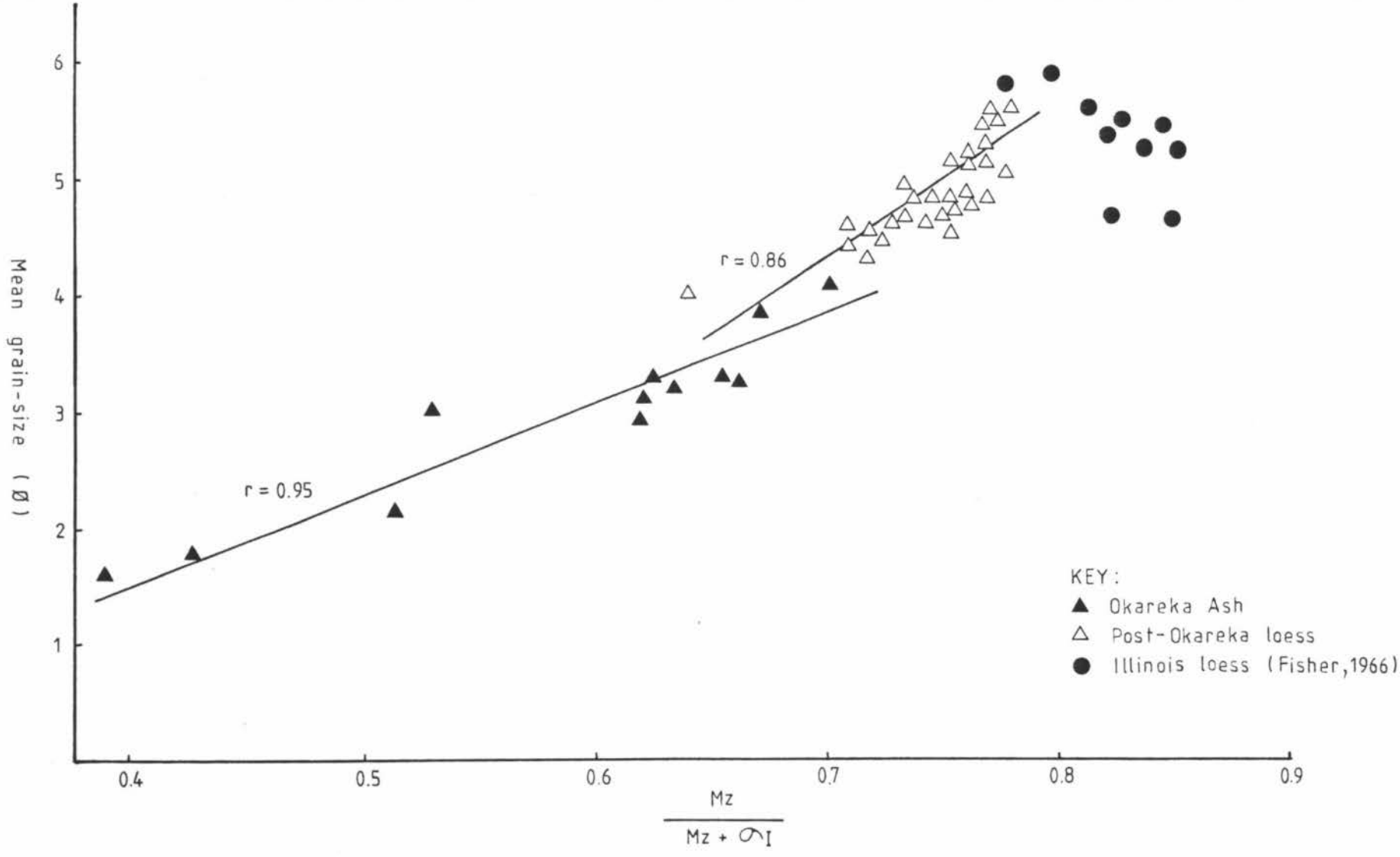

FIGURE 48: Variation of mean grain-size versus the mean grain-size - sorting coefficient ratio [Mz / Mz + σ_I] for Okareka Ash and Post-Okareka loess deposits.

with data presented by Fisher (1966), but Post-Okareka loess samples plot in a field intermediate to Okareka Ash and a 'true' loess (negative slope - Illinois loess; Figure 48). This position illustrates that tephric loess samples are still strongly influenced by their parent tephric material, and also that source has changed often, but was always local to deposition.

Fisher (1966) attributes increased sorting coefficients in airfall tephra to post-depositional alteration, which is quite significant in the tephras he analysed. The time period since deposition of Okareka Ash and overlying loess deposits is relatively short in comparison to Fisher's samples. It is conceivable, therefore, less distinctive differences between Okareka Ash and Post-Okareka loess samples in this study are a consequence of a small amount of weathering.

8.1.8 Mean grain-size versus $\frac{K_G}{K_G + Mz}$

Evaluation of the graph mean grain-size against the kurtosis - mean grain-size coefficient ratio $\frac{K_G}{K_G + Mz}$ for Okareka Ash and Post-Okareka loess samples show that ratio values become smaller as mean grain-size and kurtosis values decrease (Figure 49). Both ash and loess deposits become better sorted in the 'tails' as mean grain-size decreases with distance from source. Okareka Ash samples vary from leptokurtic at sections close to source where mean grain-size is coarsest (i.e. Trunk Rd, Lynmore, and to a lesser extent Okareka Quarry), to more platykurtic in finer grained samples from sections at distonce from source (i.e. Highland Hill and Kuhatahi). Okareka Ash deposits are better sorted at distance from source probably due to depletion in the ash cloud of heavier and coarser fragments close to source. This graph also illustrates that weathering has not affected ash sorting to any great extent. Loess deposits do not exhibit as wide a range of K_G and Mz values as ash, and therefore plot in a narrower field. Post-

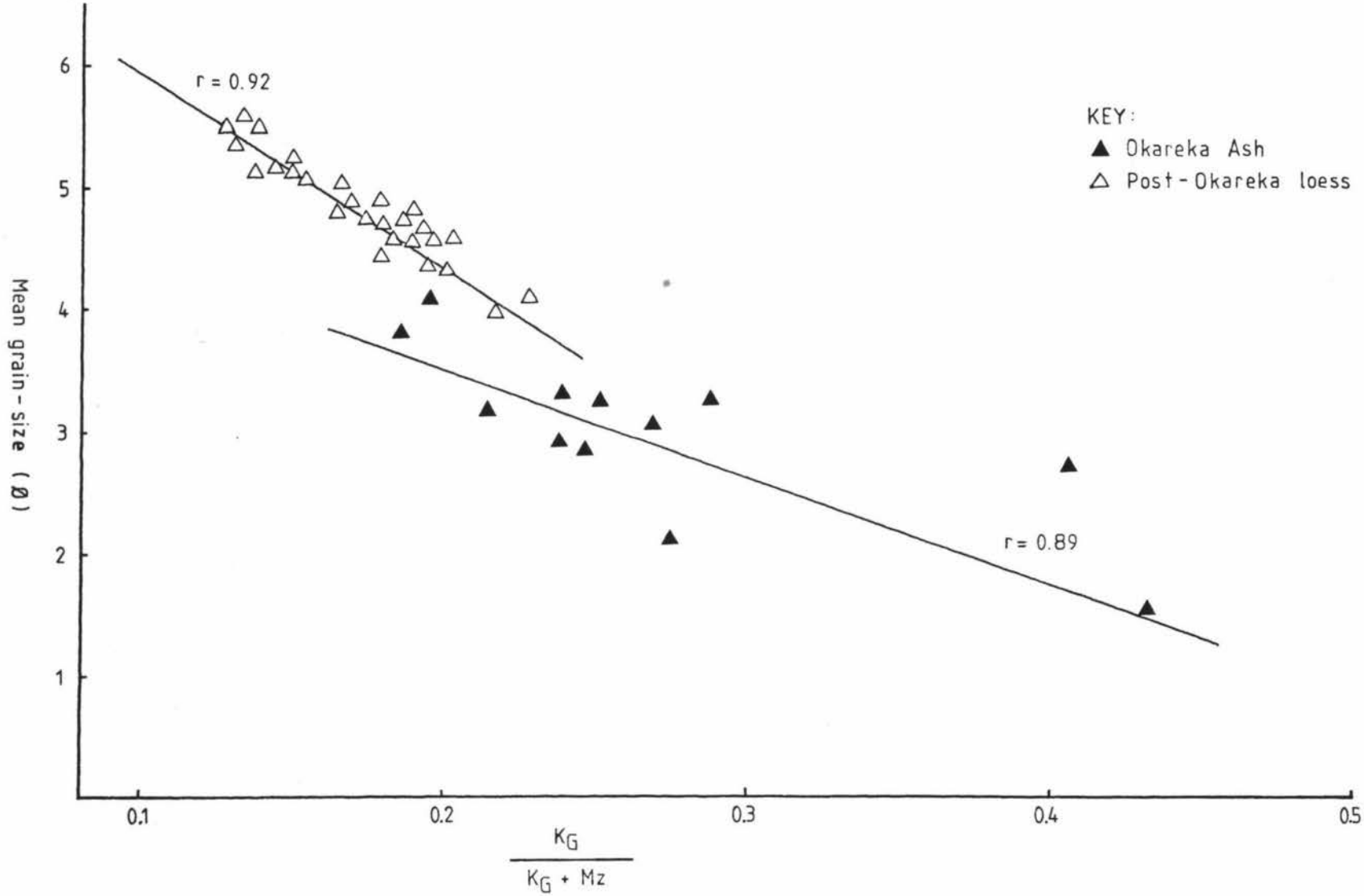

FIGURE 49: Variation of mean grain-size versus the kurtosis-mean grain-size coefficient ratio [K_G / K_G + Mz] for Okareka Ash and Post-Okareka loess deposits.

Okareka loess samples are platy/mesokurtic even at sections close to ash source. A less distinctive trend to that of Okareka Ash deposits is also evident in loess deposits, and these results further substantiate conclusions derived from the plot Mz versus $\frac{Mz}{Mz + \sigma_I}$. It is possible to differentiate Post-Okareka loess and Okareka Ash samples at sections at close and intermediate distances from ash source. However, where Okareka Ash deposits are thin, in distal areas from source, they exhibit mean grain-size and kurtosis characteristics similar to those of Post-Okareka loess samples.

Chapter 9: CONCLUSIONS

1. Mineralogical results reveal loessial material deposited in the period c.17,000 - 14,700 years B.P. is derived predominantly from the underlying rhyolitic biotite-bearing Okareka Ash erupted c.17,000 years B.P., although minor composition differences in upper loess layers indicate changes in source occurred during later stages of loess accumulation.

2. Okareka Ash particles, especially that of volcanic glass, exhibit morphological characteristics typical of a magmatic eruption of rhyolitic material. Particle size, shape and surface texture of loess grains indicate this material has been reworked by aeolian processes prior to redeposition as Post-Okareka loess deposits.

3. During late Pleistocene times, cool, semi-arid climatic conditions (glacial) and sedge-type vegetation concurrently inhibited soil development and encouraged loess deposition. Minimal weathering of particles, except at sections of high altitude and rainfall, within Okareka Ash and overlying loess deposits reflect such conditions. Increased alteration of grains in upper Post-Okareka loess samples is most probably due to warmer conditions which supported more luxuriant vegetation during later stages of loess deposition. Primary minerals feldspar, biotite mica, and mafic minerals hypersthene, hornblende, augite, and titano-magnetite are most susceptible to alteration by solution in both ash and loess deposits.

4. Irrespective of changes in topography, altitude, drainage, climate and vegetation, clay minerals halloysite, allophane and imogolite are present in clay fractions of Okareka Ash deposits. Post-Okareka loess clay samples contain more halloysite than the underlying ash clay samples, as well as allophane, imogolite and gibbsite in variable amounts. Halloysite, in Okareka Ash clay fractions, comprises predominantly squat ellipsoids,

derived from weathering rhyolitic volcanic glass, while loess clay samples, in general, contain a greater proportion of halloysite curled flakes, formed from plagioclase feldspar.

5. Despite detailed analysis of Okareka Ash and Post-Okareka loess deposits, clay mineralogical data provides insufficient evidence to make assumptions concerning weathering sequences within tephra and tephra-derived soils. The occurrence and abundance of clay minerals in such deposits is dependent upon local environmental conditions, including past and present pedogenic factions, in particular climate.

6. Comparison of grain-size parameters, mean grain-size and sorting of Okareka Ash deposits reveal greatest variation in mean grain-size and poorest sorting occurs close to source, but deposits become better sorted, and show decreasing mean grain-size with increasing distance from ash source. Okareka Ash deposits contain more sand-sized material and less clay than loess, although a greater amount of fine material in Post-Okareka loess deposits can be attributed to abrasion and attrition during reworking. Post-Okareka loess deposits exhibit a typically narrow and fine mean grain-size in the range 4 - 5.5Ø (63 - 20μm). A slight decrease in mean grain-size of loess deposits with distance from ash source suggests much of Post-Okareka loess is derived from a localised source. Loess deposits are better sorted than Okareka Ash but exhibit a wide range of skewness values, and have kurtosis coefficients similar to ash deposits. A slight increase in mean grain-size and poorer sorting shown in basal loess samples, is due to mixing of the overlying finer loessial material with the underlying Okareka Ash deposits.

7. $\frac{Mz}{Mz + \sigma_I}$ versus mean grain-size, a ratio equivalent to that of Fisher's (1966), is found to be a useful means of differentiating loess, airfall tephra and tephric loess on the basis ash deposits become better sorted as mean grain-size decreases, and the reverse is observed in loess deposits. Tephric loess deposits such as Post-Okareka loess plot in an intermediate field between ash (positive slope) and loess (negative slope). Grain-size results also indicate that due to minimal weathering of Okareka Ash and Post-Okareka loess deposits, the distinction between the two deposits is less well-defined than data from similar deposits reported by Fisher (1966).

8. As mineralogical composition of Okareka Ash and Post-Okareka loess is essentially similar, and morphological characteristics of ash deposits closely resemble those of loess, where deposits are thin in distal areas from source and under certain environmental conditions (high rainfall and altitude), it is apparent grain-size parameters, in particular mean grain-size, sorting and kurtosis, are the more accurate means of differentiating ash and tephric loess deposits.

9. Post-Okareka loess is the youngest aeolian material to have accumulated in Central North Island, and, therefore, the lack of weathering observed in these deposits is a reflection of time as well as the cool climatic conditions which prevailed during loess deposition. Further study of other late Pleistocene deposits such as Post-Te Rere, Post-Kawakawa and Post-Rotoehu loess deposits is required to resolve questions concerning the affect of weathering on grain-size parameters and grain morphology. Whereas the present study found some techniques, under certain circumstances, enable identification and differentiation of ash, loess and tephric loess deposits, such techniques may not be applicable to older deposits due to changes in weathering resulting from different pedogenic conditions.

REFERENCES

ADAMS, J. 1976: Sieve size statistics from grain measurement. Journal of Geology 85: 209-227.

ALLEN, J.R.L. 1970: Physical processes of sedimentation: An Introduction. Earth Science Series 1. George Allen and Urwin Ltd. 248pp.

AOMINE, S., YOSHINAGA, N. 1955: Clay minerals of some well-drained volcanic ash soils in Japan. Soil Science 79: 345-355.

AOMINE, S., WADA, K. 1962: Differential weathering of volcanic ash and pumice resulting in formation of hydrated halloysite. American Mineralogist 42: 1024-1047.

AOMINE, S., MIZOTA, C. 1973: Distribution and genesis of imogolite in volcanic ash soils of northern Kanto, Japan. In: Serratosa, J.M. (Ed.) International Clay Conference Proceedings (1972): 207-213.

BAGNOLD, R.R. 1942: The physics of windblown sand and desert dunes. Morrow, New York, N.Y., 265pp.

BAGNOLD, R.R. 1956: The flow of cohesionless grains in fluids. Philosophical Transactions of the Royal Society, London 249: 235-290.

BERG, L.S. 1964: Loess as a product of weathering and soil formation. I.P.S.T., Jerusalem, 205pp.

BIRRELL, K.S., FIELDES, M. 1952: Allophane in volcanic ash soils. Journal of Soil Science 3: 156-166

BIRRELL, K.S., PULLAR, W.A. 1973: Weathering of paleosols in Holocene and late Pleistocene tephras in Central North Island, New Zealand. N.Z. Journal of Geology and Geophysics 16: 687-702.

BIRRELL, K.S. 1974: Tephric loess studies. In: Read,N.E. (Ed.) Soil Groups of New Zealand. Part 1: Yellow-Brown Pumice Soils. N.Z. Society of Soil Science: 56-61.

BIRRELL, K.S., PULLAR, W.A., SEARLE, P.L. 1977: Weathering of Rotoehu Ash in Bay of Plenty district. N.Z. Journal of Science 20: 303-310.

CAMPBELL. A.S., MITCHELL, B.D., BRACEWELL, J.M. 1968: Effects of particle size, pH and organic matter on the thermal analysis of allophane. Clay Minerals 7: 451-454.

COLE, J.W. 1970a: Structure and eruptive history of the Tarawera Volcanic Complex. N.Z. Journal of Geology and Geophysics 13: 879-902.

COLE, J.W. 1970b: Petrography of the rhyolitic lavas of the Tarawera Volcanic Complex. N.Z. Journal of Geology and Geophysics 13: 903-924.

COWIE, J.D., MILNE, J.D.G. 1973: Maps and sections showing the distribution and stratigraphy of North Island loess and associated cover deposits, New Zealand. N.Z. Soil Survey Report 6.

DOEGLAS, D.J. 1946: Interpretation of the results of mechanical analysis. Journal of Sedimentary Petrology 16: 19-40.

DOUGLAS, L.A. 1977: Vermiculites. In: Dixon, J.B. Weed, S.B. (Eds.) Minerals in Soil Environments 8: 259-292. Soil Science Society of America. 948pp.

EMBLETON, C., KING, C. 1975: Periglacial Geomorphology.

EWART, A. 1963: Petrology and petrogenesis of the Quaternary pumice ash in the Taupo area, New Zealand. Journal of Petrology 4: 392-431.

FARMER, V.C., FRASER, A.R., TAIT, J.M. 1977: Synthesis of imogolite: A tubular aluminium silicate polymer. Journal of the Chemical Society, Chem. Comm: 462-463.

FARMER, V.C., FRASER, A.R. 1978: Synthetic imogolite: A tubular hydroxlaluminium silicate. In: Mortland, M.M., Farmer, V.C. (Eds.) International Clay Conference: 547-553.

FARMER, V.C., SMITH, B.F.L., TAIT, J.M. 1979: The stability, free energy, and heat of formation of imogolite. Clay Minerals 14: 103-107.

FEHRENBACHER, J.B. 1972: Loess stratigraphy, distribution, and time of deposition in Illinois. Soil Science 115: 176-182.

FIELDES, M. 1955: Clay Mineralogy of New Zealand soils, Part II: Allophane and related mineral colloids. N.Z. Journal of Science and Technology 37: 336-350.

FIELDES, M., FURKERT, R.J. 1966: The nature of allophane in soils, Part 2: Differences in composition. N.Z. Journal of Science 9: 608-622.

FISHER, R.V. 1964: Maximum size, median diameter, and sorting of tephra. Journal of Geophysical Research 69: 341-355.

FISHER, R.V. 1966: Textural comparison of John Day Volcanic Siltstone with loess and volcanic ash. Journal of Sedimentary Petrology 36: 706-718.

FISHER, R.V. 1971: Grain-size characteristics of pyroclastic deposits. Journal of Geological Society of London 79: 696-714.

FLEMING, C.A. 1975: Quaternary record in Australia and New Zealand. In: Suggate, R.B., Cresswell, M.M. (Eds.) Quaternary Studies: Royal Society of NZ Bulletin 13: 1-20.

FOLK, R.L., WARD, W.C. 1957: Brazos River Bar: A study in the significance of grain-size parameters. Journal of Sedimentary Petrology 27: 3-26.

FOLK, R.L. 1968: Petrology of Sedimentary Rocks. The University of Texas, Geology 370K, 383L, 383M. 170pp.

FRANZMEIER, D.P. 1970: Particle size sorting of proglacial aeolian material. Soil Science Society of America Proceedings 34: 920-924.

FRAZEE, C.J., FEHRENBACHER, J.B., KRUMBEIN, W.C. 1970: Loess distribution from a source. Soil Science Society of America Proceedings 34: 296-301.

FREIDMAN, G.M. 1961: Distinction between dune, beach and river sands from their textural characteristics. Journal of Sedimentary Petrology 31: 514-529.

FREIDMAN, G.M. 1967: Dynamic processes and statistical parameters compared for size-frequency distributions of beach and river sands. Journal of Sedimentary Petrology 37: 327-354.

HANDY, R.L. 1976: Loess distribution by variable winds. Geological Society of America Bulletin 87: 915-927.

HARDJOSOESASTRO. R.R. 1956: Preliminary note on cristobalite in clay fractions of volcanic ashes. Journal of Soil Science 7: 185-188.

HEIKEN, G. 1972: Morphology and petrography of volcanic ashes. Geological Society of America Bulletin 83: 1961-1988.

HENMI, T., WADA, K. 1976: Morphology and compostion of allophane. American Mineralogist 61: 379-390.

HSU, P.H. 1977: Aluminium hydroxides and oxyhydroxides. In: Dixon, J.B., Weed, S.B. (Eds.) Minerals in Soil Environments 4: 99-144. Soil Science Society of America, 948pp.

HUANG, T.C., WATKINS, N.D., SHAW, D.M. 1975: Atmospherically transported volcanic glass in deep sea sediments. Volcanism in subantarctic lattitudes of the South Pacific during late Pliocene and Pleistocene times. Geological Society of America Bulletin 86: 1305-1315.

INMAN, D.L. 1949: Sorting of sediment in light of fluid mechanics. Journal of Sedimentary Petrology 19: 51-70

INMAN, D.L. 1952: Measures for describing the size distribution of sediments. Journal of Sedimentary Petrology 22: 125-145

IVES, D. 1973: Nature and distribution of Loess in Canterbury, New Zealand. N.Z. Journal of Geology and Geophysics 16: 587-610

KALINSKE, A.A. 1943: Turbulence and the transport of sand and silt by wind. Ann. N.Y. Academy of Science 44: 41-54

KENNEDY, N.M. 1975: Paleosols and tephric loess associated with the Okareka and Te Rere Tephra formations. N.Z. Soil News 23: 165.

KENNEDY, N.M., PULLAR, W.A. 1977: Loess on the Mamaku Plateau. N.Z. Soil News 25: 91.

KENNEDY, N.M. 1980: Field recognition of tephric loess (c.42,000 - 15,000 years B.P.) in Central North Island. N.Z. Soil News 28: 55-58

KIRKMAN, J.H. 1975: Clay mineralogy of some tephra beds of Rotorua areas, North Island, New Zealand. Clay Minerals 10: 437-449.

KIRKMAN, J.H. 1977: Possible structure of halloysite disks and cylinders observed in some New Zealand rhyolitic tephras. Clay Minerals 12: 199-216

KIRKMAN, J.H. 1978: Clay mineralogy of New Zealand volcanic ash soils and tephras. N.Z. Soil News 26: 12-18.

KIRKMAN, J.H. 1980: Mineralogy of the Kauroa Ash Formation of southwest and west Waikato, North Island, New Zealand. N.Z. Journal of Geology and Geophysics 23: 113-120.

KIRKMAN, J.H., McHARDY, W.J. 1980: A comparative study of the morphology, chemical composition and weathering of rhyolitic and andesitic glass. Clay Minerals 15: 165-173.

KIRKMAN, J.H. 1981: Morphology and structure of halloysite in New Zealand tephras. Clays and Clay Minerals 29: 1-9.

KITIGAWA, Y. 1971: The unit particle of allophane. American Mineralogist 56: 465-475.

KRUMBEIN, W.C. 1937: Sediments and exponential curves. Journal of Geology 45: 577-601.

KRUMBEIN, W.C. 1938: Size frequency distributions and the normal phi curve. Journal of Sedimentary Petrology 8: 84-90.

LEWIS, K.B., EADE, J.V. 1974: Sedimentation in the vicinity of the Maui gas field, New Zealand. N.Z. Oceanography Institute, Oceanographical Summary No.6.

LOWE, D.J. 1980: Tephric loess. N.Z. Soil News 28: 217-219.

MARGOLIS, S.V., KRINSLEY, D.H. 1971: Submicroscopic features on eolian and subaqueous quartz sand grains. Geological Society of America Bulletin 82: 3395-3406.

MASUI, J., SHOJI, S., UCHIYAMA, N. 1966: Clay mineral properties of volcanic ash soils in north-eastern parts of Japan. Tohoku Journal of Agricultural Research 17: 17-36.

McGRAW, J.D. 1975: Quaternary airfall deposits of New Zealand. In: Suggate, R.B., Cresswell, M.M. (Eds.) Quaternary Studies: Royal Society of New Zealand Bulletin 13: 35-44.

MITCHELL, B.D., SMITH, B.F.L., de ENDREDY, A.S. 1971: The effect of buffered sodium dithionite solution and ultrasonic agitation on soil clays. Israel Journal of Chemistry 9: 45-52.

MIYAUCHI, N., AOMINE, S. 1964: Does allophane B exist in Japanese volcanic ash soils? Soil Science and Plant Nutrition (Tokyo) 10: 199-203.

MIZOTA, C. 1976: Relationships between the primary mineral and the clay mineral compositions of recent andosols. Soil Science and Plant Nutrition (Tokyo) 22: 257-268.

MOSS, A.J. 1962: The physical nature of common sandy and pebbly deposits - Part 1. American Journal of Science 260: 337-373.

MOSS, A.J. 1963: The physical nature of common sandy and pebbly deposits - Part 2. American Journal of Science 261: 297-343.

NAGASAWA, K. 1978: Weathering of volcanic ash and other pyroclastic materials. In: Sudo, T., Shimoda, S. (Eds) Clays and Clay Minerals of Japan 2: 105-125. Developments in Sedimentology No. 26, Elsevier 326pp.

NEALL, V.E. 1975: Climate-controlled tephra redeposition on Pouakai Ring plain, Taranaki, New Zealand. N.Z. Journal of Geology and Geophysics 18: 317-326.

NIETER, W.M., KRINSLEY, D.H. 1976: The production and recognition of aeolian features on sand grains by silt abrasion. Sedimentology 23: 713-720.

PARFITT, R.L., HENMI, T. 1980: Structure of some allophanes from New Zealand Clays and Clay Minerals 28: 285-294.

PARFITT, R.L., FURKERT, R.J., HENMI, T. 1980: Identification, structure and naming of two types of allophane from volcanic ash soils and tephra, proto-imogolite and proto-halloysite allophane. Clays and Clay Minerals 28: 328-334.

PARFITT, R.L., RUSSELL, M., KIRKMAN, J.H. in press: The Clay mineralogy of Yellow-Brown Loam soils. In: Neall, V.E. (Ed.) Genetic Soil groups of New Zealand - Yellow-Brown Loams. N.Z. Soil Science Society.

PASSEGA, R. 1966: Grain-size representation by CM patterns as a geological tool. Journal of Sedimentary Petrology 34: 830-847

PETTIJOHN, F.J. 1949: Sedimentary Rocks, Harper, New York, N.Y. 526pp.

PETTIJOHN, F.J. 1957: Sedimentary Rocks, Harper, New York, N.Y. 718pp.

PULLAR, W.A. 1967: Volcanic ash beds in the Waikato district. Journal of Earth Science 1: 17-36.

PULLAR, W.A., POLLOK, J.A. 1973: Paleosols and tephric loess associated with the Okareka and Te Rere Formations. N.Z. Soil News 21: 186-187.

PULLAR, W.A., BIRRELL, K.S. 1973a: Parent materials of Tirau Silt Loam. N.Z. Journal of Geology and Geophysics 16: 677-686.

PULLAR, W.A., BIRRELL, K.S. 1973b: Age and distribution of late Quaternary pyroclastic and associated cover deposits of Central North Island, New Zealand. N.Z. Soil Survey Report - Parts 1 and 2.

PULLAR, W.A., KENNEDY, N.M. 1978: New Zealand Loess. Search 9: 435.

PULLAR, W.A. 1980: Tephra and loess cover deposits on Kaingaroa Plateau including detailed lithology of upper Taupo Pumice. N.Z. Soil Bureau Report 44.

RAESIDE, J.D. 1964: Loess deposits of the South Island, New Zealand, and soils formed on them. N.Z. Journal of Geology and Geophysics 7: 811-838.

RUSSELL, M., PARFITT, R.L., CLARIDGE, G.G. 1981: Estimation of the amounts of allophane and other minerals in the clay fraction of an Egmont Loam profile and other volcanic ash soils, New Zealand. Australian Journal of Soil Research 19:

RUSSELL, R.J. 1944a: Lower Mississippi Valley loess. Geological Society of America Bulletin 55: 1-40.

RUSSELL, R.J. 1944b: Origin of loess - a reply. American Journal of Science 242: 447-450

SARGUSA, M., SHOJI, S., KATO, T. 1978: Origin and nature of halloysite in Andosoils from Towada Tephra, Japan. Geoderma 20: 115-129

SCHEIDIGGER, A.E., POTTER P.E. 1968: Textural studies in grading: Volcanic ash falls. Sedimentology 11: 163-170.

SELBY, M.J. 1976: Loess. N.Z. Journal of Geography 61: 1-18.

SEKI, T. 1913: Zwei Vulkanogene Lehms aus Japan. Landw. Versuch. Sta 79/80: 871-890.

SHERMAN, G.D., CADY, J.G., IKAMA, H., BLUMSBERG, N.E. 1967: Genesis of the bauxitic Hailu soils. Hawaii Agriculture Experimental Station, Technical Bulletin No. 56.

SMALLEY, I.J. 1966: Properties of glacial loess and the formation of loess deposits. Journal of Sedimentary Petrology 36: 699-766.

SMALLEY, I.J., VITA-FINZI, C. 1968: The formation of fine particles in sandy deserts and the nature of 'desert' loess. Journal of Sedimentary Petrology 38: 766-774.

SMALLEY, I.J., CABRERA, J.G. 1970: The shape and surface texture of loess particles. Geological Society of America Bulletin 81: 1591-1596.

SMITH, G.D. 1942: Illinois loess - variations in its properties and distribution. Illinois Agriculture Experimental Station Bulletin 490: 139-184.

SOIL BUREAU, 1978: Field data for 26th N.Z. Soil Bureau Conference, Rotorua, 1978.

STEWART, R.B., NEALL, V.E., POLLOK, J.A., SYERS, J.K. 1977: Parent material stratigraphy of an Egmont Loam profile, Taranaki, New Zealand. Australian Journal of Soil Research 15: 177-190.

SUDO, T. 1953a: Clay minerals formed by alteration of volcanic glass in Japan. Clay Minerals 2: 96-106.

SUDO, T, YOTSUMOTO, H. 1977: The formation of halloysite tubes from spherutic halloysite. Clays and Clay Minerals 25: 155-159.

SUGGATE, R.B., MOAR, N.T. 1970: Revision of chronology of the late Otiran Glacial. N.Z. Journal of Geology and Geophysics 13: 742-746.

SWINEFORD, A., FRYE, J.C. 1945: A mechanical analysis of wind-blown dust compared with analyses of loess. American Journal of Science 243: 249-255.

SWINEFORD, A., FRYE, J.C. 1955: Petrographic comparison of some loess samples from Western Europe with Kansas loess. Journal of Sedimentary Petrology 25: 3-23.

TAYLOR, N.H. 1933: Soil processes in volcanic ash beds. N.Z. Journal of Science and Technology 14: 338-52

TAZAKI, K. 1979: Scanning electron microscope study of imogolite formation from plagioclase. Clays and Clay Minerals 27: 209-212.

TERUGGI, M.E. 1957: The nature and origin of Argentine Loess. Journal of Sedimentary Petrology 27: 322-332.

THOMPSON, B.D. 1958: The geology of the Atiamuri Dam site. N.Z. Journal of Geology and Geophysics 1: 275-305.

THOMPSON, B.D. 1964: Quaternary volcanism of the Central volcanic region. N.Z. Journal of Geology and Geophysics 7: 45-66.

THORARINSSON, S. 1954: The tephra-fall from Hekla on March 29th, 1947. In: Erinarsson, T., Kjartansson, G., Thorarinsson, S. (Eds.) The eruption of Hekla 1947-1948; Part 2: 1-68. Reykjavik.

TOPPING, W.W., KOHN, B.P. 1973: Rhyolitic tephra marker beds in the Tongariro area, North Island, New Zealand. N.Z. Journal of Geology and Geophysics 16: 375-395.

VISHER, G.S. 1969: Grain-size distribution and depositional processes. Journal of Sedimentary Petrology 39: 1074-1106.

VUCETICH, C.G. 1963: Ash beds and soils in Rotorua district. Proceedings of the N.Z. Ecological Society 10: 65-72.

VUCETICH, C.G., PULLAR, W.A. 1964: Stratigraphy and chronology of late Quaternary volcanic ash in Taupo, Rotorua and Gisborne districts. Geological Survey Bulletin 73 (Part 2): 43-88.

VUCETICH, C.G. 1968: Soil-Age relationships for New Zealand based on tephrochronology. Transactions of the 9th International Congress of the Soil Science Society IV: 121-130.

VUCETICH, C.G., PULLAR, W.A. 1969: Stratigraphy and chronology of late Peistocene volcanic ash beds in Central North Island, New Zealand. N.Z. Journal Geology and Geophysics 12: 784-837.

WADA, K. 1977: Allophane and Imogolite. In: Dixon, J.B., Weed, S.B. (Eds.) Minerals in Soil Environments 16: 603-638. Soil Science Society of America, 948pp.

WADA, K. 1978: Allophane and imogolite. In: Sudo, T., Shimoda, S. (Eds.) Clays and Clay Minerals of Japan 4: 147-188. Developments in Sedimentology No.26, Elsevier. 326pp.

WAGGONER, P.E., BINGHAM, C. 1961: Depth of loess and distance from source. Soil Science 92: 396-401.

WALKER, G.P.L. 1971: Grain-size characteristics of pyroclastic deposits. Journal of Geology 79: 696-714.

WALKER, G.P.L., CROASDALE, R. 1971: Two plinian-type eruptions in the Azores. Geological Society of London Journal 127: 17-55.

WALKER, G.P.L., CROASDALE, R. 1972: The characteristics of some basaltic pyroclastics. Bulletin of Volcanology 35: 303-317.

WATKINS, N.D., HUANG, T.C. 1977: Tephras in abyssal sediments, east of the North Island, New Zealand: Chronology, paleowind velocity, and paleoexplosivity. N.Z. Journal of Geology and Geophysics 20: 179-198.

WILDING, L.P., SMECK, N.E., DREES, L.R. 1977: Silica in soils: Quartz, Cristobalite, Tridymite and Opal. In: Dixon, J.B., Weed, S.B. (Eds.) Minerals in Soil Environments 14: 471-552. Soil Science Society of America, 948pp.

WILSON, M.J. 1975: Chemical weathering of some primary rock-forming minerals. Soil Science 119: 349-355.

YOSHINAGA, N., AOMINE, S. 1962a: Allophane in some Ando soils. Soil Science and Plant Nutrition (Tokyo) 8: 6-13.

YOSHINAGA, N., AOMINE, S. 1962b: Imogolite in some Ando soils. Soil Science and Plant Nutrition (Tokyo) 8: 22-29.

YOSHINAGA, N., TAIT, J.M., SOONG, R. 1973: Occurrence of imogolite in some volcanic ash soils of New Zealand. Clay Minerals 10: 127-130.

APPENDICES

LIST OF APPENDICES

63-125μm	VG	Qz	Fds	Bt	Opx	Cpx	Hb	FeO
Te Ngae	84	6	4	1	3	1	<1	2
Gavin Rd	82	9	3	<1	2	-	1	2
Okareka Quarry	78	9	7	<1	2	-	1	3
Lynmore	77	8	7	<1	1	-	2	2
Pukehangi Rd	81	6	9	1	1	-	<1	1
Ngongotaha	88	3	5	2	2	-	2	2
Tarukenga	79	9	5	<1	2	-	2	2
Dalbeth Rd	84	5	3	<1	2	-	<1	4
Highland Hill	82	5	8	2	2	-	2	<1
Kuhatahi	74	8	11	1	3	-	2	1
125-250μm	VG	Qz	Fds	Bt	Opx	Cpx	Hb	FeO
Te Ngae	70	14	7	2	4	-	2	3
Gavin Rd	74	10	11	1	1	-	2	2
Okareka Quarry	66	15	10	<1	2	-	<1	6
Lynmore	65	17	15	1	1	-	-	<1
Pukehangi Rd	68	14	15	2	1	-	<1	<1
Ngongotaha	70	7	16	2	2	-	2	2
Tarukenga	71	17	6	1	2	-	1	1
Dalbeth Rd	78	11	5	1	2	-	<1	2
Highland Hill	72	10	14	2	2	-	2	<1
Kuhatahi	59	13	20	1	3	-	2	1

APPENDIX 1: Frequency of mineral species (percent) in very fine sand (63 - 125μm) and fine sand (125 - 250μm) fractions from Okareka Ash deposits.

63-125μm		VG	Qz	Fds	Bt	Opx	Cpx	Hb	FeO
Te Ngae	HL_1	86	3	6	<1	2	<1	<1	<1
	HL_2	84	3	7	1	2	<1	<1	2
Gavin Rd	GL_1	95	<1	3	<1	1	<1	<1	-
	GL_2	93	2	4	-	<1	-	<1	<1
	GL_3	92	2	2	<1	<1	<1	<1	<1
Okareka Quarry	AL_1	78	6	15	<1	2	<1	<1	<1
	AL_2	80	5	11	<1	2	<1	<1	<1
	AL_3	78	5	12	<1	2	-	<1	2
Lynmore	IL_1	88	2	9	<1	1	-	<1	<1
	IL_2	88	3	6	<1	1	-	<1	<1
Pukehangi Rd	BL	88	2	7	<1	2	-	<1	-
Ngongotaha	JL_1	87	2	9	<1	<1	-	<1	<1
	JL_2	78	3	12	1	27	-	2	<1
Tarukenga	CL_1	87	2	7	<1	<1	<1	<1	3
	CL_2	86	2	9	<1	1	<1	<1	<1
	CL_3	80	3	14	<1	2	-	<1	<1
Dalbeth Rd	DL_1	88	3	6	<1	1	<1	<1	<1
	DL_2	83	4	8	<1	1	<1	<1	<1
	DL_3	81	5	11	<1	2	<1	<1	<1
	DL_4	82	3	7	<1	1	-	<1	<1
Highland Hill	EL_1	77	2	18	<1	2	<1	-	<1
	EL_2	75	3	18	<1	2	<1	<1	<1
	EL_3	78	3	16	-	2	-	<1	<1
Kuhatahi	KL_1	78	2	17	-	2	<1	-	<1
	KL_2	87	<1	10	<1	<1	-	<1	<1
	KL_3	84	3	10	<1	2	<1	<1	<1

APPENDIX 2: Frequency of mineral species (percent) in very fine sand (63 - 125μm) fraction in Post-Okareka loess deposits.

125-250μm		VG	Qz	Fds	Bt	Opx	Cpx	Hb	FeO
Te Ngae	HL_1	75	7	14	<1	2	<1	1	2
	HL_2	75	7	11	<1	3	<1	1	2
Gavin Rd	GL_1	94	2	3	<1	<1	-	<1	<1
	GL_2	93	1	3	<1	1	<1	<1	<1
	GL_3	82	6	7	<1	1	<1	1	1
Okareka Quarry	AL_1	70	6	19	-	2	<1	<1	2
	AL_2	79	5	12	<1	<1	-	<1	3
	AL_3	71	5	18	<1	2	-	<1	3
Lynmore	IL_1	74	5	15	<1	2	<1	1	2
	IL_2	75	8	13	<1	2	-	<1	<1
Pukehangi Rd	BL	65	0	20	<1	3	<1	<1	<1
Ngongotaha	JL_1	62	10	20	2	2	<1	2	<1
	JL_2	74	6	14	1	3	<1	<1	1
Tarukenga	CL_1	72	4	19	-	1	<1	<1	5
	CL_2	80	3	12	<1	1	<1	<1	3
	CL_3	78	4	15	<1	2	-	<1	<1
Dalbeth Rd	DL_1	68	8	18	<1	3	<1	<1	2
	DL_2	74	6	13	<1	3	<1	<1	2
	DL_3	78	5	11	<1	2	<1	<1	2
	DL_4	79	6	11	<1	2	-	<1	2
Highland Hill	EL_1	61	6	28	<1	<1	<1	<1	<1
	EL_2	66	4	26	<1	2	<1	<1	1
	EL_3	62	8	19	<1	5	<1	2	2
Kuhatahi	KL_1	75	6	16	<1	1	<1	<1	<1
	KL_2	72	4	20	<1	1	<1	<1	2
	KL_3	70	6	16	<1	3	1	2	1

APPENDIX 3: Frequency of mineral species (percent) in fine sand (125 - 250μm) fraction in Post-Okareka loess deposits.

LOCATION		Mean Grain-size Ø	Mean Grain-size mm	Sorting (σ_I) Ø		Skewness (SK_I)		Kurtosis (K_G)
Trunk Rd	RAL	1.75	300	2.36	vps	0.26	fs	1.20
	RA	2.96	130	2.61	vps	0.36	sfs	0.89
Gavin Rd	GA	3.26	105	1.99	ps/vps	0.35	sfs	1.02
Te Ngae	HA	3.29	104	1.73	ps	0.46	sfs	1.35
Okareka Quarry	AA	2.13	230	2.01	vps	0.35	sfs	1.02
Lynmore	IA	1.55	345	2.42	vps	0.38	sfs	1.18
Pukehangi Rd	BA	3.27	103	1.66	ps	0.39	sfs	1.09
Ngongotaha	JA	3.09	118	1.88	ps	0.33	sfs	1.13
Tarukenga	CA	2.90	135	1.78	ps	0.28	fs → sfs	0.94
Dalbeth Rd	DA	3.16	113	1.83	ps	0.28	fs	0.86
Highland Hill	EA	3.84	70	1.87	ps	0.37	sfs	0.87
Kuhatahi	KA	4.07	59	1.72	ps	0.32	sfs	0.97

APPENDIX 4: Summary of textural analyses for Okareka Ash deposits.

LOCATION		Mean Grain-size Ø	Mean Grain-size /Mm	Sorting (σ_I) Ø		Skewness (SK_I)		Kurtosis (K_G)
Trunk Rd	PT	4.63	40	1.66	ps	0.20	fs	1.09
	L_1	4.12	57	2.09	vps	0.04	nearly sym	1.20
	L_2	3.04	120	2.14	vps	0.00	nearly sym	0.97
Gavin Rd	GL_1	4.71	38	1.52	ps	0.34	sfs	1.00
	GL_2	4.85	35	1.45	ps	0.38	sfs	1.03
	GL_3	4.57	42	1.67	ps	0.29	fs ⟶ sfs	1.14
Te Ngae	Hl_1	4.86	35	1.71	ps	0.08	nearly sym	0.90
	HL_2	4.38	48	1.75	ps	0.32	sfs	1.07
Okareka Quarry	AL_1	4.54	43	1.73	ps	0.11	nearly sym/fs	1.23
	AL_2	4.56	42	1.83	ps	0.23	fs	1.11
	AL_3	3.97	64	2.21	vps	0.20	fs	1.08
Lynmore	IL_1	4.82	35	1.54	ps	0.35	sfs	1.10
	IL_2	4.37	48	1.70	ps	0.16	fs	1.06
Pukehangi Rd	BL	4.90	33	1.76	ps	0.17	fs	0.98

APPENDIX 5A: Summary of textural analyses for Post-Okareka loess deposits.

LOCATION		Mean Grain-size Ø	Mean Grain-size μm	Sorting (σ_I) Ø		Skewness (SK_I)		Kurtosis (K_G)
Ngongotaha	JL_1	5.18	28	1.66	ps	0.	fs	0.85
	JL_2	4.49	45	1.70	ps	0.32	sfs	0.97
Tarukenga	CL_1	5.23	27	1.55	ps	0.09	nearly sym/fs	0.91
	CL_2	5.17	28	1.60	ps	0.20	fs	0.81
	CL_3	4.69	42	1.61	ps	0.34	st fs	1.01
Dalbeth Rd	DL_1	5.19	27	1.59	ps	0.12	fs	0.83
	DL_2	4.58	42	1.49	ps	0.40	sfs	1.00
	DL_3	4.84	35	1.50	ps	0.31	sfs ⟶ fs	0.95
	DL_4	4.72	38	1.54	ps	0.29	fs ⟶ sfs	1.05
Highland Hill	EL_1	5.19	28	1.54	ps	0.21	fs	0.90
	EL_2	5.09	29	1.44	ps	0.32	sfs	1.00
	EL_3	5.41	24	1.57	ps	0.07	nearly sym	0.81
Kuhatahi	KL_1	5.54	22	1.60	ps	0.08	nearly sym	0.87
	KL_2	5.56	21	1.55	ps	0.08	nearly sym	0.86
	KL_3	5.49	22	1.59	ps	0.08	nearly sym	0.81

APPENDIX 5B: Summary of textural analyses for Post-Okareka loess deposits.

APPENDIX 6A: Site description; TRUNK RD

GRID REF: N77/937136

LOCATION: forestry road east of Tarawera, past Rerewhakaaitu township

ALTITUDE: 430m

RAINFALL: 2000mm

OVERBURDEN DEPTH: 5.75m

TOPOGRAPHY: undulating landscape densely covered in native bush

DRAINAGE: free-draining

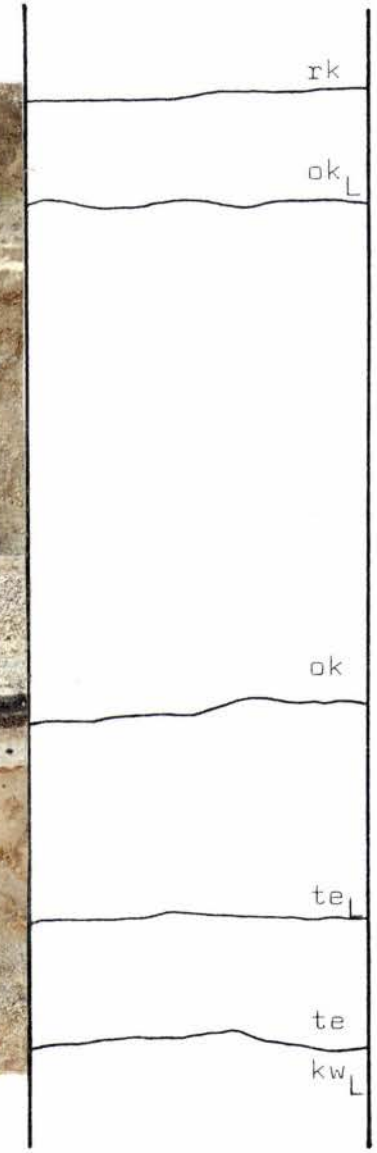

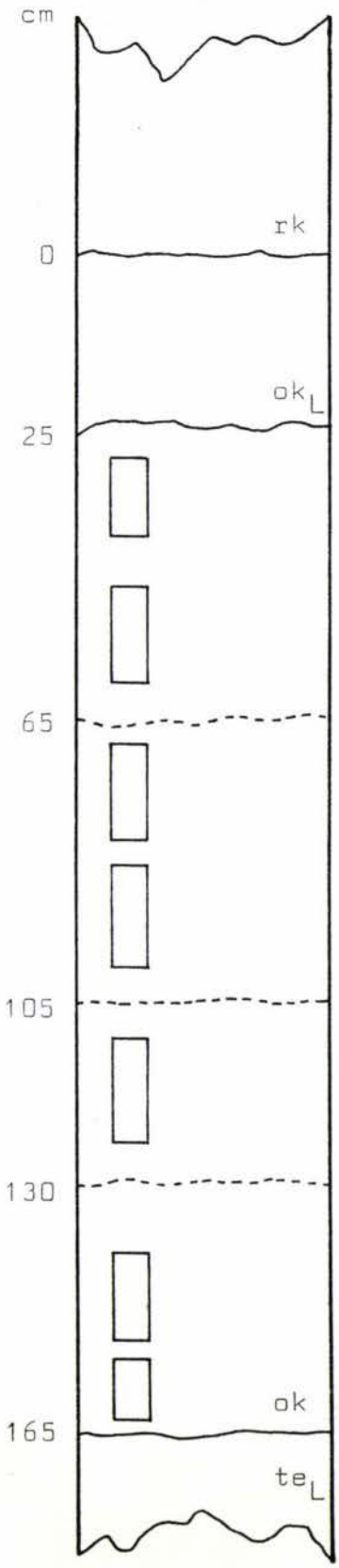

distinct boundary

2.5Y 4/4 - 10YR 5/8 silt loam; massive; moist; many pores; pinheads;
2.5YR 5/6 scattered lapilli

distinct boundary

R_{AL} 2.5Y 8/2 - 7/2 white / light grey; shower bedded very fine sandy ash and lapilli

irregular boundary

R_{FL} shower bedded fine ash and lapilli; some pin heads
2.5Y 6/2 - 7/2 light grey medium fine lapilli; irregular boundary

R_L 5Y 7/2 light grey shower bedded medium fine lapilli, lithic and pumice fragments overlying coarse lapilli; iron banding between laminae

R_A 2.5Y 7/4 pale yellow medium fine shower bedded ash and lapilli

distinct boundary

R_{CL} 2.5Y 7/2 light grey coarse lapilli banded appearance
medium coarse lapilli with some medium fine lapilli; some mottles

irregular boundary

B_{AL} 5Y 6/3 pale olive medium to coarse lapilli; grading to coarse lapilli at base

B_L 2.5Y 5/0 grey fine lapilli and ash; shower bedded

distinct boundary
some iron movement evident from basal layer of ok through to te$_L$; eluvial layer at top of te$_L$

APPENDIX 6B : Profile description; TRUNK RD

APPENDIX 7 : Profile description; GAVIN RD; section G

GRID REF: N86/991833

LOCATION: road side section east of Rerewhakaaitu township

ALTITUDE: 430m

RAINFALL: 1600mm

OVERBURDEN DEPTH: 6.85m

TOPOGRAPHY: hill surrounded by farmland

DRAINAGE: free-draining

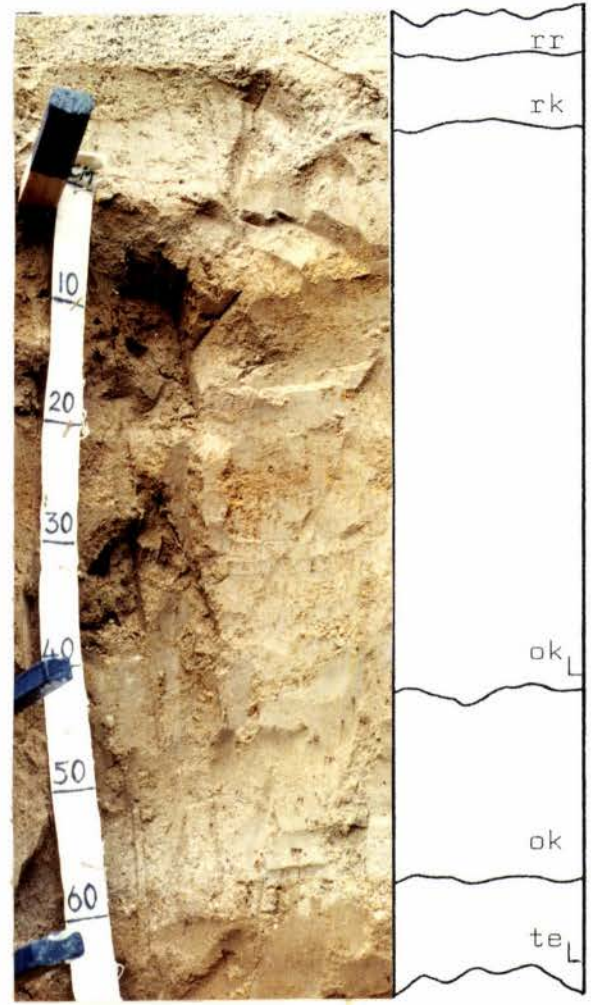

APPENDIX 8 : Profile description; TE NGAE; section H

GRID REF: N75/791112

LOCATION: roadside section on Rotorua-Tauranga state highway, 100m from turnoff to Whakatane

ALTITUDE: 290m

RAINFALL: 1750mm

OVERBURDEN DEPTH: 4.90m

TOPOGRAPHY: lakeside area surrounded by farmland

DRAINAGE: free-draining

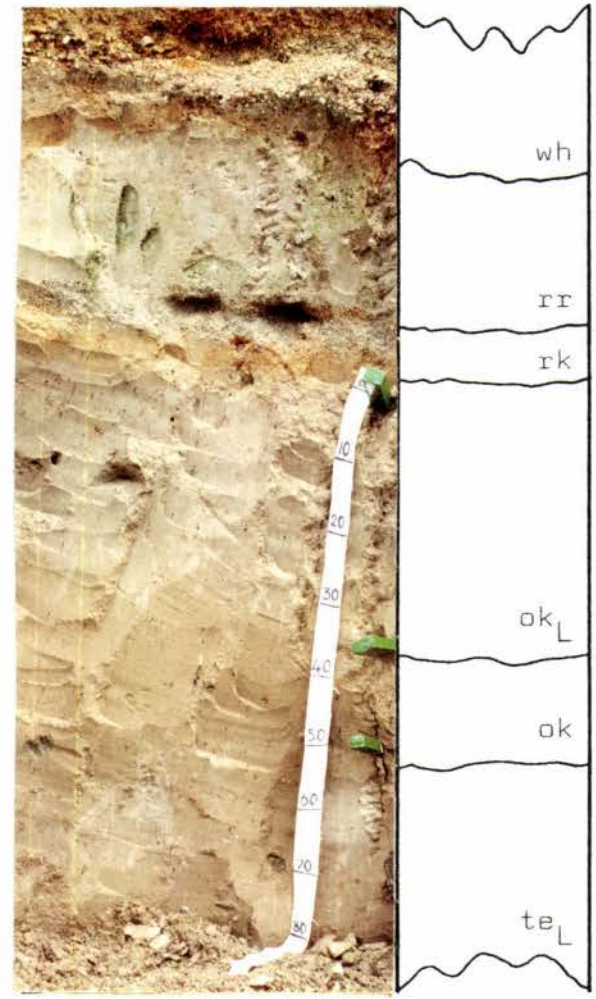

0 distinct boundary
2.5Y 5/4 - 6/4 light olive-brown massive silt loam; some pin-heads; pores; some grey mottles

2.5Y 5/4 light olive-brown silt loam; some sandy inclusions

35 irregular boundary
2.5Y 6/4 light yellow-brown shower bedded fine lapilli and
52 ash; indistinct irregular boundary

APPENDIX 9 : Profile description; OKAREKA QUARRY; section A

GRID REF: N76/798002

LOCATION: quarry site, Okareka Loop Rd east of Rotorua

ALTITUDE: 460m

RAINFALL: 1500mm

OVERBURDEN DEPTH: 7.15m

TOPOGRAPHY: site is exposed by quarrying, surrounded by forest and farmland

DRAINAGE: free-draining

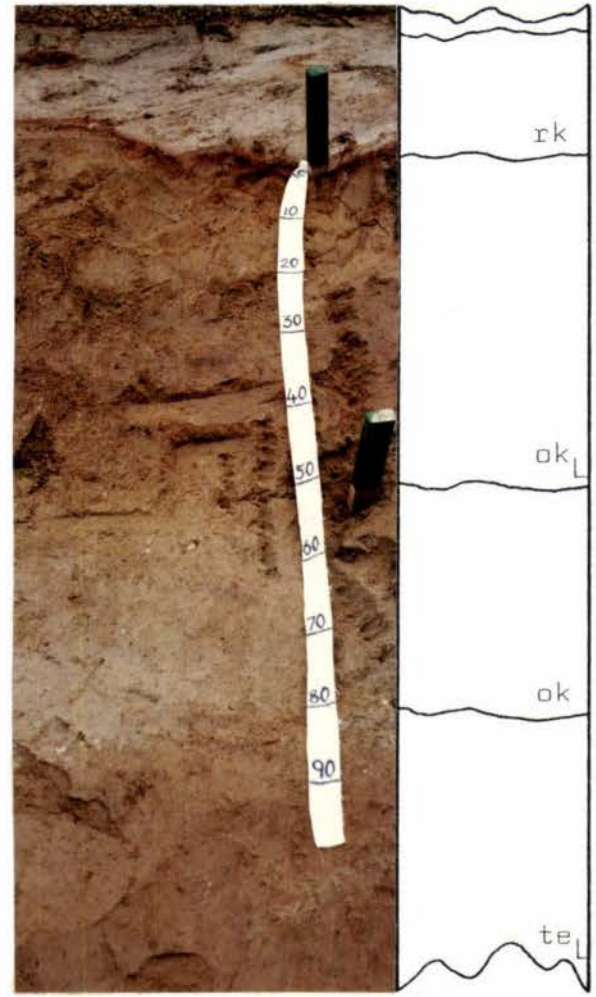

cm

rk

0 iron banding

distinct boundary
2.5Y 5/6 light olive-brown massive silt loam; pinheads

compact

2.5Y 6/6 olive-yellow sandy silt

ok_L

52-68 irregular boundary
2.5Y 6/4 light yellowish-brown shower bedded ash and lapilli

coarse lapilli at base; whiteish basal layer; scattered pin-heads

ok

84-90 irregular distinct boundary

te_L

APPENDIX 10 : Profile description; LYNMORE; section I

GRID REF: N76/757025

LOCATION: quarry pumice pit 300m from end of Walford Drive

ALTITUDE: 320m

RAINFALL: 1550mm

OVERBURDEN DEPTH: 1.40m

TOPOGRAPHY: gully area surrounded by forested hills, rim of Rotorua Basin

DRAINAGE: free-draining

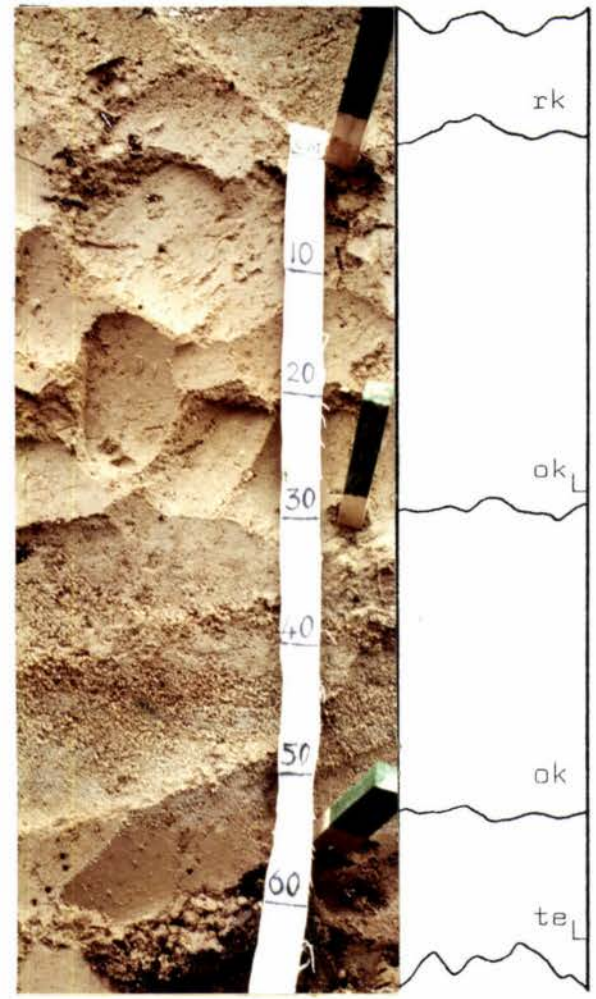

cm

rk

0 indistinct irregular boundary
2.5Y 4/4 olive-brown silt loam; massive; pinheads; pores; some roots

2.5Y 5/4 light olive-brown silt loam

ok

25-32 irregular boundary
5Y 5/3 olive shower bedded ash; coarse lapilli at base grading to fine ash

ok

50-62 irregular distinct boundary

te

APPENDIX 11 : Profile description; PUKEHANGI RD, section B

GRID REF: N76/693017

LOCATION: southwestern edge of Rotorua city, south of Rotorua stadium

ALTITUDE: 300m

RAINFALL: 1500mm

OVERBURDEN DEPTH: 1.40m

TOPOGRAPHY: low lying hummock surrounded by farmland

DRAINAGE: free-draining

cm

rk

0 indistinct boundary
2.5Y 5/4 light olive-brown massive, quite compact silt loam; some pores

ok_L

25 irregular boundary
2.5Y 6/4 light yellowish-brown shower bedded fine sandy ash; some mottles from old root channels

ok

65 irregular distinct boundary

kw_L

APPENDIX 12 : Profile description; NGONGOTAHA, section J

GRID REF: N76/672103

LOCATION: roadside section Rotorua-Tirau state highway 1km from Ngongotaha turnoff

ALTITUDE: 300m

RAINFALL: 1900mm

OVERBURDEN DEPTH: 2.00m

TOPOGRAPHY: low-lying hill sloping to L. Rotorua

DRAINAGE: free-draining

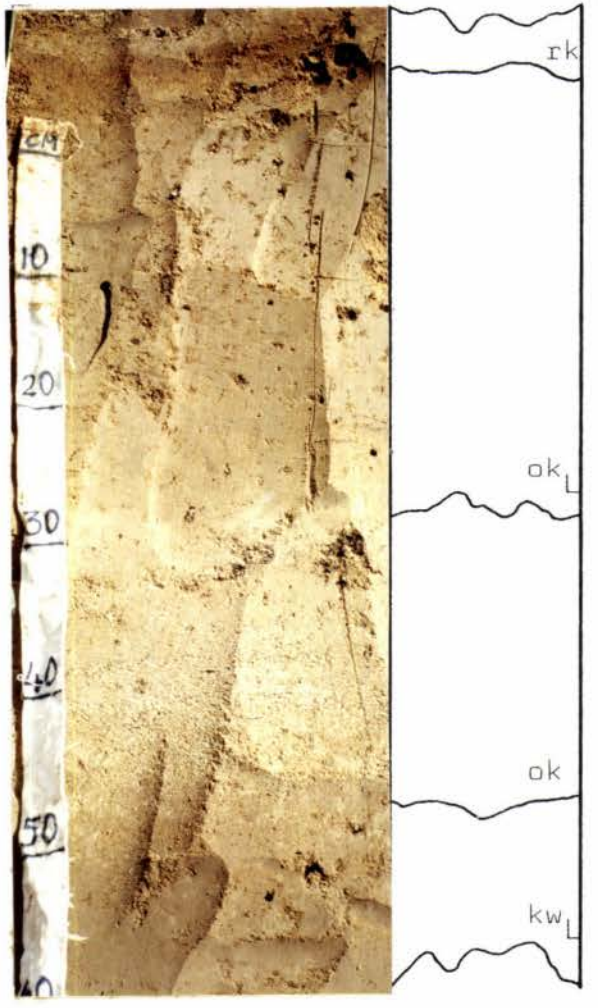

cm

0 irregular boundary
2.5Y 5/4 light olive-brown massive silt loam; some pores; pinheads and fine rootlets

26 irregular boundary
2.5Y 6/4 light-yellowish-brown shower bedded lapilli and fine sandy ash

lithic fragments

55 distinct boundary

APPENDIX 13 : Profile description; TARUKENGA, section C

GRID REF: N76/639120

LOCATION: roadside section part of Tarukenga deviation Rotorua-Tirau highway

ALTITUDE: 380m

RAINFALL: 1900mm

OVERBURDEN DEPTH: 2.75m

TOPOGRAPHY: side of Mamaku plateau surrounded by farmland

DRAINAGE: free-draining

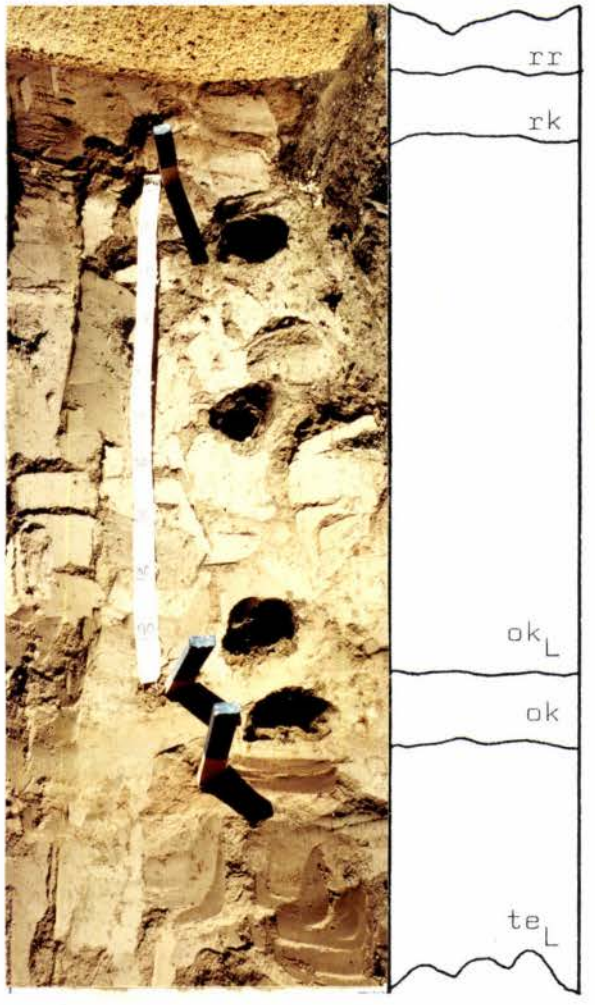

0 indistinct boundary

5Y 5/3 olive massive silt loam; many pores and fine roots; pinheads; moist

2.5Y 5/4 light olive-brown silt loam

100 indistinct boundary

2.5Y 5/4 light yellowish-brown

115 fine ash and lapilli; coarser at base; indistinct boundary

APPENDIX 14 : Profile description; DALBETH RD, section D

GRID REF: N76/628119

LOCATION: roadside section west of Dalbeth Road on Rotorua-Tirau highway

ALTITUDE: 410m

RAINFALL: 2000mm

OVERBURDEN DEPTH: 2.80m

TOPOGRAPHY: hill on down-slope, eastern side of Mamaku Plateau, surrounded by farmland

DRAINAGE: free-draining

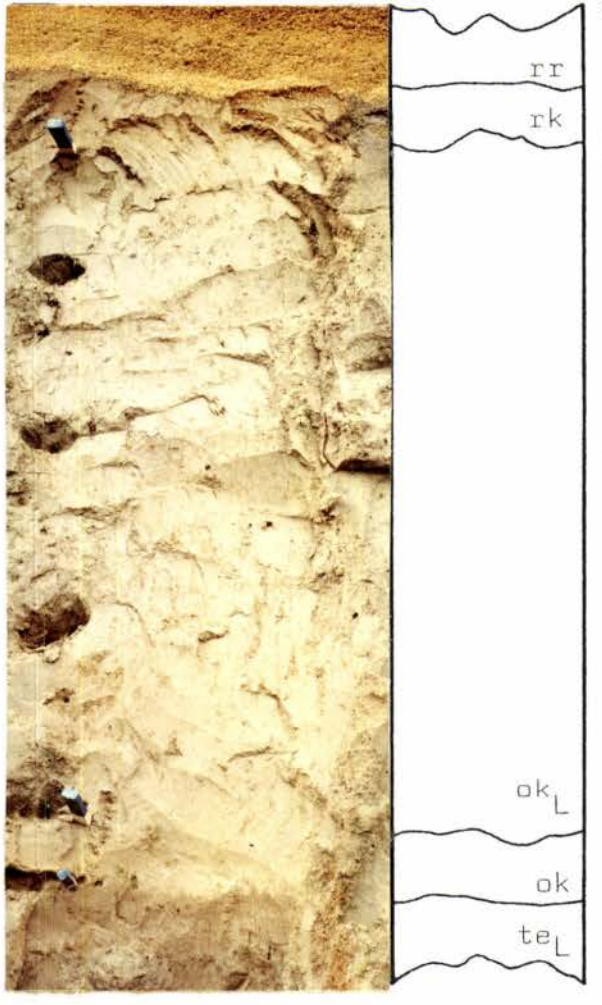

distinct boundary

indistinct boundary

5Y 5/3 olive massive silt loam; very moist with deep pores; some old root channels; many pinheads

2.5Y 4/4 olive-brown silt loam

2.5Y 5/4 light olive-brown silt loam; firm

many pinheads

indistinct boundary

2.5Y 6/4 light yellowish-brown fine ash and lapilli; distinct boundary

APPENDIX 15 : Profile description; HIGHLAND HILL, section E

GRID REF: N76/495168

LOCATION: Rotorua-Tirau highway approx. 2km east of Highland Hill Station

ALTITUDE: 550m

RAINFALL: 2200mm

OVERBURDEN DEPTH: 1.35m

TOPOGRAPHY: on crest of Mamaku Plateau covered by native forest, overlying weathered Mamaku Ignimbrite

DRAINAGE: free-draining

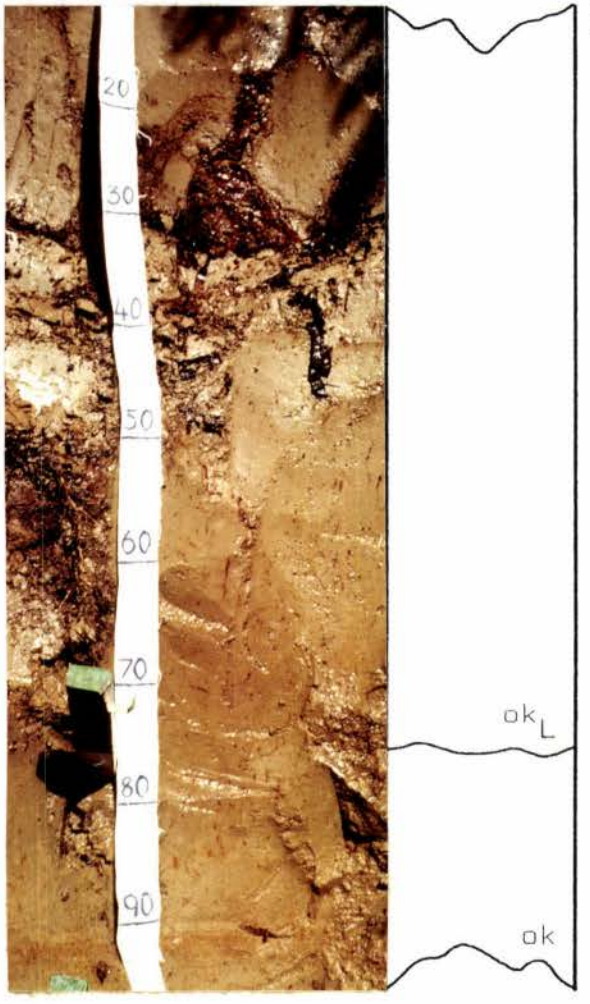

cm

10 indistinct boundary
2.5Y 5/4 light olive-brown
massive silt loam; very
moist; many roots; very
compact

2.5Y 4/4 olive-brown silt
loam

75 indistinct boundary
2.5Y 6/4 light yellowish-brown
shower bedded ash; grading from
fine ash and lapilli to very
fine sandy ash

100

APPENDIX 16 : Profile description; KUHATAHI, section K

GRID REF: N75/442183

LOCATION: recent roadside cutting on Rotorua-Tirau highway, adjacent Kuhatahi River

ALTITUDE: 450m

RAINFALL: 1900mm

OVERBURDEN DEPTH: 0.90m

TOPOGRAPHY: hill on western downslope of Mamaku Plateau, dense native bush surrounding

DRAINAGE: free-draining

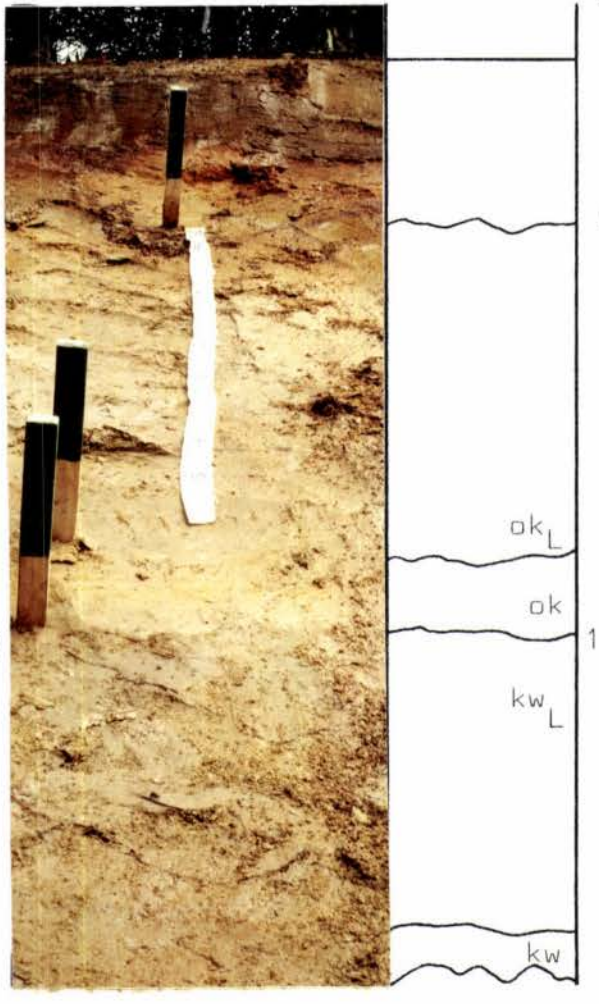

0 irregular distince boundary
10YR 4/6 dark yellowish-brown silt loam; many fine roots; massive; very moist; many pores; some orange mottles

2.5Y 5/4 light olive-brown silt loam
harder and more compact
2.5Y 4/4 olive-brown silt loam

90 irregular boundary
2.5Y 5/6 light olive-brown shower bedded fine sandy ash and lapilli; irregular boundary

105